

CP violation with ALPs and Singlet Scalars

Cosmology, Astrophysics, Theory and Collider Higgs 2024

(CATCH22+2)

Dublin May 1 - 5 2024

Belén Gavela
Univ. Autónoma de Madrid and IFT



H2020



Why CP-violation ?

Why CP-violation ?

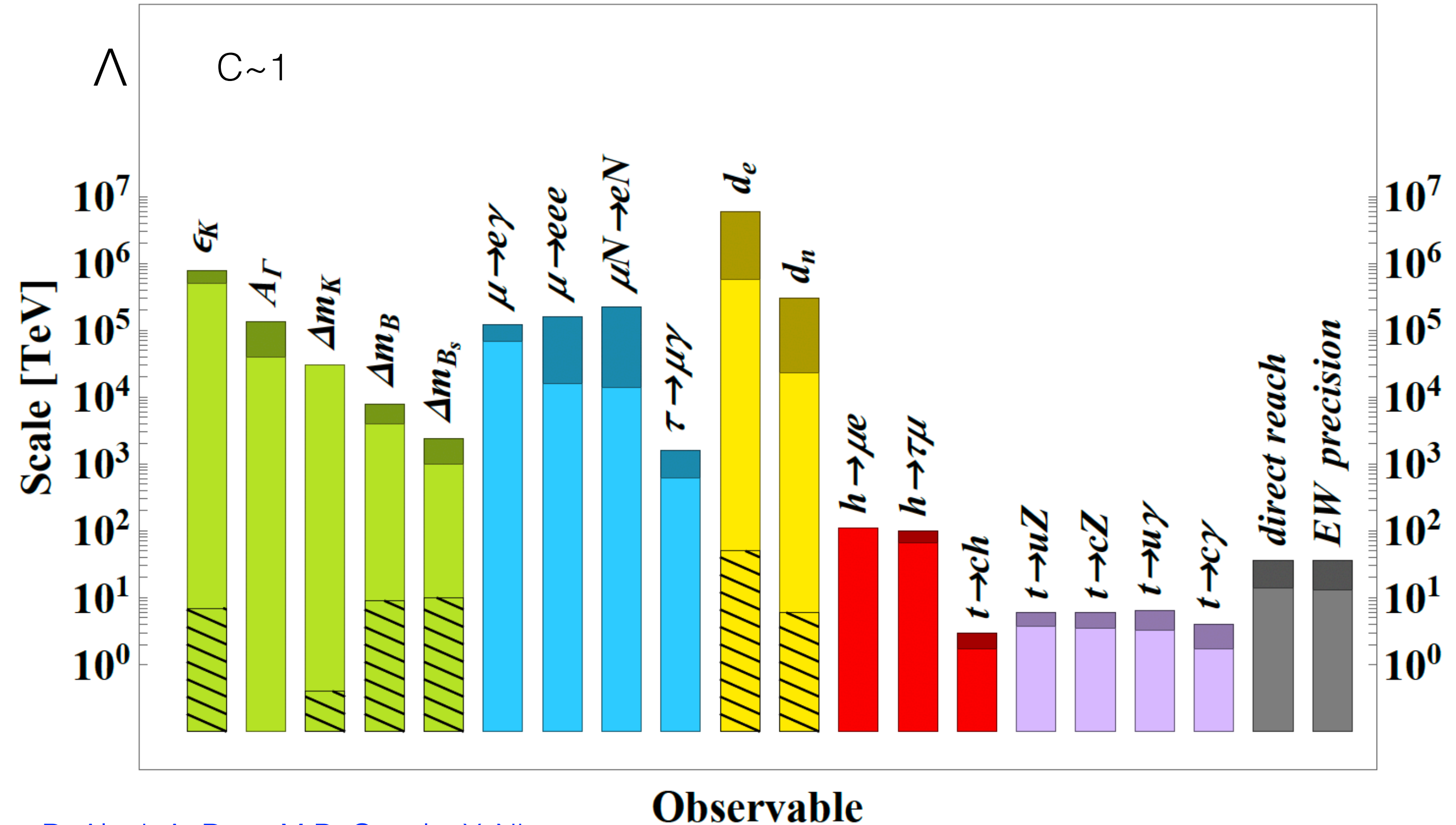
Why 3 generations of quarks and leptons, with mixing and leading to CP-violation.... for ``nothing''?

Why CP-violation ?

**CP-violation is a fantastic
window to BSM**

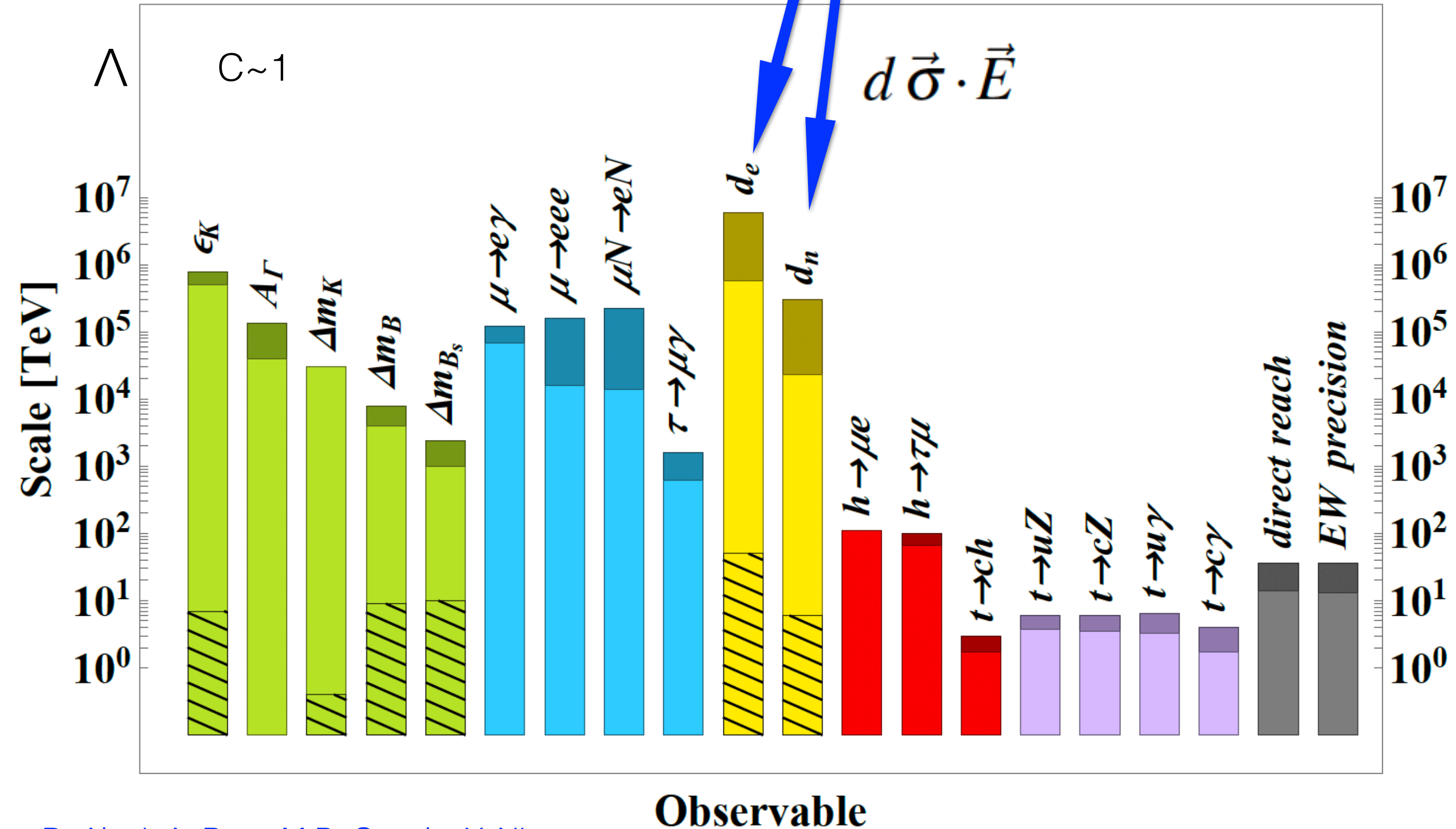
$$\frac{C_6^a}{\Lambda^2} \mathcal{O}_a^{(6)}$$

Flavour physics



$$\frac{C_6^a}{\Lambda^2} \mathcal{O}_a^{(6)}$$

Electric dipole moments



Electric dipole moments

$$d \vec{\sigma} \cdot \vec{E}$$

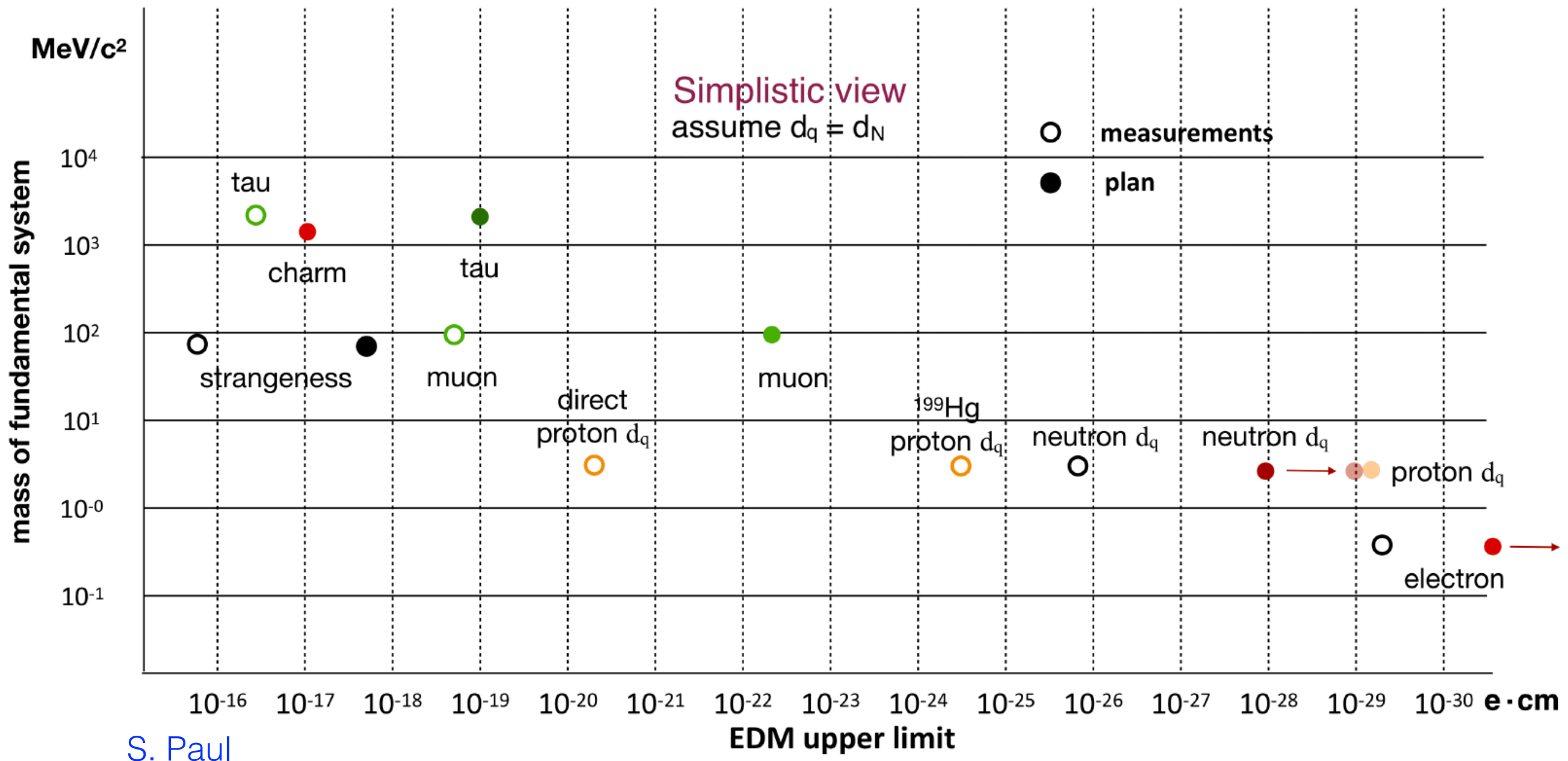
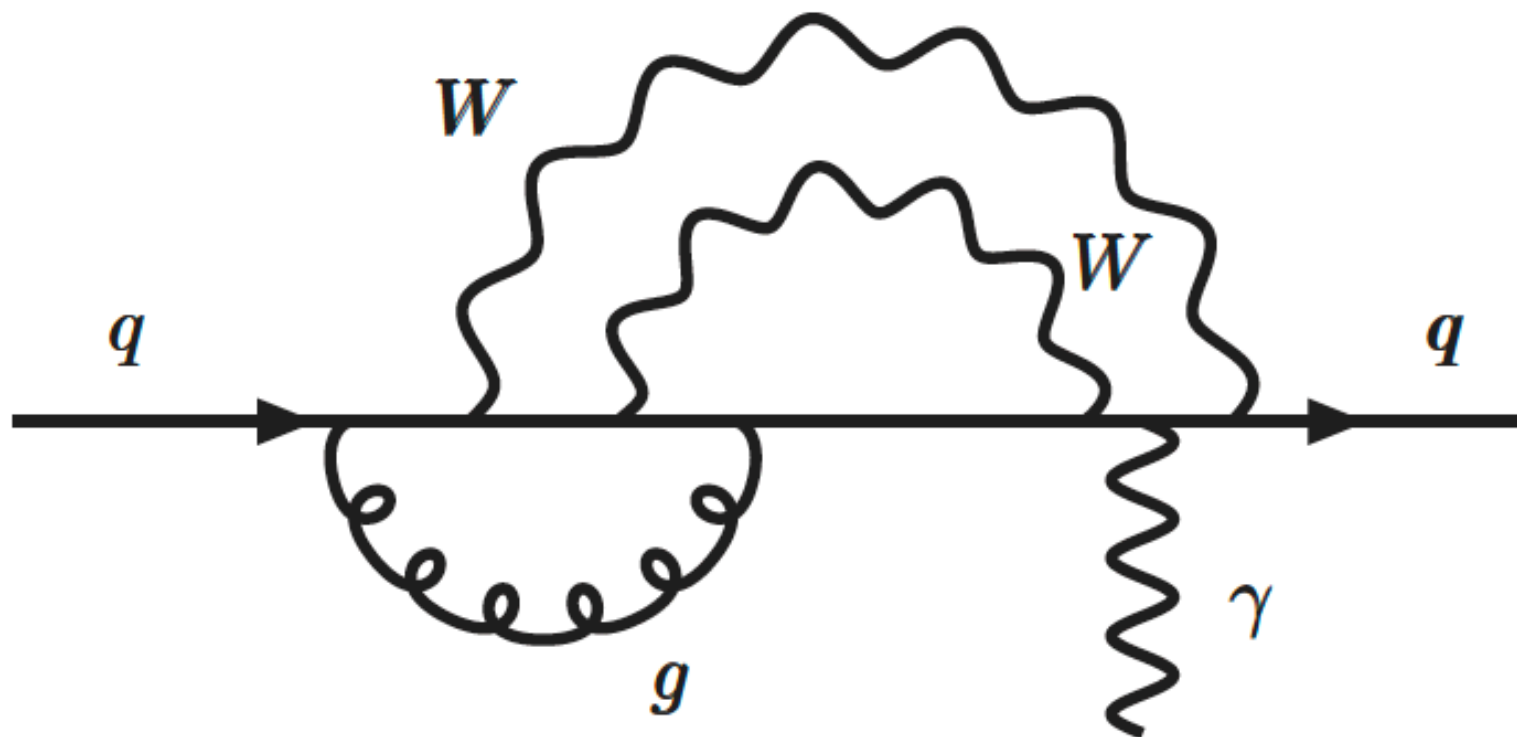


Fig. 5.3: Summary of current EDM limits (empty circles) and short/mid-term planned sensitivities (full circles) for light quarks, strange and charm quarks, electron, muon and tau [257].

In the SM the quark EDM is 3-loop suppressed

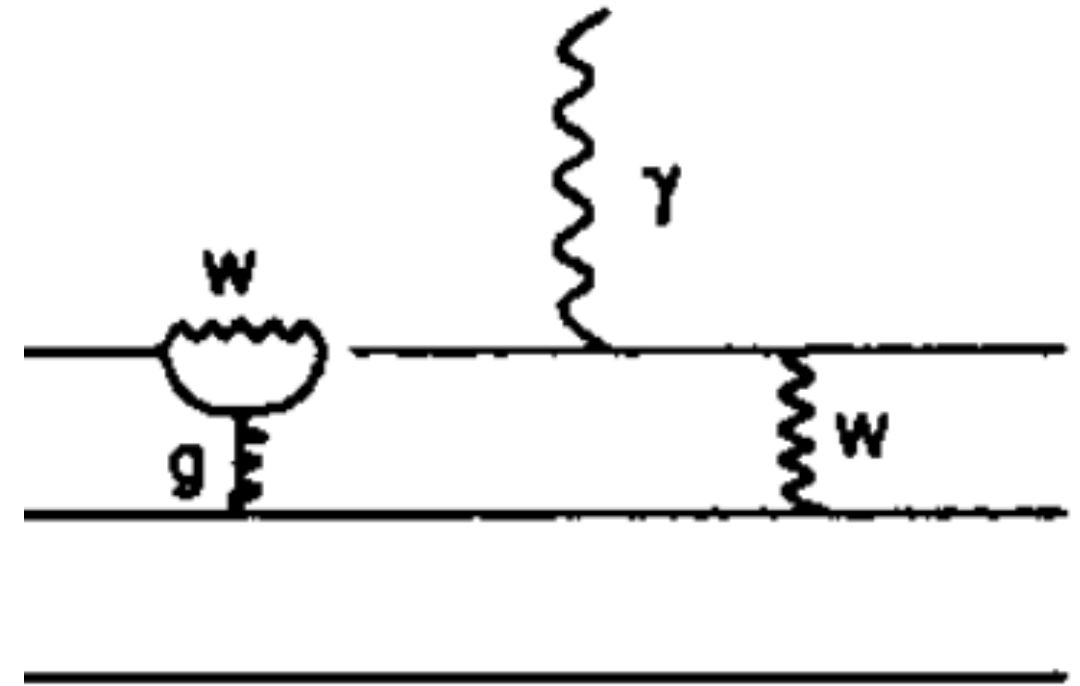
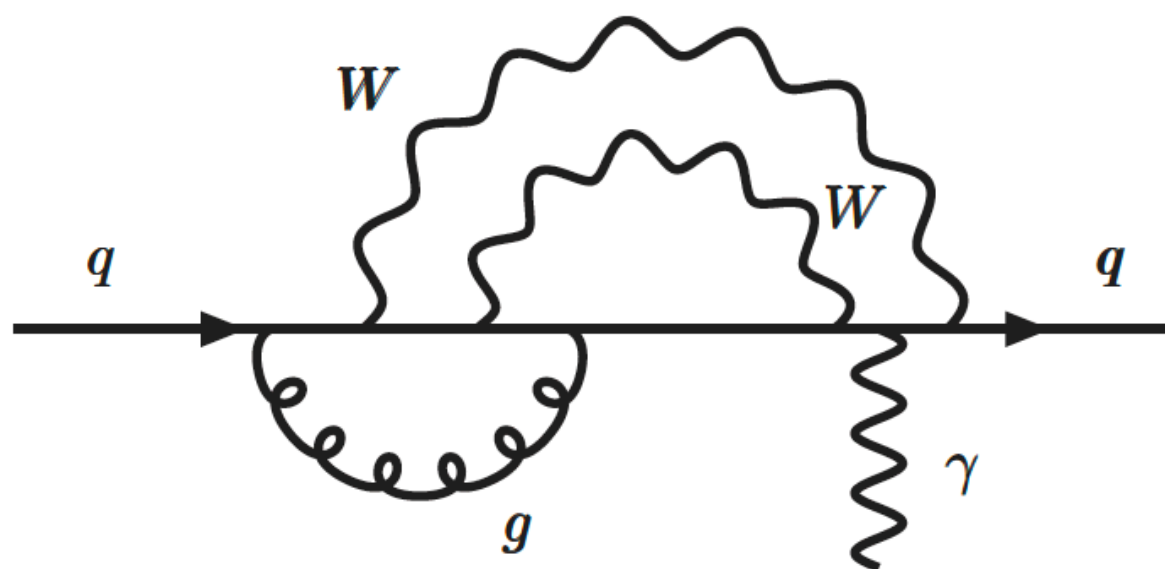


SM predicts $d_n \sim 10^{-34} \text{ e}\cdot\text{cm}$

Experiment: $d_n < 3.6 \times 10^{-26} \text{ e}\cdot\text{cm}$ at 95% CL

In the SM the neutron EDM is very suppressed

“penguin dominated”



(80's: Gavela et al.,
Khriplovich+Zhitnitsky)

SM predicts $d_n \sim 10^{-30} - 10^{-32} \text{ e}\cdot\text{cm}$

Experiment: $d_n < 3.6 \times 10^{-26} \text{ e}\cdot\text{cm}$ at 95% CL

In the SM they are 3-loop suppressed

BSM window: In general
electric dipole moments
at one loop

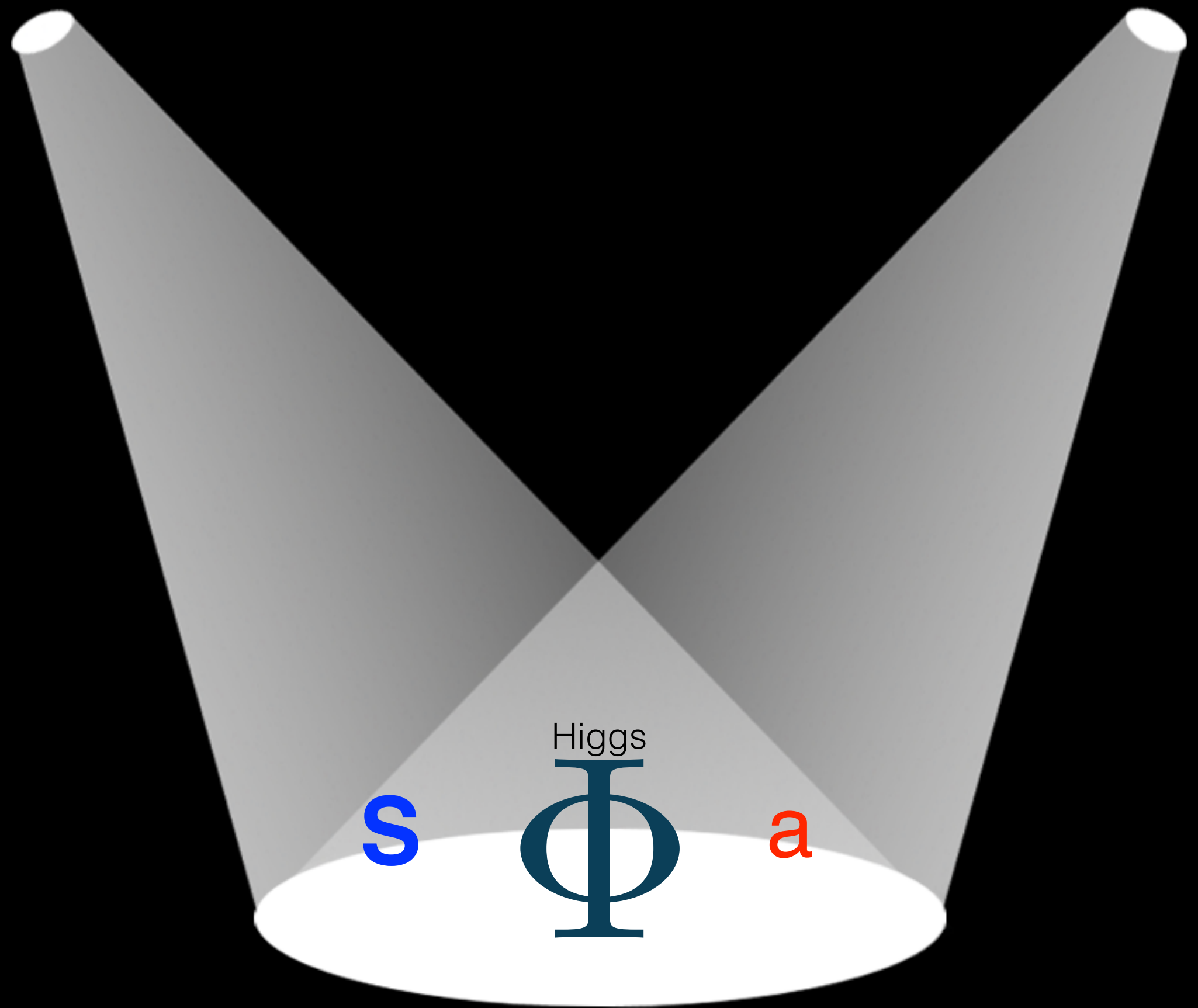


SM predicts $d_n \sim 10^{-30} - 10^{-32}$ e·cm

Experiment: $d_n < 3.6 \times 10^{-26}$ e·cm at 95% CL

Why ALPs

or general Scalars ?



Strong motivation for singlet (pseudo)scalars from fundamental SM problems

The nature of DM is unknown

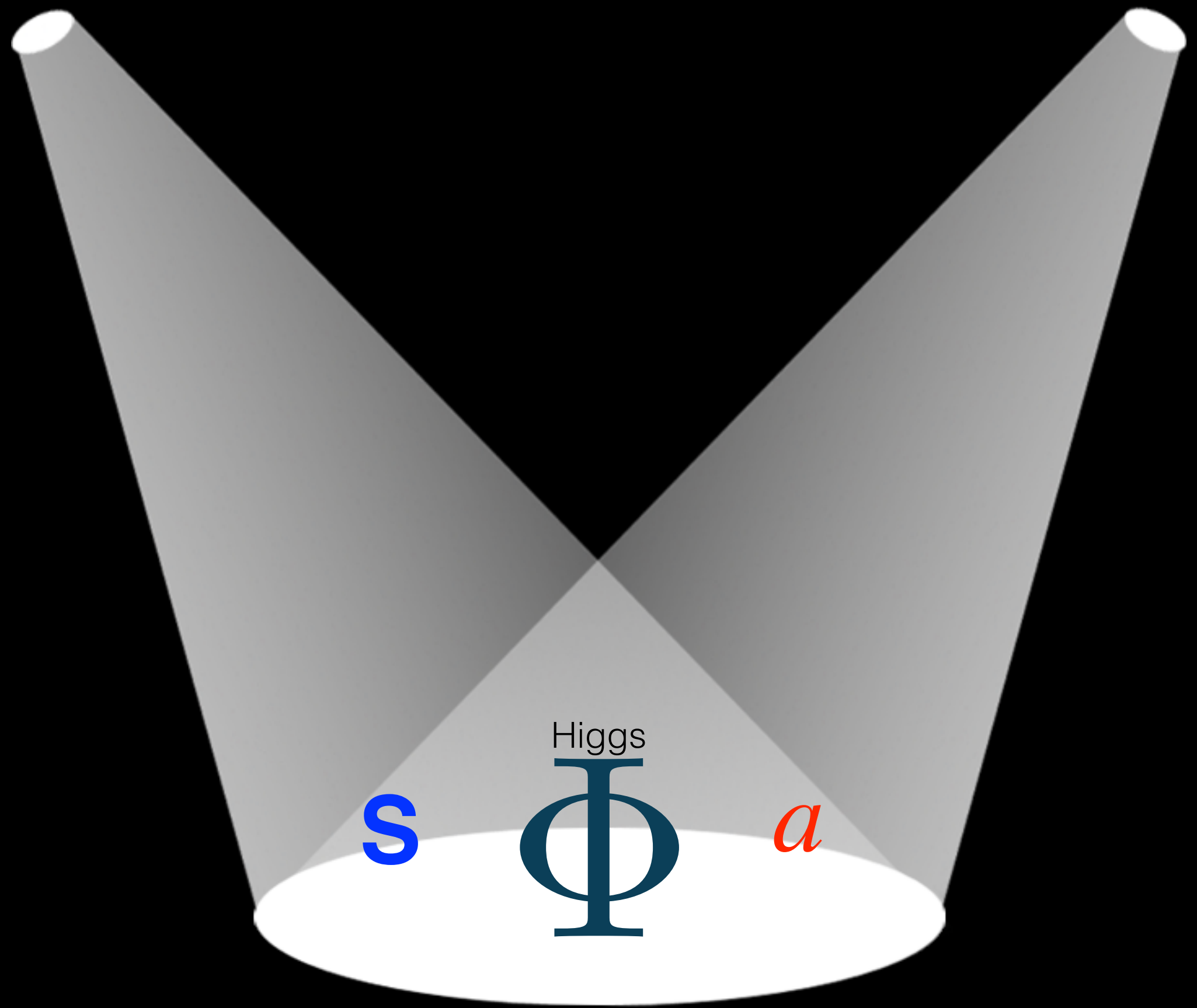


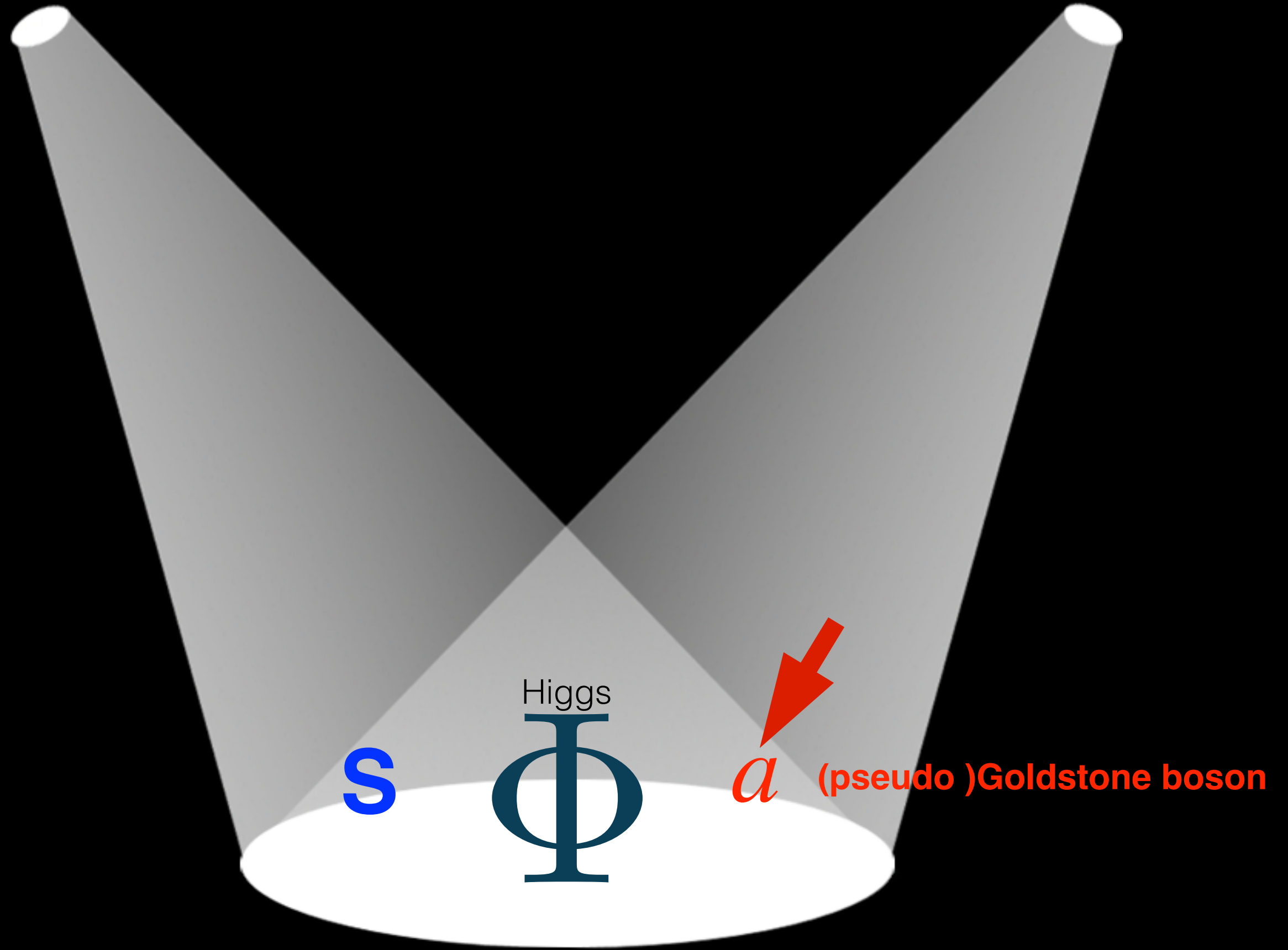
It may be a (SM singlet) scalar **S**

the “Higgs portal”

$$\delta\mathcal{L} = \Phi^+\Phi S^2$$

S has polynomial couplings





Strong motivation for singlet (pseudo)scalars from fundamental SM problems

The nature of DM is unknown



It may be a (SM singlet) scalar **S**

the “Higgs portal”

$$\delta\mathcal{L} = \Phi^+\Phi S^2$$

S has polynomial couplings

Strong motivation for singlet (pseudo)scalars from fundamental SM problems

The nature of DM is unknown



The strong CP problem

Why is the QCD θ parameter so small?

$$\mathcal{L}_{\text{QCD}} \supset \theta G_{\mu\nu} \tilde{G}^{\mu\nu}$$

It may be a (SM singlet) scalar S

the “Higgs portal”

$$\delta\mathcal{L} = \Phi^+ \Phi S^2$$

S has polynomial couplings

Silveira+Zee; Veltman+Yndurain; Patt+Wilczek...

Strong motivation for singlet (pseudo)scalars from fundamental SM problems

The nature of DM is unknown



It may be a (SM singlet) scalar S
the “Higgs portal”

$$\delta\mathcal{L} = \Phi^+\Phi S^2$$

S has polynomial couplings

Silveira+Zee; Veltman+Yndurain; Patt+Wilczek...

The strong CP problem

Why is the QCD θ parameter so small?

$$\mathcal{L}_{QCD} \ni \theta G_{\mu\nu} \tilde{G}^{\mu\nu}$$
A thick red vertical arrow pointing downwards, indicating a causal relationship or flow from the top-right text to the bottom-right text.

A dynamical $U(1)_A$ solution

Peccei+Quinn; Wilczek...

Strong motivation for singlet (pseudo)scalars from fundamental SM problems

The nature of DM is unknown



It may be a (SM singlet) scalar S
the “Higgs portal”

$$\delta\mathcal{L} = \Phi^+\Phi S^2$$

S has polynomial couplings

Silveira+Zee; Veltman+Yndurain; Patt+Wilczek...

The strong CP problem

Why is the QCD θ parameter so small?

$$\mathcal{L}_{QCD} \supset \frac{a}{f_a} G_{\mu\nu} \tilde{G}^{\mu\nu}$$


A dynamical $U(1)_A$ solution

→ the axion a

Peccei+Quinn; Wilczek...

Strong motivation for singlet (pseudo)scalars from fundamental SM problems

The nature of DM is unknown



It may be a (SM singlet) scalar S
the “Higgs portal”

$$\delta\mathcal{L} = \Phi^+\Phi S^2$$

S has polynomial couplings

Silveira+Zee; Veltman+Yndurain; Patt+Wilczek...

The strong CP problem

Why is the QCD θ parameter so small?

$$\mathcal{L}_{QCD} \supset \frac{a}{f_a} G_{\mu\nu} \tilde{G}^{\mu\nu}$$

A dynamical $U(1)_A$ solution

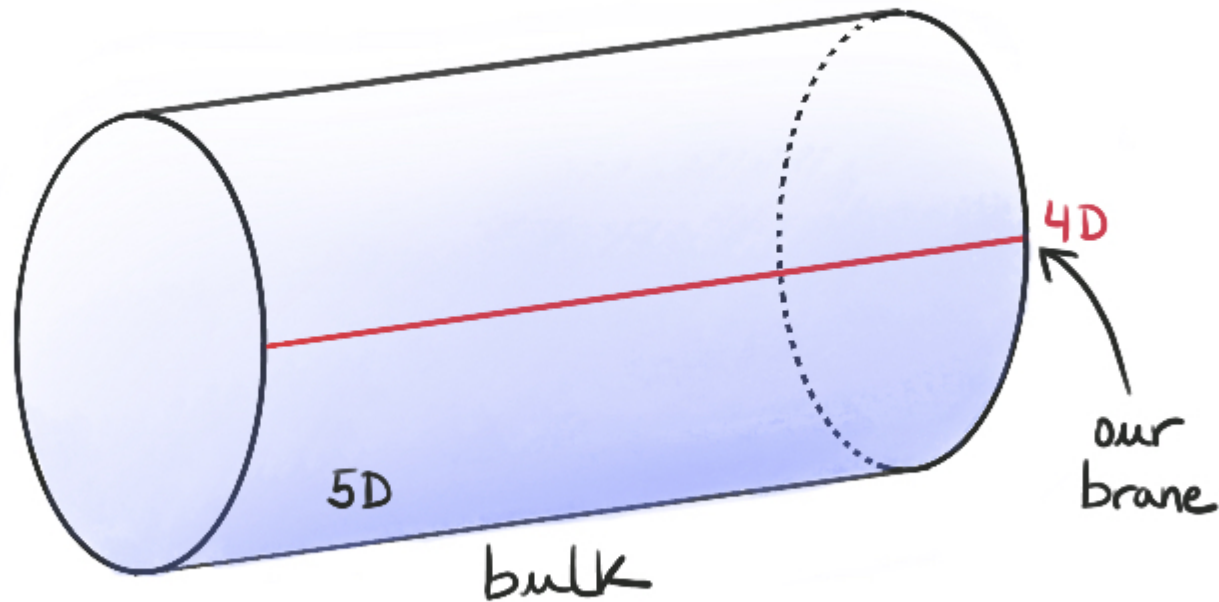
→ the axion a

It is a pGB: \sim derivative couplings
 $\sim \partial_\mu a$

Also excellent DM candidate
Peccei+Quinn; Wilczek...

(Pseudo)Goldstone Bosons appear in many BSM theories

- * e.g. Extra-dim Kaluza-Klein: 5d gauge field compactified to 4d
The Wilson line around the circle is a GB, which behaves as an axion in 4d



- * Majorons, for dynamical neutrino masses
- * From string models
- * The Higgs itself may be a pGB ! (“composite Higgs” models)
- * Axions a that solve the strong CP problem, and ALPs (axion-like particles)

.....

Because they are (pseudo)Goldstone bosons,

Axions and ALPs a

are the tell-tale of hidden

symmetries

awaiting discovery

**Think of the pions...
and of the massive W and Z...**

\mathcal{ALPs} (axion-like-particles)

An ALP (axion-like particle) is a generic scalar field a
with derivative couplings to SM particles

and free scale f_a :

$$\mathcal{L} = \mathcal{L}_{\text{SM}} + \frac{\partial_\mu a}{f_a} \times \text{SM}^\mu$$

general effective couplings

$$\{m_a, f_a\}$$

An ALP (axion-like particle) is a generic scalar field a
with derivative couplings to SM particles

and free scale f_a :

$$\mathcal{L} = \mathcal{L}_{\text{SM}} + \frac{\partial_\mu a}{f_a} \times \text{SM}^\mu + C_i \frac{a X_{\mu\nu} \tilde{X}^{\mu\nu}}{f_a} + \dots$$

general effective couplings

$X^{\mu\nu} = F^{\mu\nu}, G^{\mu\nu}, Z^{\mu\nu}, W^{\mu\nu}, \dots$

$$\{m_a, f_a\}$$

An ALP (axion-like particle) is a generic scalar field a
with derivative couplings to SM particles

and free scale f_a :

$$\mathcal{L} = \mathcal{L}_{\text{SM}} + \frac{\partial_\mu a}{f_a} \times \text{SM}^\mu + C_i \frac{a X_{\mu\nu} \tilde{X}^{\mu\nu}}{f_a} + \dots$$

general effective couplings

$$X^{\mu\nu} = F^{\mu\nu}, G^{\mu\nu}, Z^{\mu\nu}, W^{\mu\nu}, \dots$$

$$\left\{ m_a, \frac{C_i}{f_a} \right\}$$

ALP-Linear effective Lagrangian at NLO

II
SM EFT

Complete basis (bosons+fermions):

$$\mathcal{L}_{\text{eff}} = \mathcal{L}_{\text{SM}} + \frac{1}{2}(\partial_\mu a)(\partial^\mu a) + \sum_i^{\text{total}} c_i \mathbf{O}_i^{d=5} - \frac{1}{2} m_a^2 a^2$$

$$\mathbf{O}_{\tilde{B}} = -B_{\mu\nu}\tilde{B}^{\mu\nu} \frac{a}{f_a} \quad \mathbf{O}_{\tilde{G}} = -G_{\mu\nu}^a \tilde{G}^{a\mu\nu} \frac{a}{f_a}$$

$$\mathbf{O}_{\tilde{W}} = -W_{\mu\nu}^a \tilde{W}^{a\mu\nu} \frac{a}{f_a} \quad \frac{\partial_\mu a}{f_a} \sum_{\substack{\psi=Q_L, Q_R, \\ L_L, L_R}} \bar{\psi} \gamma_\mu X_\psi \psi$$

where X_ψ is a general 3x3 matrix in flavour space

Georgi + Kaplan + Randall 1986

Choi + Kang + Kim, 1986

Salvio + Strumia + Shue, 2013

ALP-Linear effective Lagrangian at NLO

II
SM EFT

Complete basis (bosons+fermions):

$$\mathcal{L}_{\text{eff}} = \mathcal{L}_{\text{SM}} + \frac{1}{2}(\partial_\mu a)(\partial^\mu a) + \sum_i^{\text{total}} c_i \mathbf{O}_i^{d=5} - \frac{1}{2} m_a^2 a^2$$

$$\mathbf{O}_{\tilde{B}} = -B_{\mu\nu}\tilde{B}^{\mu\nu} \frac{a}{f_a}$$

$$\mathbf{O}_{\tilde{G}} = -G_{\mu\nu}^a \tilde{G}^{a\mu\nu} \frac{a}{f_a}$$

$$\mathbf{O}_{\tilde{W}} = -W_{\mu\nu}^a \tilde{W}^{a\mu\nu} \frac{a}{f_a}$$

$$\frac{\partial_\mu a}{f_a} \sum_{\substack{\psi=Q_L, Q_R, \\ L_L, L_R}} \bar{\psi} \gamma_\mu X_\psi \psi$$

where X_ψ is a general 3x3 matrix in flavour space

Georgi + Kaplan + Randall 1986
 Choi + Kang + Kim, 1986
 Salvio + Strumia + Shue, 2013

$$\left\{ \mathbf{m}_a, \frac{c_i}{f_a} \right\}$$

A diagram showing a ghost line (dashed red) entering from the left, labeled a . A wavy line (ghost-gauge boson) enters from the top-left, labeled G , and exits to the top-right, also labeled G . A ghost-gauge boson vertex is shown at the top-right corner. The ghost-gauge boson line has a self-energy insertion, represented by a loop of two wavy lines. The loop is labeled $a G_{\mu\nu} \tilde{G}^{\mu\nu}$.

A diagram showing a ghost line (dashed red) entering from the left, labeled a . A wavy line (ghost-gauge boson) enters from the top-left, labeled G , and exits to the top-right, also labeled G . A ghost-gauge boson vertex is shown at the top-right corner. The ghost-gauge boson line has a self-energy insertion, represented by a loop of two wavy lines. The loop is labeled $a F_{\mu\nu} \tilde{F}^{\mu\nu}, a F^{\mu\nu} \tilde{Z}_{\mu\nu}, a Z^{\mu\nu} \tilde{Z}_{\mu\nu}, a W^{\mu\nu} \tilde{W}_{\mu\nu}$.

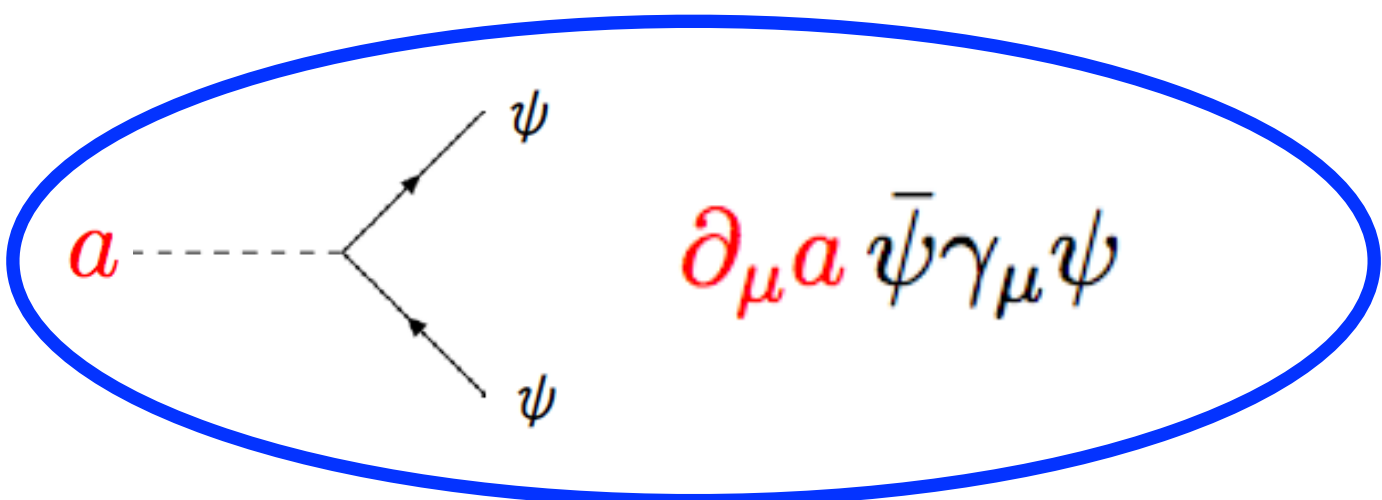
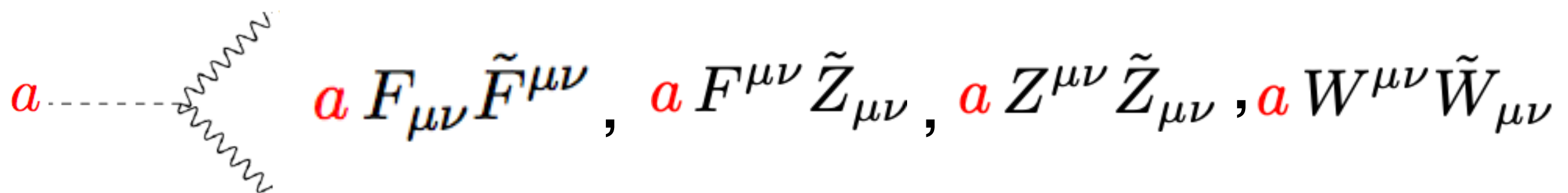
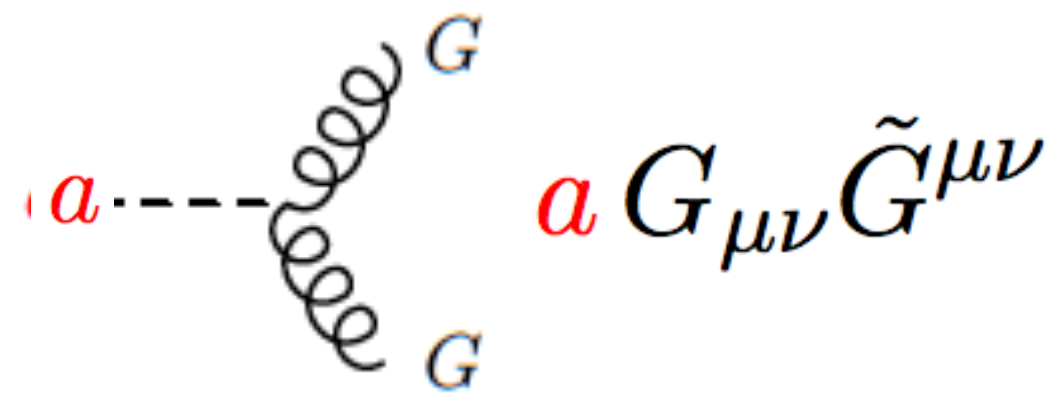
A diagram showing a ghost line (dashed red) entering from the left, labeled a . A wavy line (ghost-gauge boson) enters from the top-left, labeled ψ , and exits to the top-right, also labeled ψ . A ghost-gauge boson vertex is shown at the top-right corner. The ghost-gauge boson line has a self-energy insertion, represented by a loop of two wavy lines. The loop is labeled $\partial_\mu a \bar{\psi} \gamma_\mu \psi$.

Feynman diagram showing a loop interaction. A dashed red line labeled a enters from the left, interacts with a wavy blue line labeled G , and exits as a dashed red line labeled a . The loop is labeled $a G_{\mu\nu} \tilde{G}^{\mu\nu}$.

Feynman diagram showing a loop interaction. A dashed red line labeled a enters from the left, interacts with a wavy blue line labeled F , and exits as a dashed red line labeled a . The loop is labeled $a F_{\mu\nu} \tilde{F}^{\mu\nu}$, $a F^{\mu\nu} \tilde{Z}_{\mu\nu}$, $a Z^{\mu\nu} \tilde{Z}_{\mu\nu}$, or $a W^{\mu\nu} \tilde{W}_{\mu\nu}$.

Feynman diagram showing a loop interaction. A dashed red line labeled a enters from the left, splits into two solid black lines labeled ψ , which then interact and recombine into a single solid black line labeled ψ . The loop is labeled $\partial_\mu a \bar{\psi} \gamma_\mu \psi$.

neutron, proton, top,
electron, muon...



neutron, proton, top,
electron, muon...

neutrinos

Bonilla, B.G, Machado [arXiv:2309.15910]

ALPs (axion-like-particles)

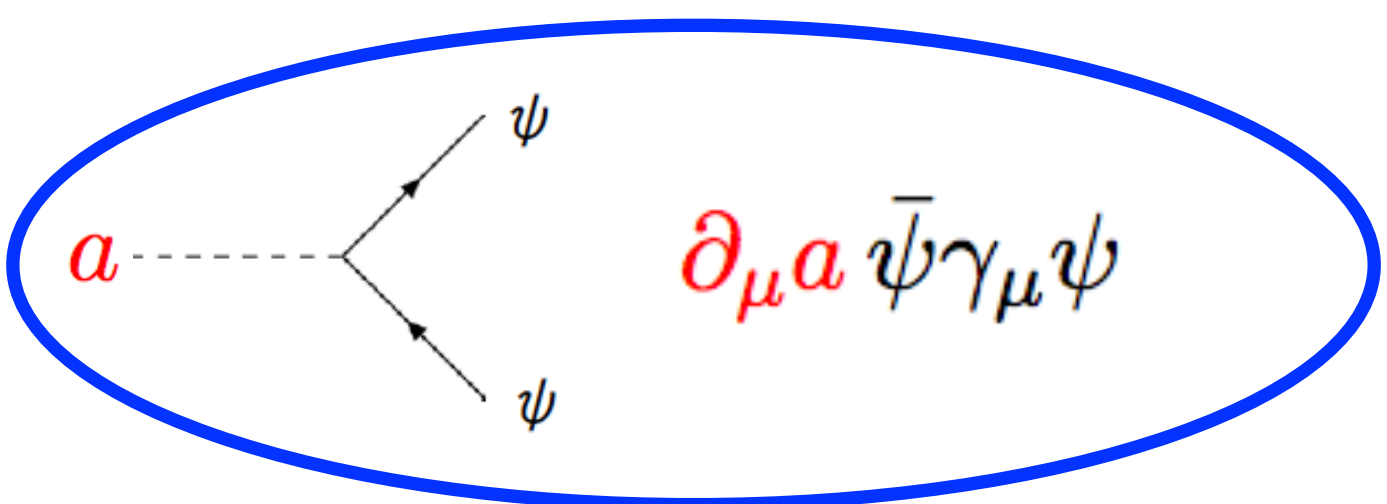
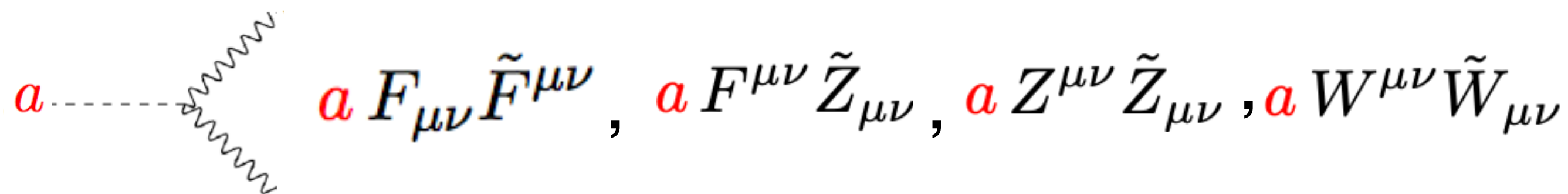
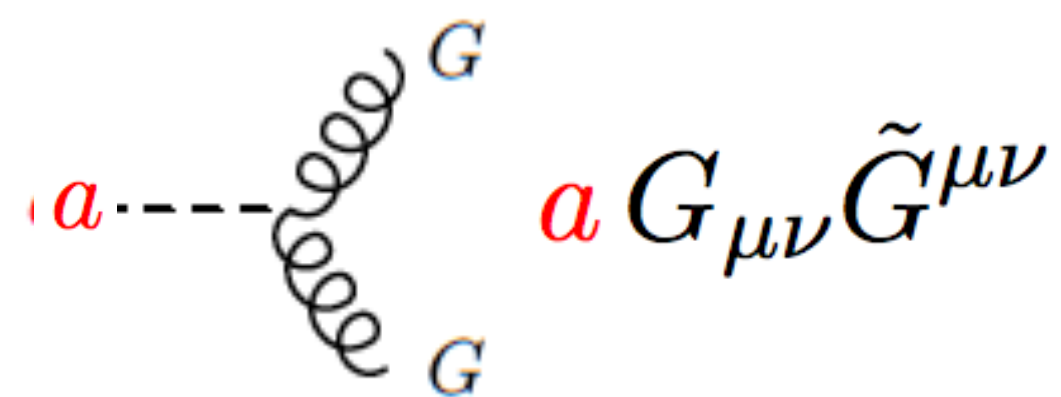
CP-violation

$$\mathcal{L} = \mathcal{L}_{SM} + \mathcal{L}_a$$

CP-violation

$m_a > 1 \text{ GeV}$

V. Enguita, M.B. Gavela, B. Grinstein, P. Quilez, arXiv: 2403.13133



The ALP EFT

$$\mathcal{L}_a \supset \frac{\partial_\mu a}{f_a} (\bar{Q}_L \gamma^\mu \textcolor{red}{C}_Q Q_L + \bar{u}_R \gamma^\mu \textcolor{orange}{C}_{u_R} u_R + \bar{d}_R \gamma^\mu \textcolor{brown}{C}_{d_R} d_R)$$

CP-violation in flavor-nondiagonal entries

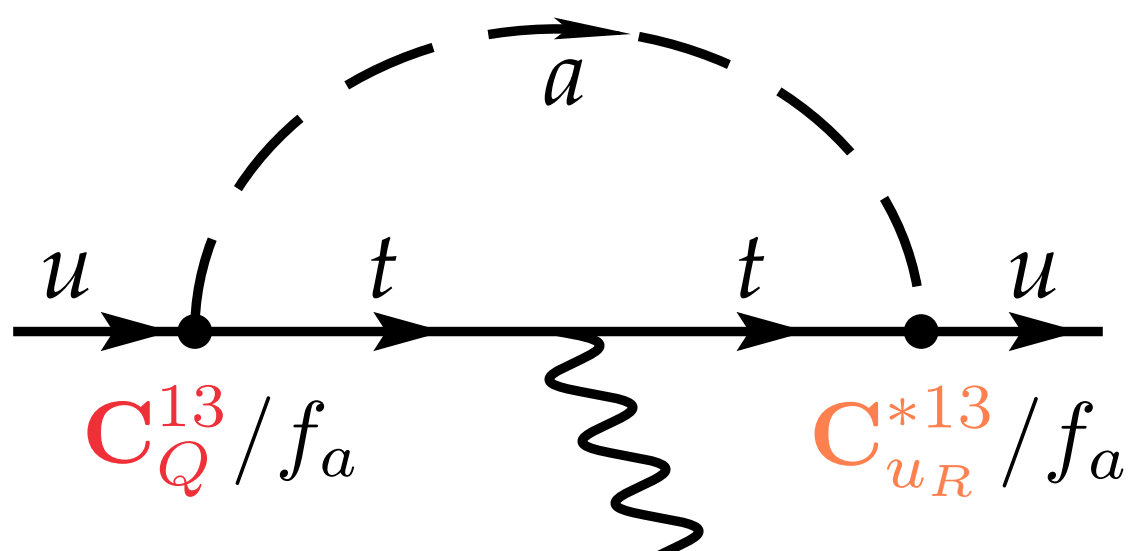
It will source CP-violation observables, e.g. EDMs... at one loop!

The ALP EFT

$$\mathcal{L}_a \supset \frac{\partial_\mu a}{f_a} (\bar{Q}_L \gamma^\mu \textcolor{red}{C}_Q Q_L + \bar{u}_R \gamma^\mu \textcolor{orange}{C}_{u_R} u_R + \bar{d}_R \gamma^\mu \textcolor{brown}{C}_{d_R} d_R)$$

CP-violation in flavor-nondiagonal entries

It will source CP-violation observables, e.g. EDMs... at one loop!

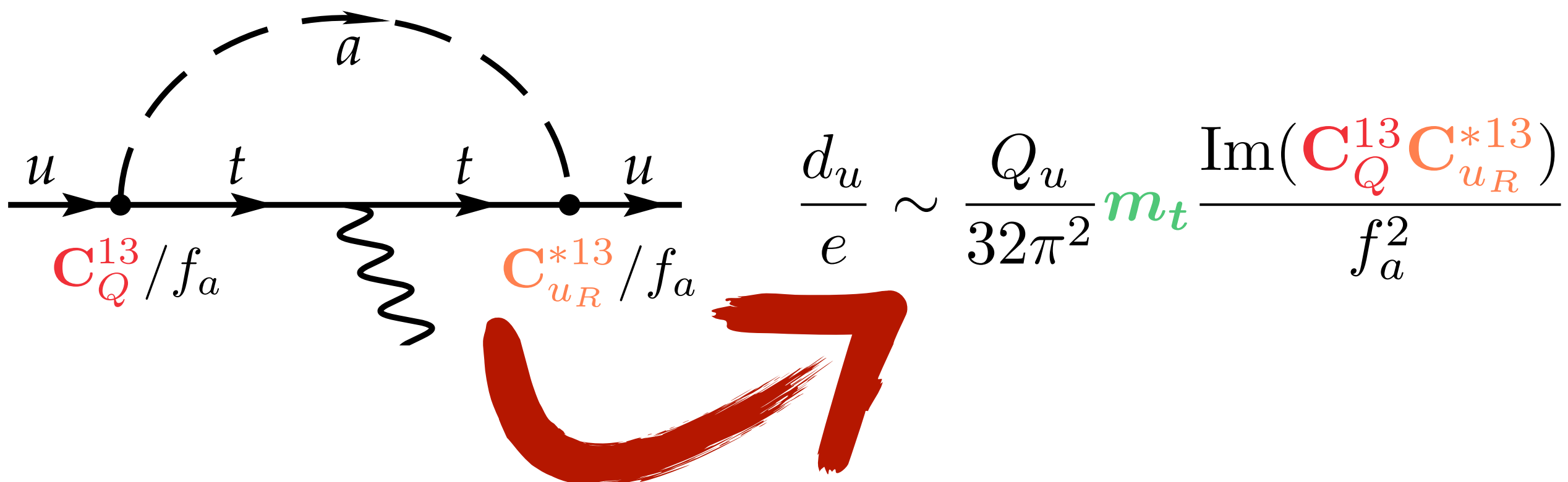


The ALP EFT

$$\mathcal{L}_a \supset \frac{\partial_\mu a}{f_a} (\bar{Q}_L \gamma^\mu \textcolor{red}{C}_Q Q_L + \bar{u}_R \gamma^\mu \textcolor{orange}{C}_{u_R} u_R + \bar{d}_R \gamma^\mu \textcolor{brown}{C}_{d_R} d_R)$$

CP-violation in flavor-nondiagonal entries

It will source CP-violation observables, e.g. EDMs... at one loop!



[Di Luzio et al., 2010.13760]

The ALP EFT

$$\mathcal{L}_a \supset \frac{1}{2} \partial_\mu a \partial^\mu a - \frac{1}{2} \textcolor{violet}{m}_a^2 a^2$$

$$+\left(\bar{u}_L\textcolor{teal}{M}_{\textcolor{teal}{u}} u_R + \bar{d}_L\textcolor{brown}{M}_{\textcolor{brown}{d}} d_R + \mathrm{h.c.}\right) + \theta \, \frac{\alpha_s}{8\pi} G_{\mu\nu} \tilde{G}^{\mu\nu}$$

$$+ \frac{\partial_\mu a}{f_a} \left(\bar{Q}_L \gamma^\mu \textcolor{red}{C}_{\textcolor{red}{Q}} Q_L + \bar{u}_R \gamma^\mu \textcolor{red}{C}_{u_{\textcolor{red}{R}}} u_R + \bar{d}_R \gamma^\mu \textcolor{brown}{C}_{d_{\textcolor{brown}{R}}} d_R \right)$$

The ALP EFT

$$\mathcal{L}_a \supset$$

$$\frac{1}{2} \partial_\mu a \partial^\mu a - \frac{1}{2} m_a^2 a^2$$

$$+ (\bar{u}_L \textcolor{green}{M}_u u_R + \bar{d}_L \textcolor{blue}{M}_d d_R + \text{h.c.}) + \theta \frac{\alpha_s}{8\pi} G_{\mu\nu} \tilde{G}^{\mu\nu}$$

$$+ \frac{\partial_\mu a}{f_a} (\bar{Q}_L \gamma^\mu \textcolor{red}{C}_Q Q_L + \bar{u}_R \gamma^\mu \textcolor{violet}{C}_u u_R + \bar{d}_R \gamma^\mu \textcolor{brown}{C}_d d_R)$$


Related by the $U_A(1)$ anomaly

physical $\bar{\theta} = \theta + \text{Arg det}(\textcolor{green}{M}_u \textcolor{blue}{M}_d)$

nEDM data imply $\bar{\theta} < \sim 10^{-10}$

The ALP EFT

$$\mathcal{L}_a \supset \frac{1}{2} \partial_\mu a \partial^\mu a - \frac{1}{2} \textcolor{violet}{m}_a^2 a^2$$

$$+\left(\bar{u}_L\textcolor{teal}{M}_{\textcolor{teal}{u}} u_R + \bar{d}_L\textcolor{brown}{M}_{\textcolor{brown}{d}} d_R + \mathrm{h.c.}\right) + \theta \, \frac{\alpha_s}{8\pi} G_{\mu\nu} \tilde{G}^{\mu\nu}$$

$$+ \frac{\partial_\mu a}{f_a} \left(\bar{Q}_L \gamma^\mu \textcolor{red}{C}_{\textcolor{red}{Q}} Q_L + \bar{u}_R \gamma^\mu \textcolor{red}{C}_{u_{\textcolor{red}{R}}} u_R + \bar{d}_R \gamma^\mu \textcolor{brown}{C}_{d_{\textcolor{brown}{R}}} d_R \right)$$

The ALP EFT

$$\mathcal{L}_a \supset \frac{1}{2} \partial_\mu a \partial^\mu a - \frac{1}{2} m_a^2 a^2$$

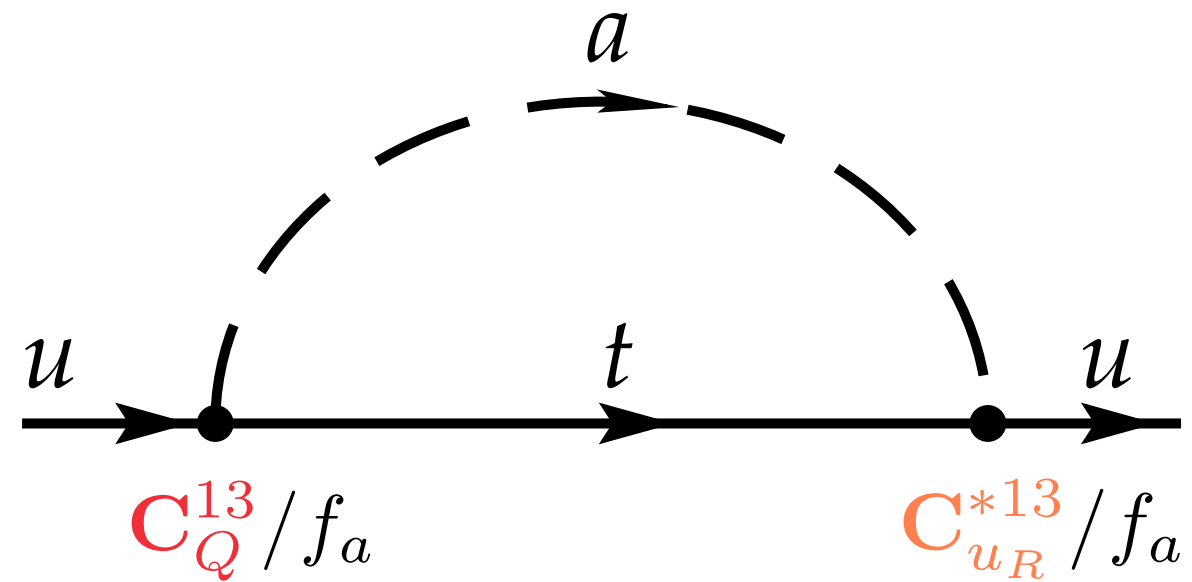
$$+ (\bar{u}_L M_u u_R + \bar{d}_L M_d d_R + \text{h.c.}) + \theta \frac{\alpha_s}{8\pi} G_{\mu\nu} \tilde{G}^{\mu\nu}$$

$$+ \frac{\partial_\mu a}{f_a} \underbrace{(\bar{Q}_L \gamma^\mu C_Q Q_L + \bar{u}_R \gamma^\mu C_{u_R} u_R + \bar{d}_R \gamma^\mu C_{d_R} d_R)}$$

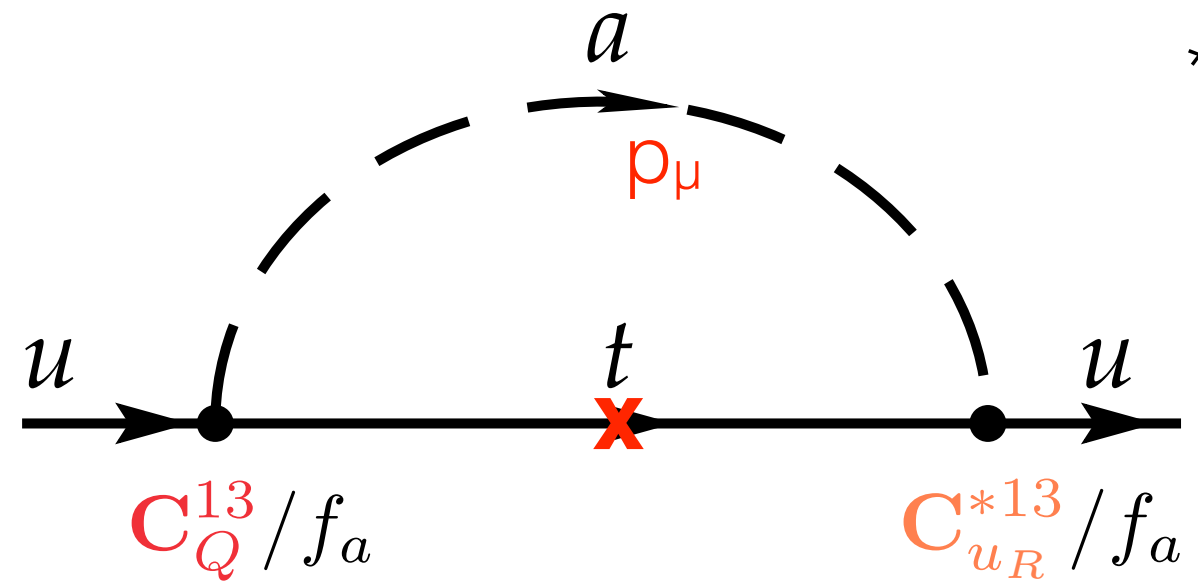
**ALPs contribute at one-loop to the quark mass terms,
i.e. ALPs contribute to $\bar{\theta}$**

physical $\bar{\theta} = \theta + \text{Arg det}(M_u M_d)$

ALP contribution to $\dot{\theta}$

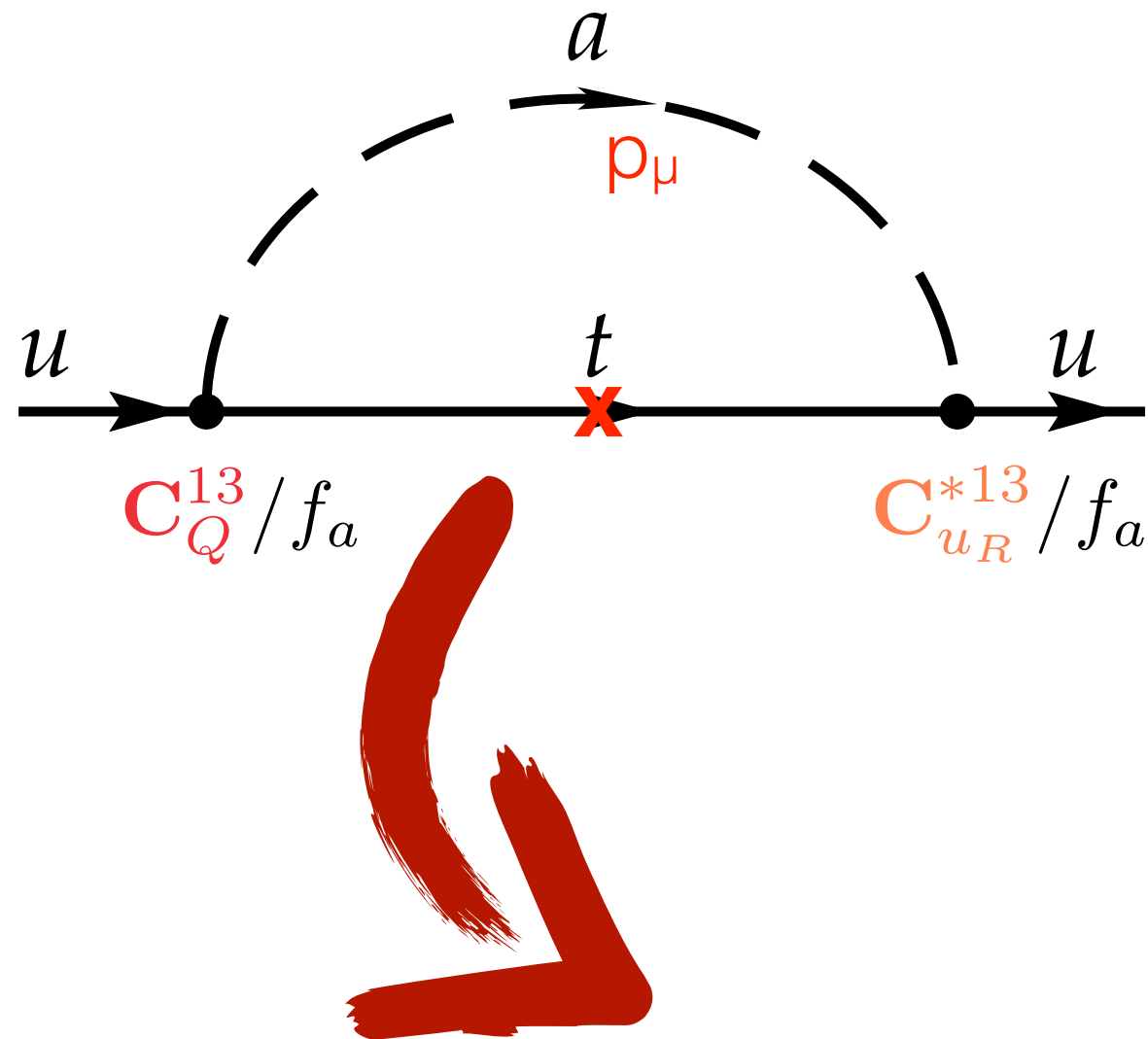


ALP contribution to $\bar{\theta}$



- * Factor m_t for chirality flip
- * Factor p_μ^2 from vertices

ALP contribution to $\bar{\theta}$



- * Factor m_t for chirality flip
- * Factor p_μ^2 from vertices

$$\Delta\bar{\theta}_{\text{ALP}} \simeq \frac{m_t \max(m_a^2, m_t^2)}{16\pi^2 f_a^2 m_u} \text{Im}(C_Q^{13} C_{u_R}^{*13})$$

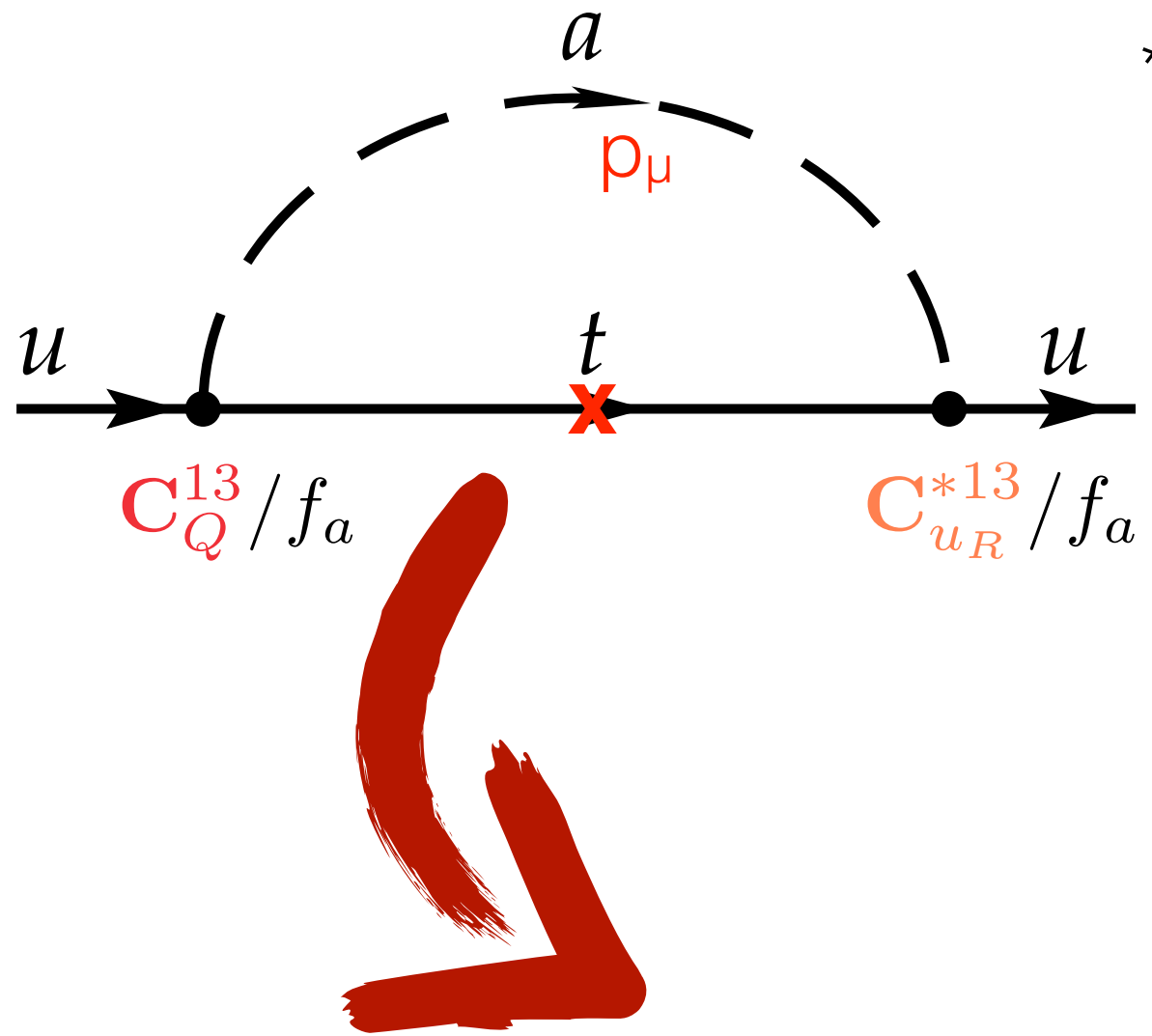
Neglecting threshold corrections

For an ALP:

$$\bar{\theta}(\mu_{\text{IR}}) \simeq \bar{\theta}_0 +$$

$$\sum_{u_i=\{u,c,t\}} \frac{m_{u_k} (m_a^2 + \hat{m}_{u_k}^2)}{16\pi^2 f_a^2 m_{u_i}} \text{Im} \left(C_Q^{ik} C_{u_R}^{*ik} \right) \log \frac{f_a^2}{\max(m_a^2, m_{u_k}^2)}$$
$$+ \sum_{d_i=\{d,s,b\}} \frac{m_{d_k} (m_a^2 + \hat{m}_{d_k}^2)}{16\pi^2 f_a^2 m_{d_i}} \text{Im} \left(C_Q^{ik} C_{d_R}^{*ik} \right) \log \frac{f_a^2}{\max(m_a^2, m_{d_k}^2)}$$

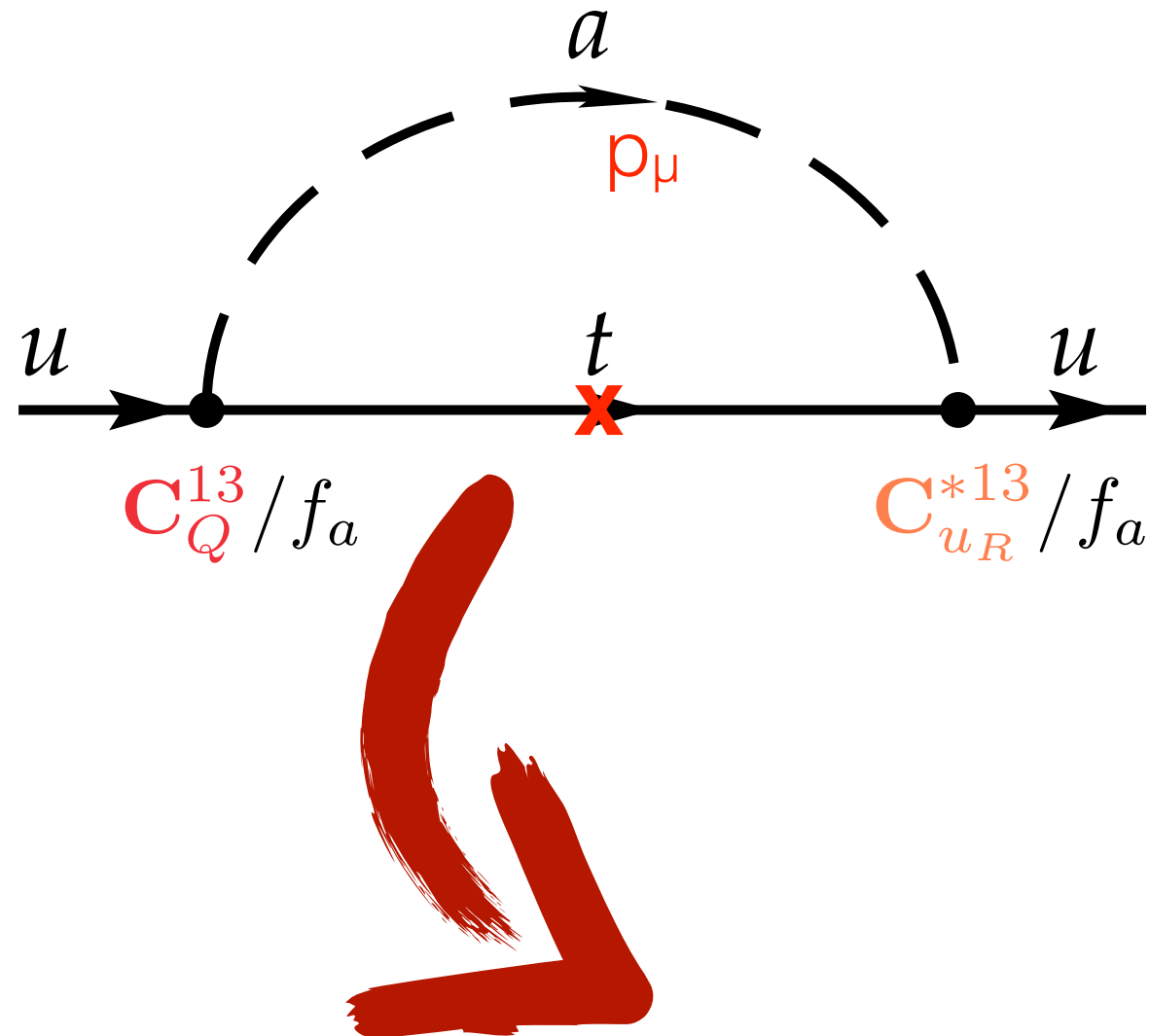
ALP contribution to $\bar{\theta}$



- * Factor m_t for chirality flip
- * Factor p_μ^2 from vertices

$$\Delta\bar{\theta}_{\text{ALP}} \simeq \frac{m_t \max(m_a^2, m_t^2)}{16\pi^2 f_a^2 m_u} \text{Im}(C_Q^{13} C_{u_R}^{*13})$$

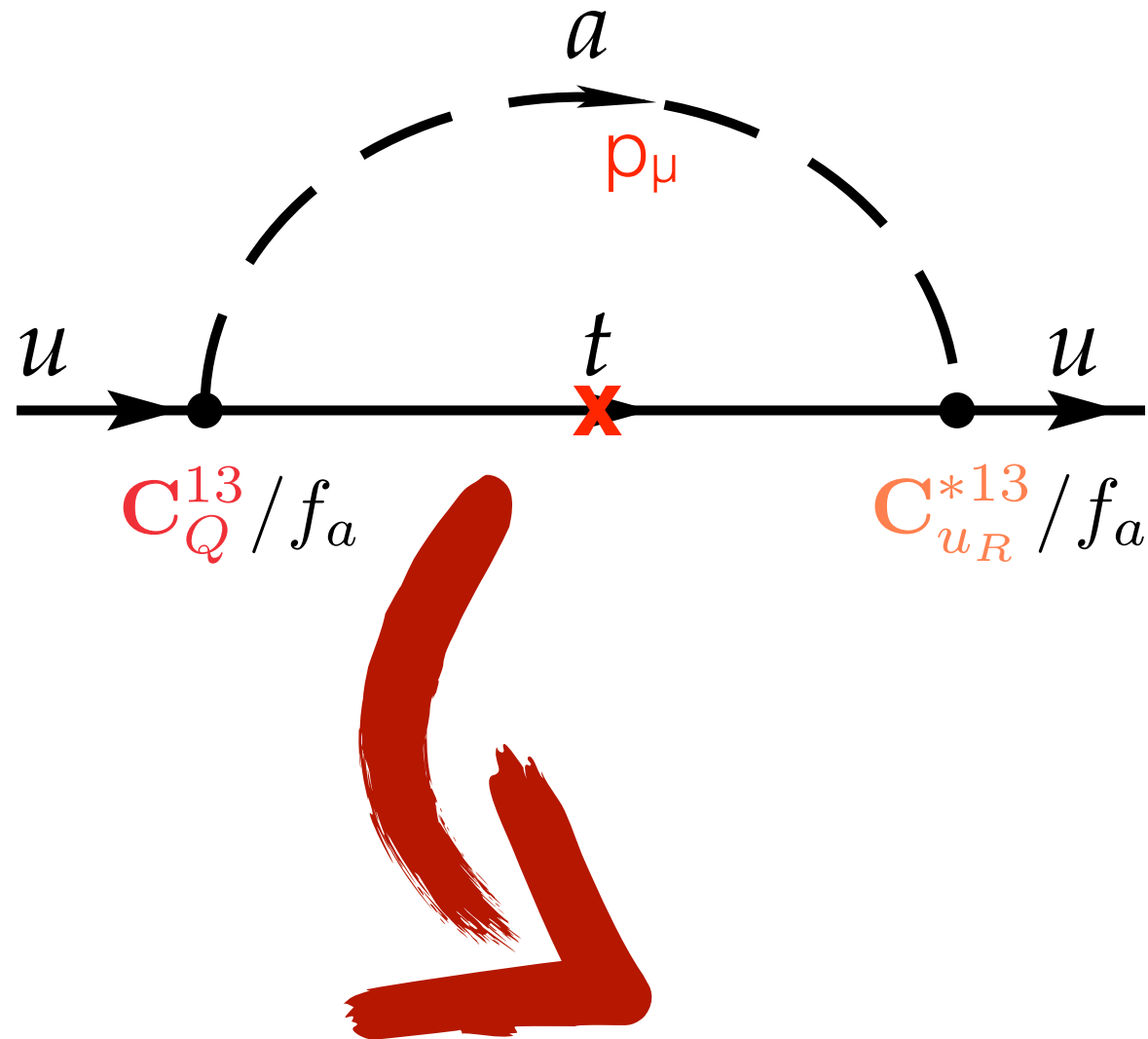
ALP contribution to $\bar{\theta}$



- * Factor m_t for chirality flip
- * Factor p_μ^2 from vertices

$$m_a < m_t: \quad \Delta \bar{\theta}_{\text{ALP}} \sim \frac{1}{16\pi^2} \left(\frac{m_t^3}{m_u} \right) \frac{\text{Im}(C_Q^{13} C_{u_R}^{*13})}{f_a^2}$$

ALP contribution to $\bar{\theta}$

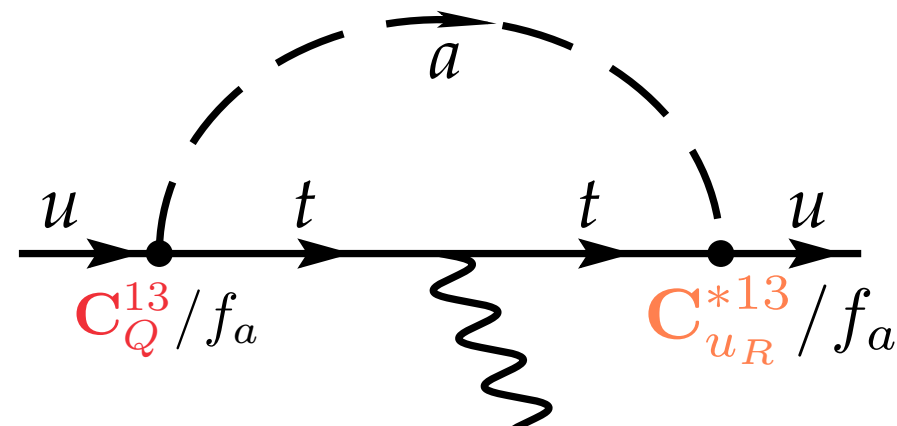


- * Factor m_t for chirality flip
- * Factor p_μ^2 from vertices

$m_a < m_t$:

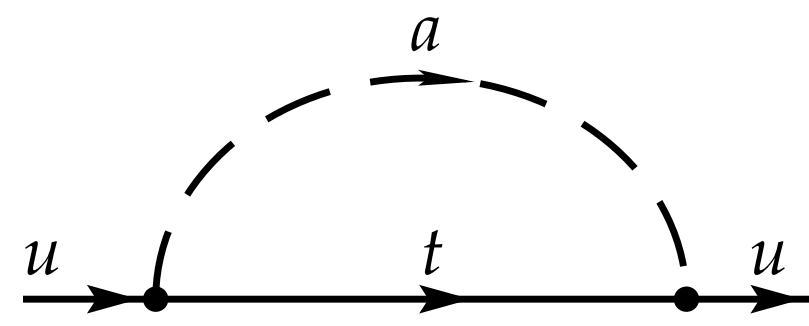
$$\left. \frac{d_n}{e} \right|_{\bar{\theta}} \sim \frac{\mathcal{O}(10^{-3} \text{ GeV}^{-1})}{16\pi^2} \times \left(\frac{m_t^3}{m_u} \right) \frac{\text{Im}(C_Q^{13} C_{u_R}^{*13})}{f_a^2}$$

nEDM limits on ALP-fermion couplings



$$\frac{d_n}{e} \Big|_{d_q, \tilde{d}_q} \sim \mathcal{O}(1) \times \frac{Q_u}{32\pi^2} \textcolor{green}{m_t} \frac{\text{Im}(\mathbf{C}_Q^{13} \mathbf{C}_{u_R}^{*13})}{f_a^2}$$

OLD



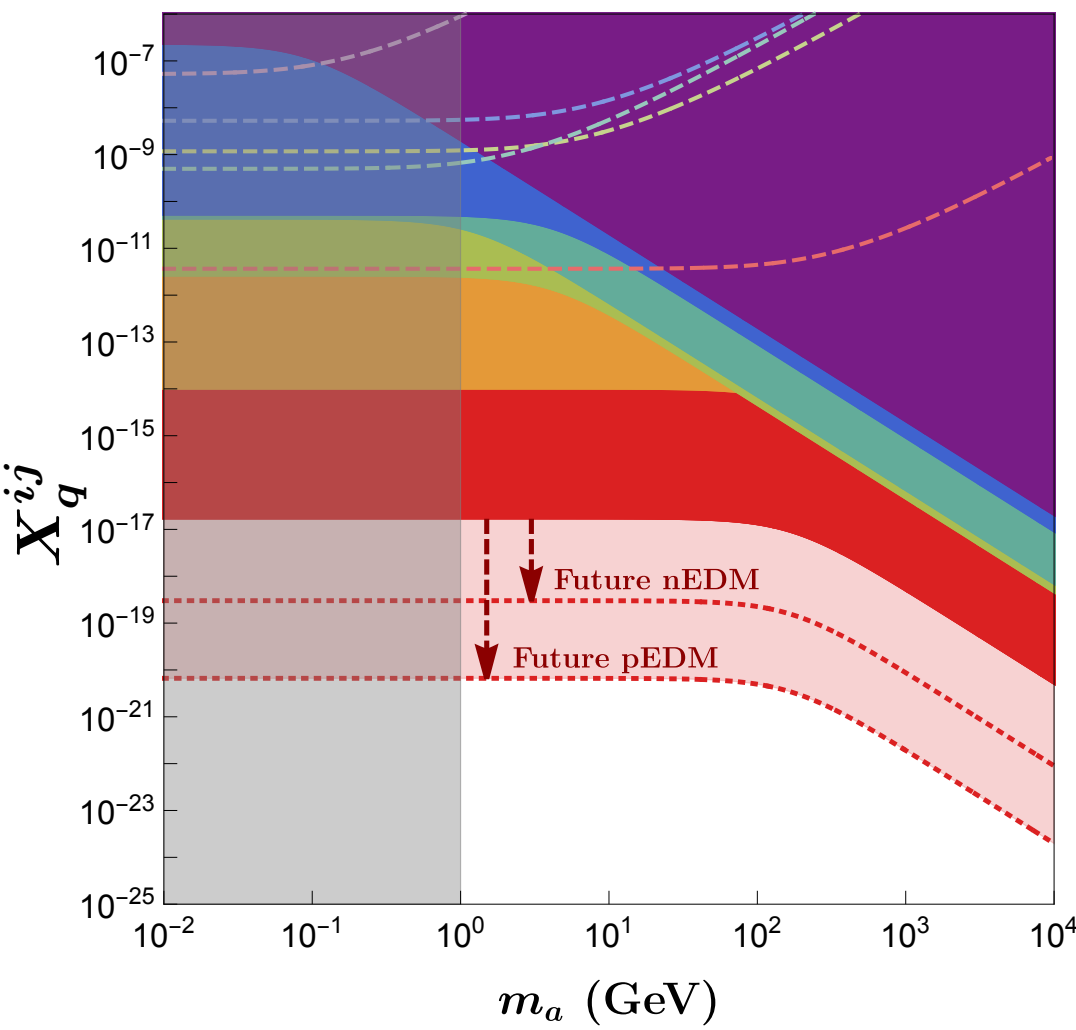
$$\frac{d_n}{e} \Big|_{\bar{\theta}} \sim \frac{\mathcal{O}(10^{-3} \text{ GeV}^{-1})}{16\pi^2} \times \left(\frac{\textcolor{green}{m_t}^3}{m_u} \right) \frac{\text{Im}(\mathbf{C}_Q^{13} \mathbf{C}_{u_R}^{*13})}{f_a^2}$$

Bounds many orders of magnitude stronger

NEW

nEDM limits on ALP-fermion couplings

$$X_q^{ij} = \text{Im}(\mathbf{C}_L^{ij} \mathbf{C}_{qR}^{*ij}) / f_a^2 \text{ (GeV}^{-2}\text{)}$$



Dotted lines:

$$\left. \frac{d_n}{e} \right|_{d_q, \tilde{d}_q} \sim \mathcal{O}(1) \times \frac{Q_u}{32\pi^2} \mathbf{m_t} \frac{\text{Im}(\mathbf{C}_Q^{13} \mathbf{C}_{uR}^{*13})}{f_a^2}$$

OLD

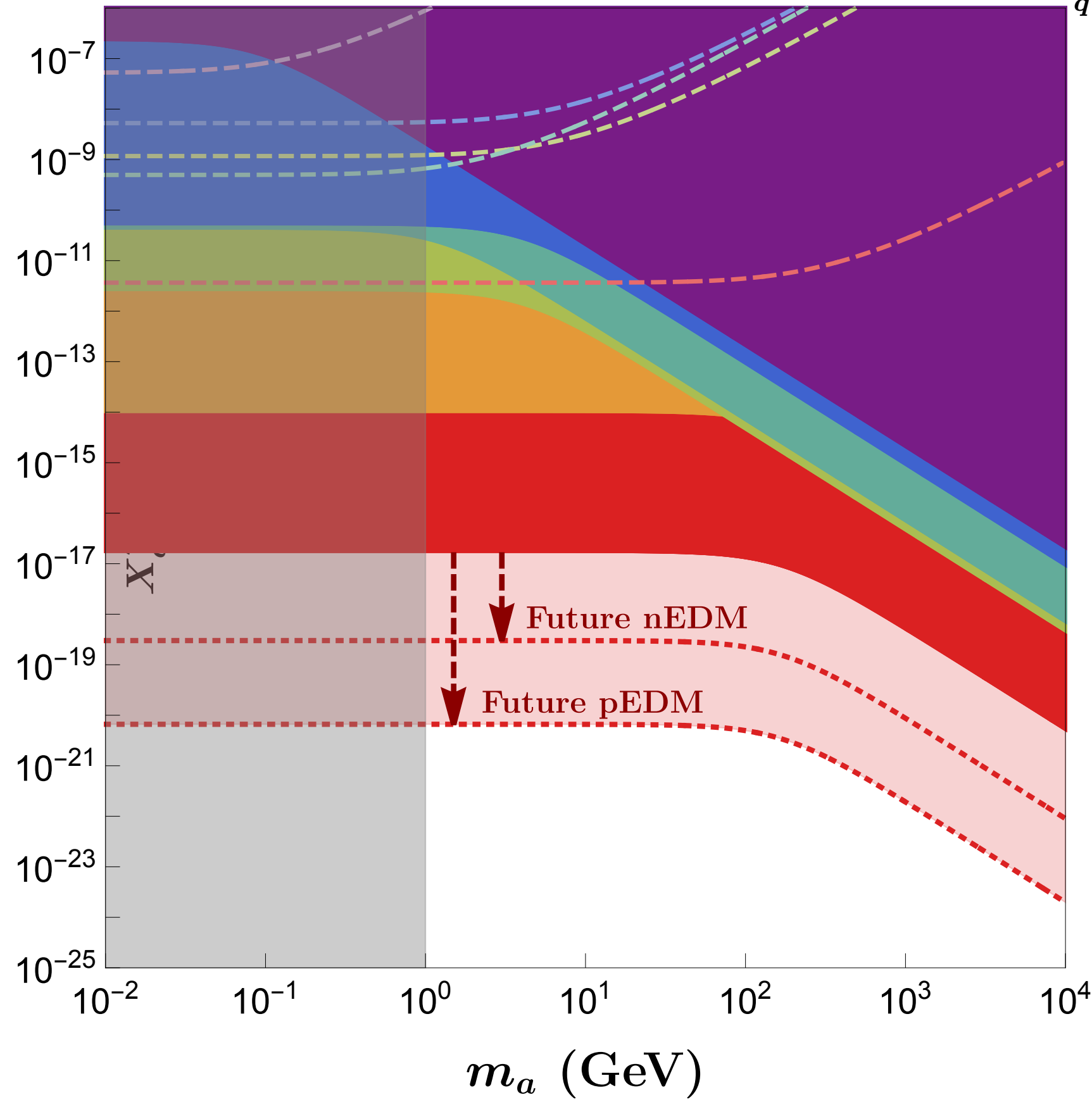
Solid regions:

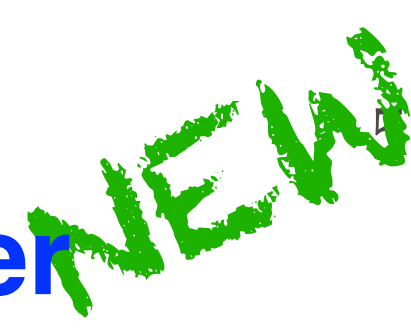
$$\left. \frac{d_n}{e} \right|_{\bar{\theta}} \sim \frac{\mathcal{O}(10^{-3} \text{ GeV}^{-1})}{16\pi^2} \times \left(\frac{\mathbf{m_t}^3}{\mathbf{m_u}} \right) \frac{\text{Im}(\mathbf{C}_Q^{13} \mathbf{C}_{uR}^{*13})}{f_a^2}$$

Bounds many orders of magnitude stronger

NEW

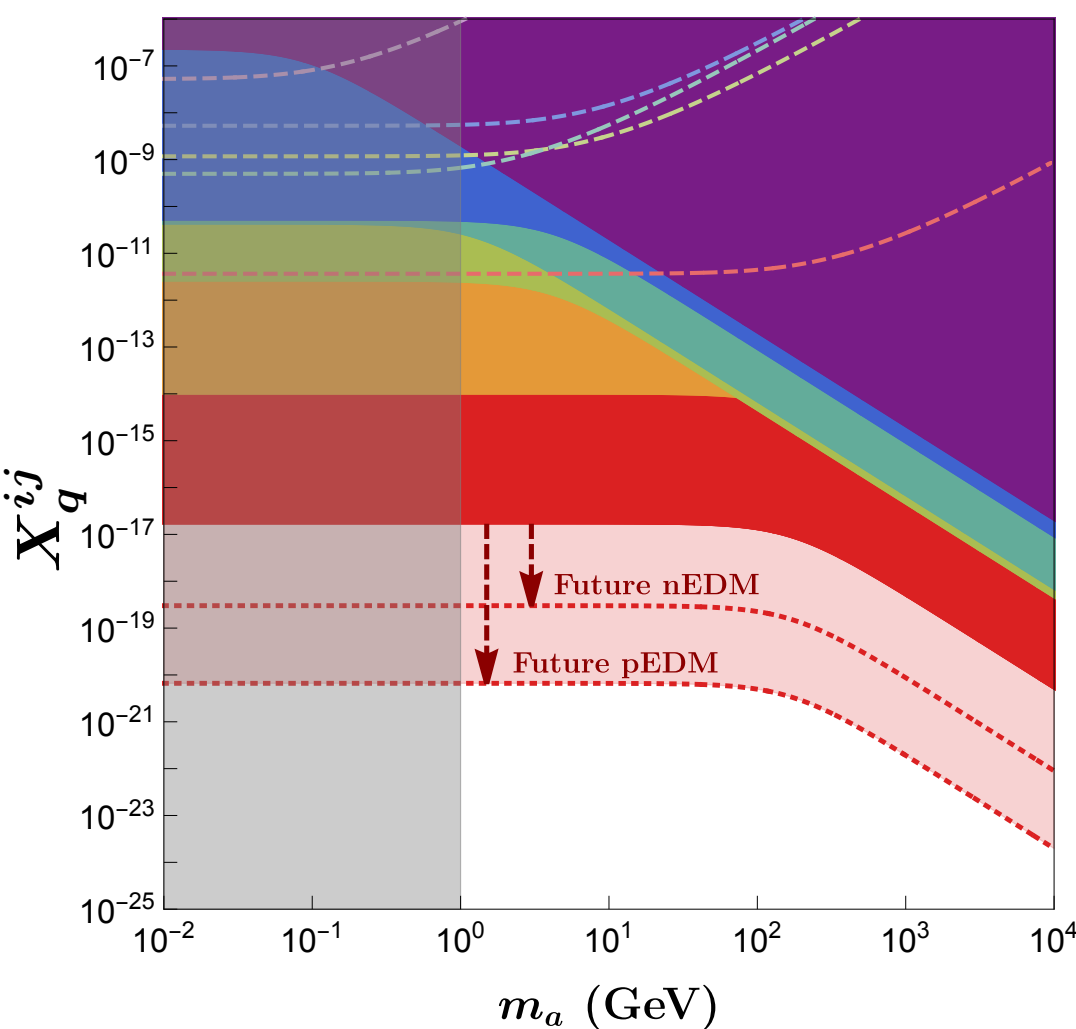
$$X_q^{ij} = \text{Im}(\mathcal{C}_L^{ij} \mathcal{C}_{qR}^{*ij})/f_a^2 \text{ (GeV}^{-2}\text{)}$$



Bounds many orders of magnitude stronger 

nEDM limits on ALP-fermion couplings

$$X_q^{ij} = \text{Im}(\mathbf{C}_L^{ij} \mathbf{C}_{qR}^{*ij}) / f_a^2 \text{ (GeV}^{-2}\text{)}$$

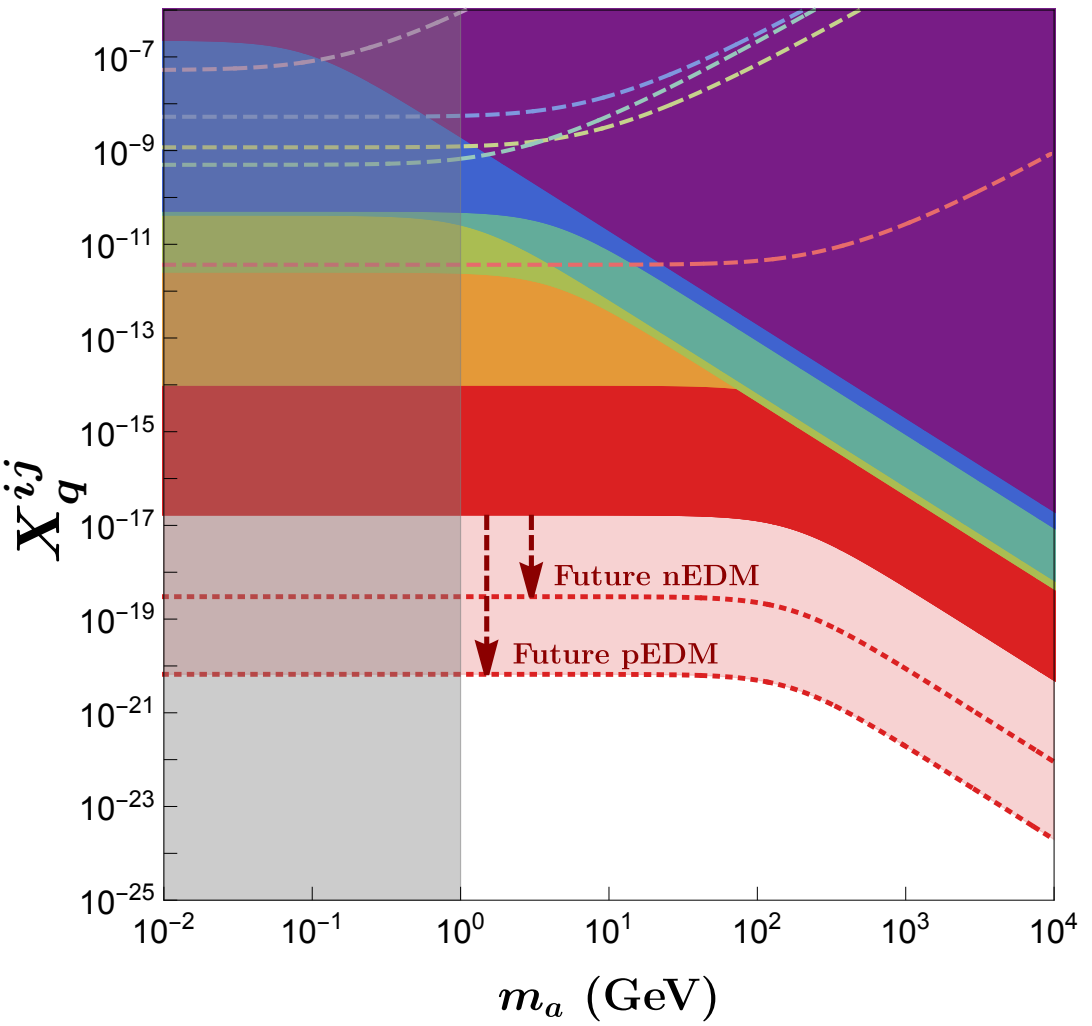


Combination	$\bar{\theta}$ -bounds (GeV $^{-2}$)	qEDM & cEDM (GeV $^{-2}$)
X_u^{13} Im[$\mathbf{C}_Q^{13} \mathbf{C}_{uR}^{*13}$] / f_a^2	1.8×10^{-17}	3.7×10^{-12}
X_u^{23} Im[$\mathbf{C}_Q^{23} \mathbf{C}_{uR}^{*23}$] / f_a^2	1.1×10^{-14}	—
X_d^{13} Im[$\mathbf{C}_Q^{13} \mathbf{C}_{dR}^{*13}$] / f_a^2	1.1×10^{-12}	1.9×10^{-9}
X_u^{12} Im[$\mathbf{C}_Q^{12} \mathbf{C}_{uR}^{*12}$] / f_a^2	2.7×10^{-12}	2.3×10^{-9}
X_d^{23} Im[$\mathbf{C}_Q^{23} \mathbf{C}_{dR}^{*23}$] / f_a^2	2.3×10^{-11}	8.7×10^{-9}
X_d^{12} Im[$\mathbf{C}_Q^{12} \mathbf{C}_{dR}^{*12}$] / f_a^2	8.6×10^{-11}	1.2×10^{-5}

$m_a = 5 \text{ GeV}$

nEDM limits on ALP-fermion couplings

$$X_q^{ij} = \text{Im}(\mathbf{C}_L^{ij} \mathbf{C}_{qR}^{*ij}) / f_a^2 \text{ (GeV}^{-2}\text{)}$$



As a function of m_a

X_u^1	$\text{Im}[\mathbf{C}_Q^{13} \mathbf{C}_{uR}^{*13}] / f_a^2 < \left(\frac{m_t^2}{m_a^2 + m_t^2} \right) 2 \times 10^{-17}$
X_u^2	$\text{Im}[\mathbf{C}_Q^{23} \mathbf{C}_{uR}^{*23}] / f_a^2 < \left(\frac{m_t^2}{m_a^2 + m_t^2} \right) 1 \times 10^{-14}$
X_d^1	$\text{Im}[\mathbf{C}_Q^{13} \mathbf{C}_{dR}^{*13}] / f_a^2 < \left(\frac{m_b^2}{m_a^2 + m_b^2} \right) 3 \times 10^{-12}$
X_u^1	$\text{Im}[\mathbf{C}_Q^{12} \mathbf{C}_{uR}^{*12}] / f_a^2 < \left(\frac{m_c^2}{m_a^2 + m_c^2} \right) 5 \times 10^{-11}$
X_d^2	$\text{Im}[\mathbf{C}_Q^{23} \mathbf{C}_{dR}^{*23}] / f_a^2 < \left(\frac{m_b^2}{m_a^2 + m_b^2} \right) 6 \times 10^{-11}$
X_d^1	$\text{Im}[\mathbf{C}_Q^{12} \mathbf{C}_{dR}^{*12}] / f_a^2 < \left(\frac{m_s^2}{m_a^2 + m_s^2} \right) 3 \times 10^{-7}$

LP case. Bounds on $\text{Im}[\mathbf{C}_Q^{ij} \mathbf{C}_{qR}^{*ij}] / f_a^2$ in GeV^{-2} obtained from the $\bar{\theta}$ correction.

We checked our results in the ``chirality-flip'' basis

$$\mathcal{L}_a \supset \frac{\partial_\mu a}{f_a} (\bar{Q}_L \gamma^\mu \mathbf{C}_Q Q_L + \bar{u}_R \gamma^\mu \mathbf{C}_{u_R} u_R + \bar{d}_R \gamma^\mu \mathbf{C}_{d_R} d_R)$$

Chiral rot.:
$$\begin{cases} u_L \rightarrow e^{i \frac{a}{f_a} \mathbf{C}_Q} u_L, & d_L \rightarrow e^{i \frac{a}{f_a} \mathbf{C}_Q} d_L, \\ u_R \rightarrow e^{i \frac{a}{f_a} \mathbf{C}_{u_R}} u_R, & d_R \rightarrow e^{i \frac{a}{f_a} \mathbf{C}_{d_R}} d_R \end{cases}$$

We checked our results in the ``chirality-flip'' basis

$$\mathcal{L}_a \supset \frac{\partial_\mu a}{f_a} (\bar{Q}_L \gamma^\mu \mathbf{C}_Q Q_L + \bar{u}_R \gamma^\mu \mathbf{C}_{u_R} u_R + \bar{d}_R \gamma^\mu \mathbf{C}_{d_R} d_R)$$

Chiral rot.: $\begin{cases} u_L \rightarrow e^{i\frac{a}{f_a}} \mathbf{C}_Q u_L, & d_L \rightarrow e^{i\frac{a}{f_a}} \mathbf{C}_Q d_L, \\ u_R \rightarrow e^{i\frac{a}{f_a}} \mathbf{C}_{u_R} u_R, & d_R \rightarrow e^{i\frac{a}{f_a}} \mathbf{C}_{d_R} d_R \end{cases}$

$\rightarrow \mathcal{L} \supset \bar{u}_L v \left[i \frac{a}{f_a} \mathbf{K}_u + \frac{a^2}{f_a^2} \mathbf{F}_u \right] u_R$

$+ \bar{d}_L v \left[i \frac{a}{f_a} \mathbf{K}_d + \frac{a^2}{f_a^2} \mathbf{F}_d \right] d_R + \text{h.c.} + \dots$

We checked our results in the ``chirality-flip'' basis

$$\mathcal{L}_a \supset \frac{\partial_\mu a}{f_a} (\bar{Q}_L \gamma^\mu \mathbf{C}_Q Q_L + \bar{u}_R \gamma^\mu \mathbf{C}_{u_R} u_R + \bar{d}_R \gamma^\mu \mathbf{C}_{d_R} d_R)$$

Chiral rot.: $\begin{cases} u_L \rightarrow e^{i\frac{a}{f_a}} \mathbf{C}_Q u_L, & d_L \rightarrow e^{i\frac{a}{f_a}} \mathbf{C}_Q d_L, \\ u_R \rightarrow e^{i\frac{a}{f_a}} \mathbf{C}_{u_R} u_R, & d_R \rightarrow e^{i\frac{a}{f_a}} \mathbf{C}_{d_R} d_R \end{cases}$

$\rightarrow \mathcal{L} \supset \bar{u}_L v \left[i \frac{a}{f_a} \mathbf{K}_u + \frac{a^2}{f_a^2} \mathbf{F}_u \right] u_R$

$+ \bar{d}_L v \left[i \frac{a}{f_a} \mathbf{K}_d + \frac{a^2}{f_a^2} \mathbf{F}_d \right] d_R + \text{h.c.} + \dots$

where

$$v \mathbf{K}_q \equiv \mathbf{C}_Q \mathbf{M}_q - \mathbf{M}_q \mathbf{C}_{q_R},$$

$$2v \mathbf{F}_q \equiv 2\mathbf{C}_Q \mathbf{M}_q \mathbf{C}_{q_R} - \mathbf{C}_Q^2 \mathbf{M}_q - \mathbf{M}_q \mathbf{C}_{q_R}^2$$

We checked our results in the ``chirality-flip'' basis

$$\mathcal{L}_a \supset \frac{\partial_\mu a}{f_a} (\bar{Q}_L \gamma^\mu \mathbf{C}_Q Q_L + \bar{u}_R \gamma^\mu \mathbf{C}_{u_R} u_R + \bar{d}_R \gamma^\mu \mathbf{C}_{d_R} d_R)$$

Chiral rot.: $\begin{cases} u_L \rightarrow e^{i \frac{a}{f_a} \mathbf{C}_Q} u_L, \\ u_R \rightarrow e^{i \frac{a}{f_a} \mathbf{C}_{u_R}} u_R, \end{cases}$

$$d_L \rightarrow e^{i \frac{a}{f_a} \mathbf{C}_Q} d_L,$$

$$d_R \rightarrow e^{i \frac{a}{f_a} \mathbf{C}_{d_R}} d_R$$

\rightarrow

$$\mathcal{L} \supset \bar{u}_L v \left[i \frac{a}{f_a} \mathbf{K}_u + \frac{a^2}{f_a^2} \mathbf{F}_u \right] u_R$$

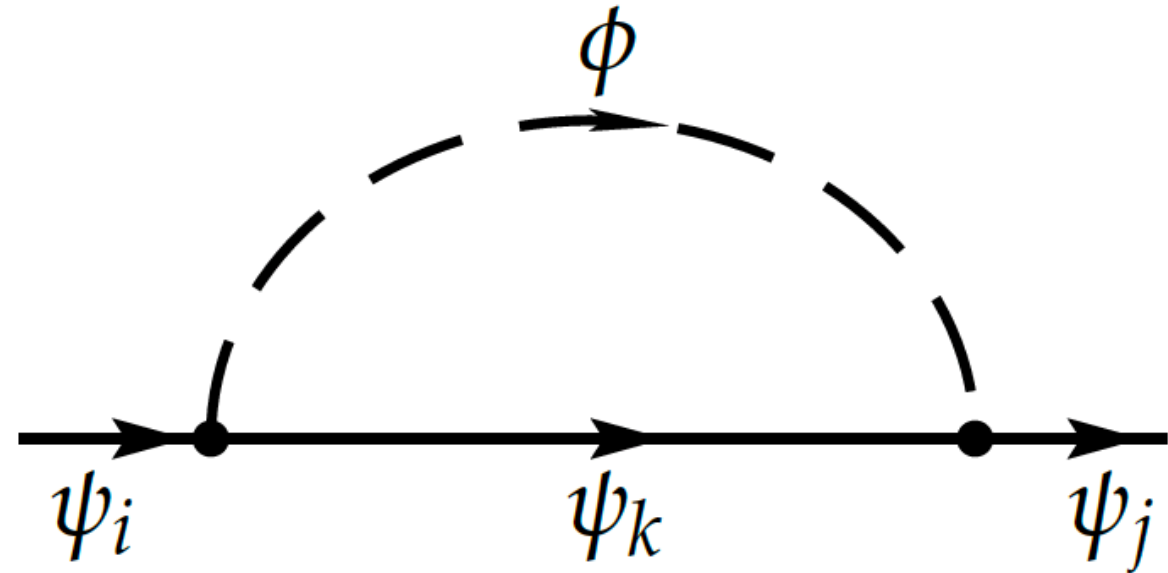
$$+ \bar{d}_L v \left[i \frac{a}{f_a} \mathbf{K}_d + \frac{a^2}{f_a^2} \mathbf{F}_d \right] d_R + \text{h.c.} + \dots$$

where

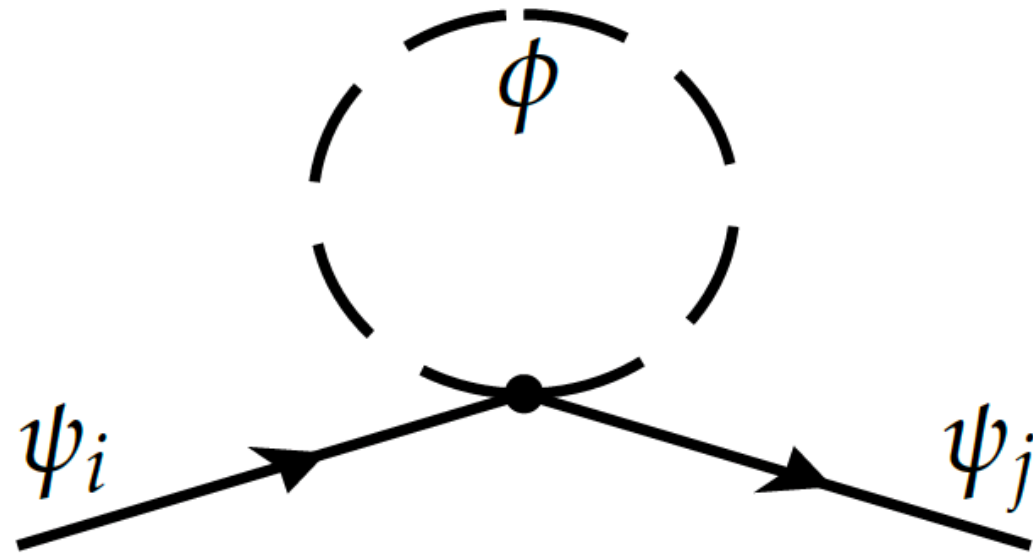
$$v \mathbf{K}_q \equiv \mathbf{C}_Q \mathbf{M}_q - \mathbf{M}_q \mathbf{C}_{q_R},$$

$$2v \mathbf{F}_q \equiv 2\mathbf{C}_Q \mathbf{M}_q \mathbf{C}_{q_R} - \mathbf{C}_Q^2 \mathbf{M}_q - \mathbf{M}_q \mathbf{C}_{q_R}^2$$

There are two diagrams in the “chirality-flip” basis:



+



General Scalar

$$\mathcal{L} = \mathcal{L}_{SM} + \mathcal{L}_S$$

CP-violation

Generic scalar

$$\begin{aligned}\mathcal{L} \supset & \bar{u}_L v \left[i \mathbf{K}_u \frac{S}{\Lambda} + \mathbf{F}_u \frac{S^2}{\Lambda^2} \right] u_R \\ & + \bar{d}_L v \left[i \frac{S}{\Lambda} \mathbf{K}_d + \frac{S^2}{\Lambda^2} \mathbf{F}_d \right] d_R + \text{h.c.}\end{aligned}$$

K and **F** arbitrary: more parameters than for ALPs

e.g. CP-violation in flavour-diagonal couplings

Generic scalar

$$\mathcal{L} \supset \bar{u}_L v \left[i \mathbf{K}_u \frac{S}{\Lambda} + \mathbf{F}_u \frac{S^2}{\Lambda^2} \right] u_R + \bar{d}_L v \left[i \frac{S}{\Lambda} \mathbf{K}_d + \frac{S^2}{\Lambda^2} \mathbf{F}_d \right] d_R + \text{h.c.}$$

K and **F** arbitrary: more parameters than for ALPs

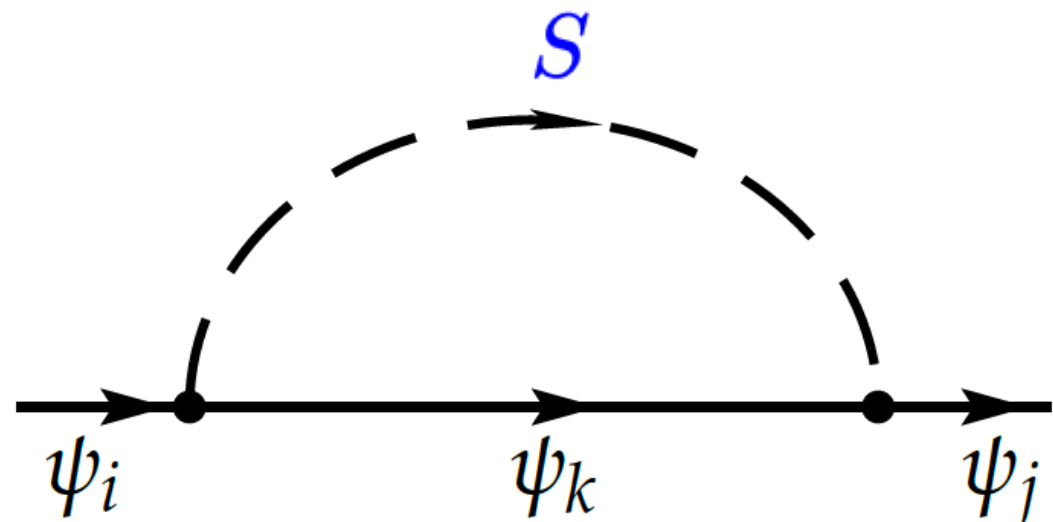
e.g. CP-violation in flavour-diagonal couplings

Generic scalar

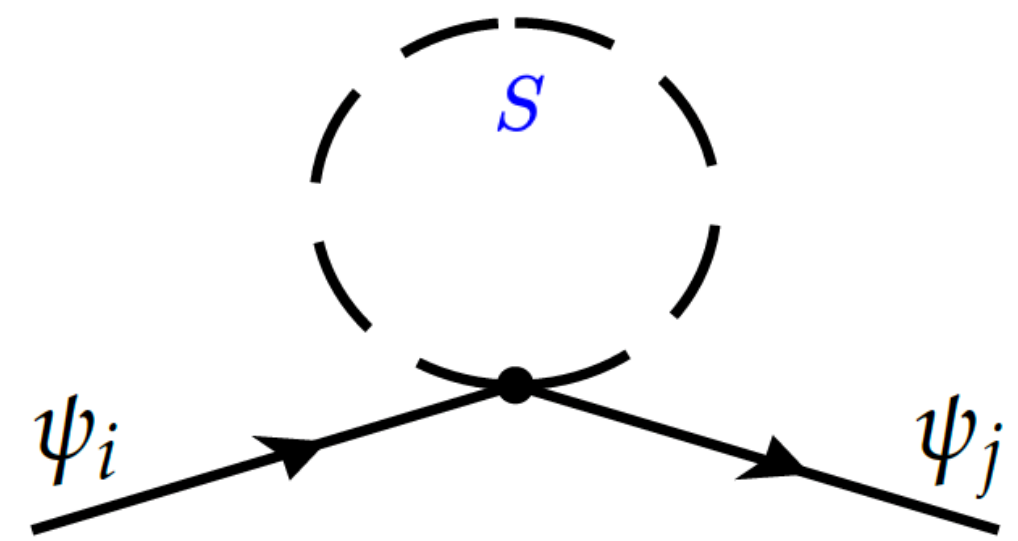
$$\begin{aligned}\mathcal{L} \supset & \bar{u}_L v \left[i \mathbf{K}_u \frac{S}{\Lambda} + \mathbf{F}_u \frac{S^2}{\Lambda^2} \right] u_R \\ & + \bar{d}_L v \left[i \frac{S}{\Lambda} \mathbf{K}_d + \frac{S^2}{\Lambda^2} \mathbf{F}_d \right] d_R + \text{h.c.}\end{aligned}$$

K and **F** arbitrary: more parameters than for ALPs

Contribution to $\bar{\theta}$ from:



+



bounds also improved by orders of magnitude

Generic scalar

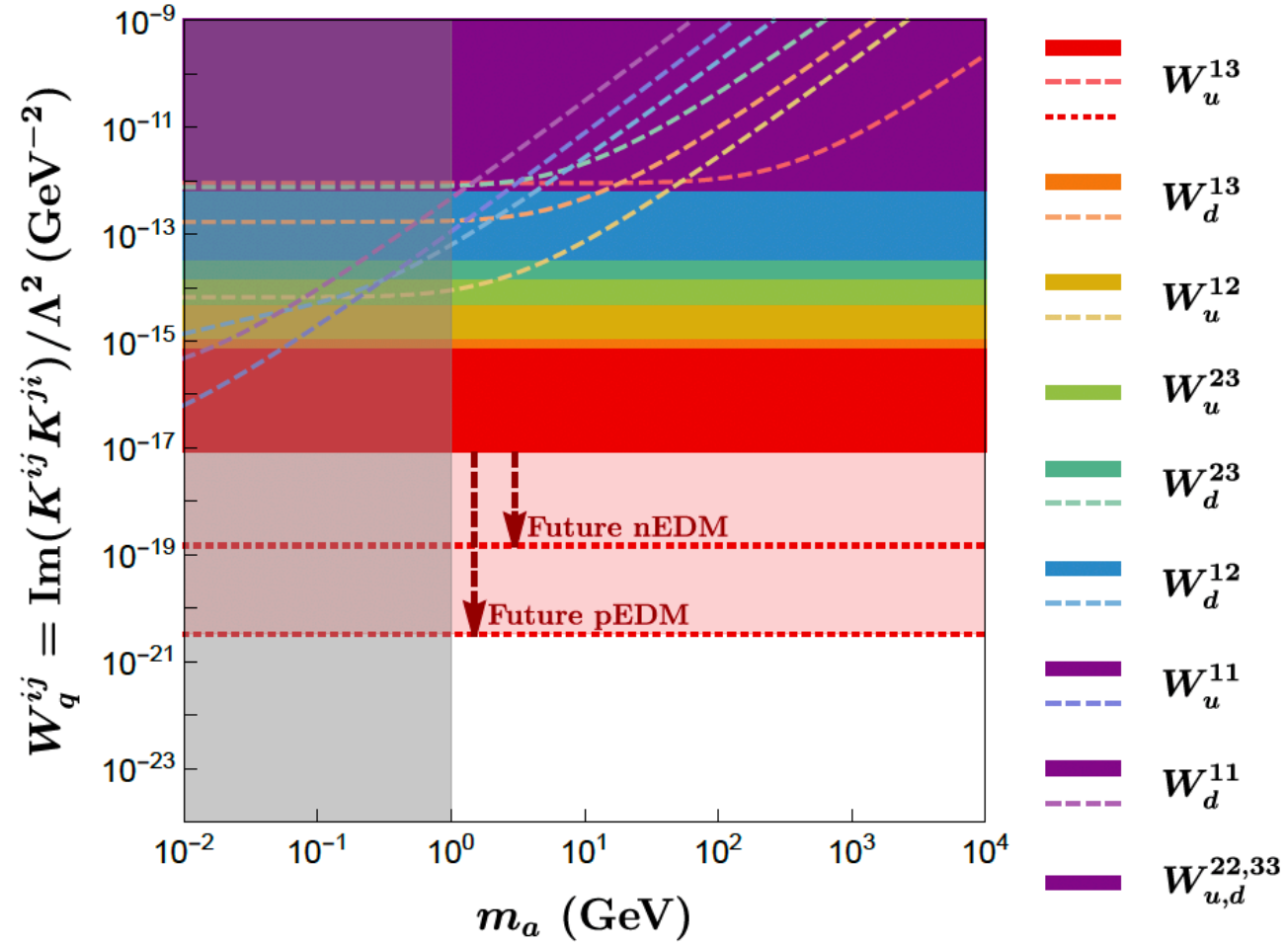


FIG. 5: *General scalar.* Upper bounds on $W_q^{ij} \equiv \text{Im}(K_q^{ij} K_q^{ji})/\Lambda^2$ stemming from the contributions of $\bar{\theta}$ (solid regions) and from the sum of qEDMs and cEDMs (dashed lines) to the nEDM. The red dotted line shows the projected bounds on W_u^{13} from future nEDM and pEDM experiments [44, 45]. The grey shaded area is as described in Fig. 2.

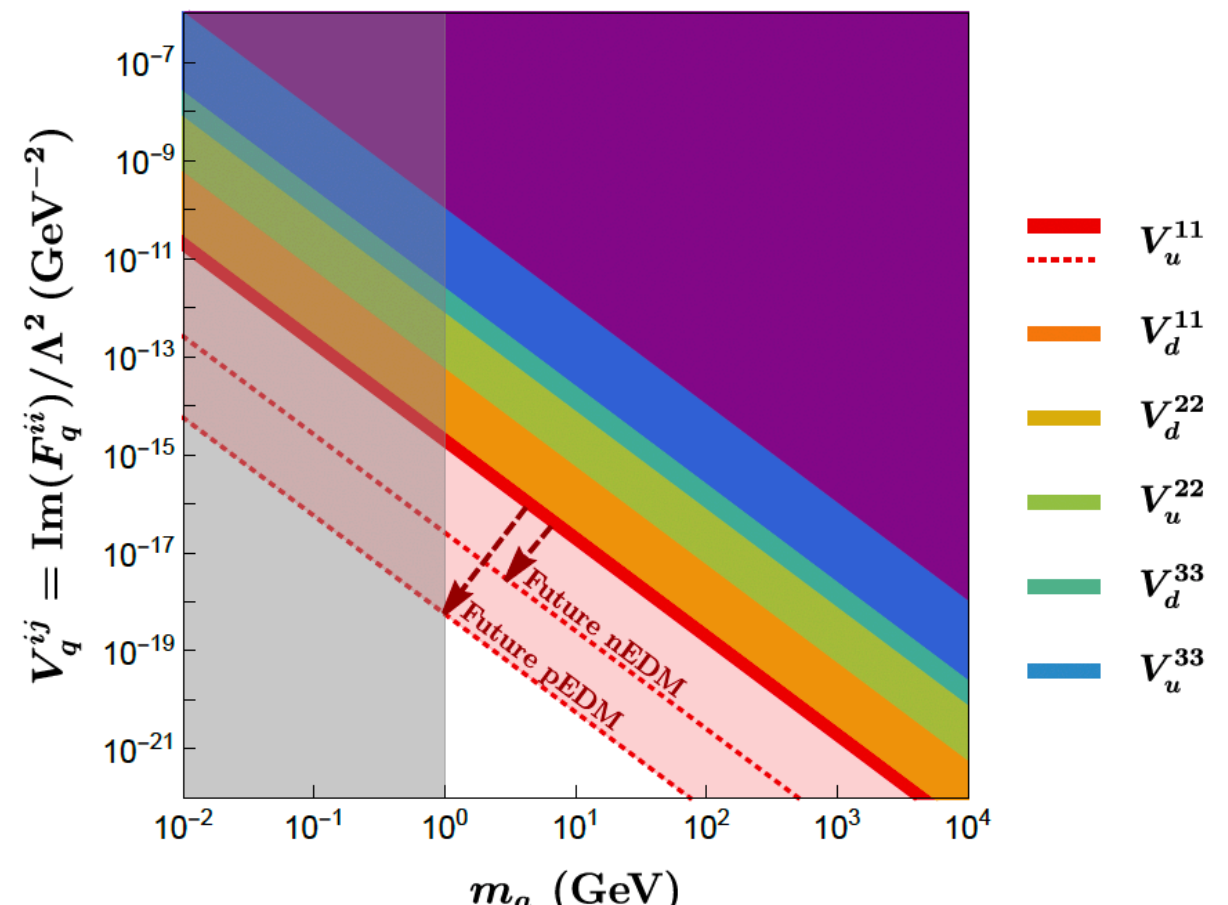


FIG. 6: *General scalar.* Upper bounds on $V_q^{ij} \equiv \text{Im}(F_q^{ij})/\Lambda^2$ stemming from the contributions of $\bar{\theta}$ (solid regions) to the nEDM. The red dotted line shows the projected bounds on V_u^{11} from future nEDM and pEDM experiments [44, 45]. The grey shaded area is as described in previous plots.

*What happens if there is a
PQ symmetry (in addition) ?*

either for ALPs or generic scalars

With a PQ symmetry present:

$\bar{\theta}$ disappears but a residual $\bar{\theta}$ induced remains:

Vafa-Witten theorem does not apply with extra explicit CP sources and

$$\bar{\theta}_{\text{ind}} = \frac{m_0^2}{2} \sum_{q=u,d,s} \frac{\tilde{d}_q}{m_q}$$

we have updated the bounds in this case

Without a PQ mechanism:

$$\begin{aligned} d_n &= 0.6(3) \times 10^{-16} \bar{\theta} [e \cdot \text{cm}] \\ &\quad - 0.204(11)d_u + 0.784(28)d_d - 0.0028(17)d_s \\ &\quad - 0.32(15) e \tilde{d}_u + 0.32(15) e \tilde{d}_d - 0.014(7)e\tilde{d}_s. \end{aligned}$$

In the presence of a PQ mechanism:

$$\begin{aligned} d_n^{\text{PQ}} &= -0.204(11)d_u + 0.784(28)d_d - 0.0028(17)d_s \\ &\quad - 0.31(15)e\tilde{d}_u + 0.62(31)e\tilde{d}_d \end{aligned}$$

Without a PQ mechanism:

$$d_n = 0.6(3) \times 10^{-16} \bar{\theta} [e \cdot \text{cm}]$$
$$- 0.204(11)d_u + 0.784(28)d_d - 0.0028(17)d_s$$
$$- 0.32(15) e \tilde{d}_u + 0.32(15) e \tilde{d}_d - 0.014(7)e \tilde{d}_s.$$

↑
chromo-electric EDMs

In the presence of a PQ mechanism:

$$d_n^{\text{PQ}} = -0.204(11)d_u + 0.784(28)d_d - 0.0028(17)d_s$$
$$- 0.31(15)e \tilde{d}_u + 0.62(31)e \tilde{d}_d$$

↑
chromo-electric EDMs

Without a PQ mechanism:

$$d_n = 0.6(3) \times 10^{-16} \bar{\theta} [e \cdot \text{cm}]$$
$$- 0.204(11)d_u + 0.784(28)d_d - 0.0028(17)d_s$$
$$- 0.32(15)e\tilde{d}_u + 0.32(15)e\tilde{d}_d - 0.014(7)e\tilde{d}_s.$$

*Lattice
+ sum rules*

sum rules

Hisano et al.

In the presence of a PQ mechanism:

$$d_n^{\text{PQ}} = -0.204(11)d_u + 0.784(28)d_d - 0.0028(17)d_s$$
$$- 0.31(15)e\tilde{d}_u + 0.62(31)e\tilde{d}_d$$

ALPs

Combination	With PQ (GeV ⁻²)	Without PQ (GeV ⁻²)
$\text{Im}(\mathbf{C}_L^{13}\mathbf{C}_{u_R}^{13})/f_a^2$	3.7×10^{-12}	3.7×10^{-12}
$\text{Im}(\mathbf{C}_L^{13}\mathbf{C}_{d_R}^{13})/f_a^2$	1.9×10^{-9}	3.2×10^{-9}
$\text{Im}(\mathbf{C}_L^{12}\mathbf{C}_{u_R}^{12})/f_a^2$	2.3×10^{-9}	2.4×10^{-9}
$\text{Im}(\mathbf{C}_L^{23}\mathbf{C}_{d_R}^{23})/f_a^2$	8.7×10^{-9}	1.2×10^{-7}
$\text{Im}(\mathbf{C}_L^{12}\mathbf{C}_{d_R}^{12})/f_a^2$	1.2×10^{-5}	1.9×10^{-6}

TABLE IV: *ALP case.* Comparison of bounds w/o the presence of a PQ symmetry. All bounds are in units of GeV⁻², and $m_a = 5$ GeV has been assumed for illustration.

Generic scalar

Combination	With PQ (GeV ⁻²)	Without PQ (GeV ⁻²)
$\text{Im}(\mathbf{K}_u^{13} \mathbf{K}_u^{31})/\Lambda^2$	9.0×10^{-7}	9.2×10^{-7}
$\text{Im}(\mathbf{K}_d^{13} \mathbf{K}_d^{31})/\Lambda^2$	2.8×10^{-7}	4.6×10^{-8}
$\text{Im}(\mathbf{K}_u^{12} \mathbf{K}_u^{21})/\Lambda^2$	3.1×10^{-8}	3.1×10^{-8}
$\text{Im}(\mathbf{K}_d^{23} \mathbf{K}_d^{23})/\Lambda^2$	1.3×10^{-6}	1.8×10^{-5}
$\text{Im}(\mathbf{K}_d^{12} \mathbf{K}_d^{21})/\Lambda^2$	8.2×10^{-7}	1.4×10^{-7}
$\text{Im}(\mathbf{K}_d^{22} \mathbf{K}_d^{22})/\Lambda^2$	3.8×10^{-6}	5.3×10^{-5}
$\text{Im}(\mathbf{K}_u^{11} \mathbf{K}_u^{11})/\Lambda^2$	2.2×10^{-6}	2.2×10^{-6}
$\text{Im}(\mathbf{K}_d^{11} \mathbf{K}_d^{11})/\Lambda^2$	8.7×10^{-6}	1.4×10^{-6}

V. Enguita, M.B. Gavela, B. Grinstein, P. Quilez, arXiv: 2403.13133

TABLE V: *General scalar.* Comparison of bounds w/o the presence of a PQ symmetry. All bounds are in units of GeV⁻², and for $m_\phi = 5$ GeV.

CONCLUSIONS

- * ALP couplings to fermions induce one-loop corrections to $\bar{\theta} \rightarrow$ to the nEDM
- * We have improved the bounds on CP-odd ALP-fermion couplings by ~ 4 orders of magnitude
- * The same kind of improvement applies to generic singlet scalars
- * Novel bounds on ALP-neutrino couplings

Backup

$$\boldsymbol{M}_{u,d}^{\text{1 loop}} = \boldsymbol{M}_{u,d} + \Delta \boldsymbol{M}_{u,d}$$

$$\begin{aligned}\Delta\bar{\theta}_{\text{ALP}}(\mu) &= \sum_{q=u,d} \arg [\det (\boldsymbol{M}_q (1 + \boldsymbol{M}_q^{-1} \Delta \boldsymbol{M}_q))] \\ &\simeq \sum_{q=u,d} \text{Im Tr} (\boldsymbol{M}_q^{-1} \Delta \boldsymbol{M}_q)\end{aligned}$$

$$\Delta\bar{\theta}_{\text{ALP}}(\mu) \simeq \frac{1}{f_a^2} \sum_{q=u,d} \text{Im Tr} [\boldsymbol{M}_q^{-1} \mathbf{C}_Q \mathbf{L} \mathbf{C}_{q_R}]$$

$$\boldsymbol{L} \equiv \text{diag}(L_1,L_2,L_3)$$

$$\begin{aligned}L_k &= \frac{m_{q_k}}{16\pi^2} \left[\left(m_a^2 + m_{q_k}^2 \right) \left(1 + \log \frac{\mu^2}{m_a^2} \right) \right. \\ &\quad \left. + \frac{m_{q_k}^4}{m_{q_k}^2 - m_a^2} \log \frac{m_a^2}{m_{q_k}^2} \right]\end{aligned}$$

$$\begin{aligned} \frac{d\bar{\theta}}{d\mu} &= \sum_{q=u,d} \text{Im} \frac{d}{d\mu} \ln \det \mathcal{M}_q = \sum_{q=u,d} \text{Im} \frac{d}{d\mu} \text{Tr} \ln \mathcal{M}_q \\ &= \sum_{q=u,d} \text{Im} \text{Tr} \left(\mathcal{M}_q^{-1} \frac{d}{d\mu} \mathcal{M}_q \right) \end{aligned}$$

$$\mu \frac{d\bar{\theta}}{d\mu} \simeq \frac{1}{f_a^2} \sum_{q=u,d} \text{Im} \text{Tr} \left[M_q^{-1} \mathbf{C}_Q \mathcal{L} \mathbf{C}_{q_R} \right]$$

$$\mathcal{L}_k=\frac{m_{q_k}}{8\pi^2}\left(m_a^2+m_{q_k}^2\right)$$

$$\boldsymbol{M}_{u,d}^{\text{1 loop}} = \boldsymbol{M}_{u,d} + \Delta \boldsymbol{M}_{u,d}$$

$$\Delta\bar{\theta}_{\text{ALP}}(\mu) = \sum_{q=u,d} \arg \left[\det \left(\boldsymbol{M}_q \left(1 + \boldsymbol{M}_q^{-1} \Delta \boldsymbol{M}_q \right) \right) \right]$$

$$\simeq \sum_{q=u,d} \text{Im Tr} \left(\boldsymbol{M}_q^{-1} \Delta \boldsymbol{M}_q \right)$$

$$\Delta\bar{\theta}_{\text{ALP}}(\mu) \simeq \frac{1}{f_a^2} \sum_{q=u,d} \text{Im Tr} \left[\boldsymbol{M}_q^{-1} \mathbf{C}_Q \mathbf{L} \mathbf{C}_{q_R} \right]$$

$$\boldsymbol{L}\equiv\text{diag}(L_1,L_2,L_3)$$

Neglecting threshold corrections

For an ALP:

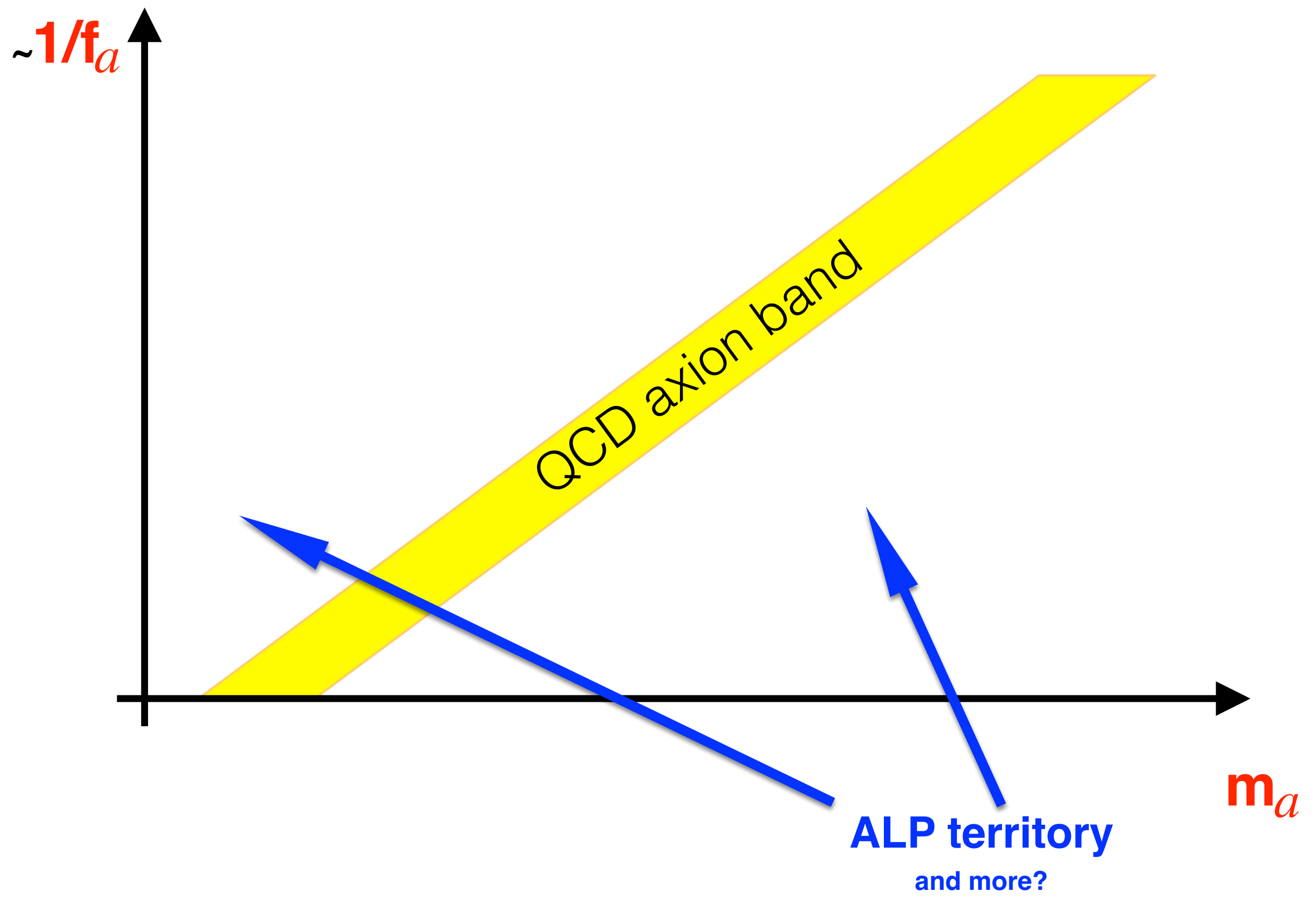
$$\bar{\theta}(\mu_{\text{IR}}) \simeq \bar{\theta}_0 +$$

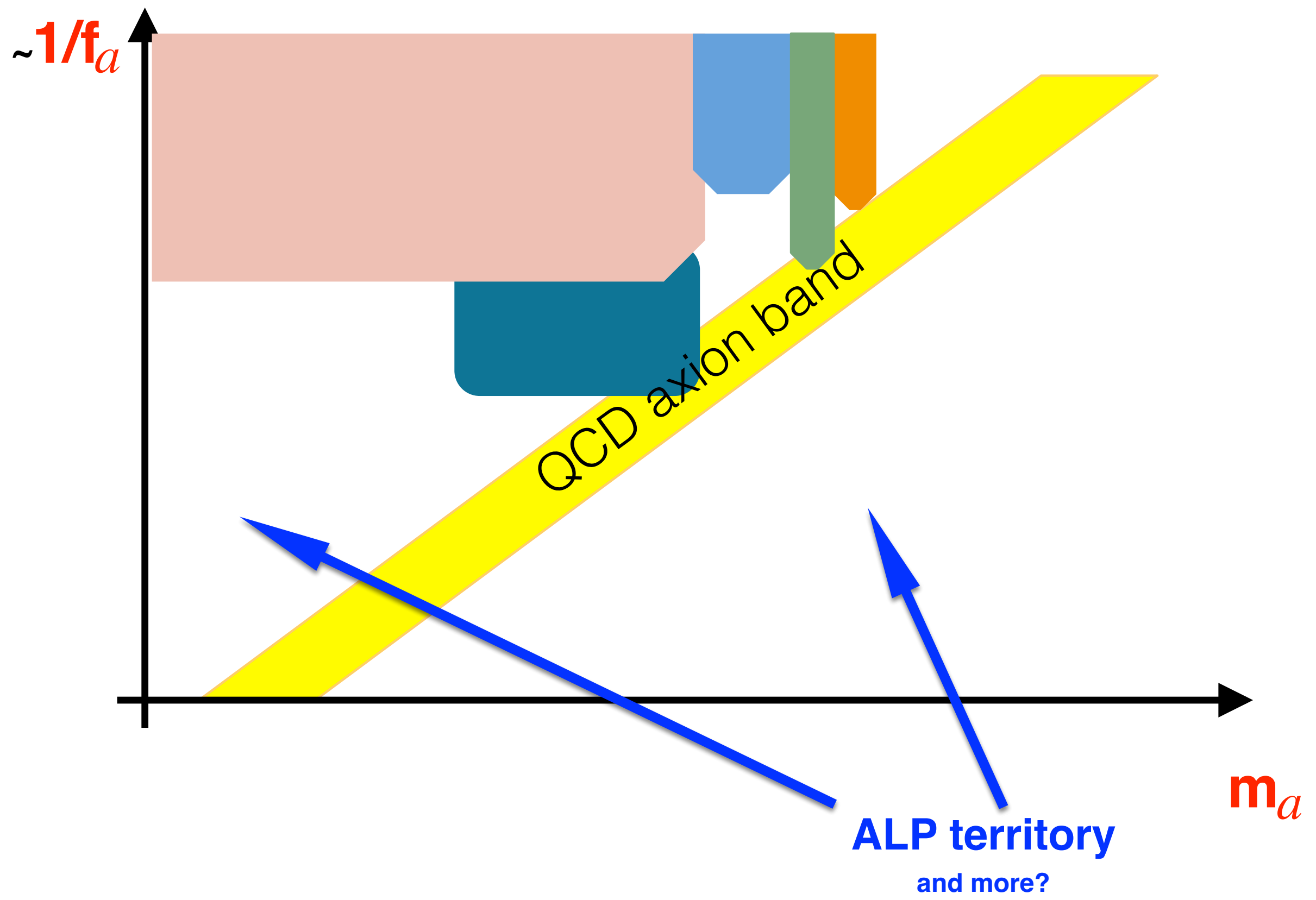
$$\sum_{u_i=\{u,c,t\}} \frac{m_{u_k} (m_a^2 + \hat{m}_{u_k}^2)}{16\pi^2 f_a^2 m_{u_i}} \text{Im} \left(C_Q^{ik} C_{u_R}^{*ik} \right) \log \frac{f_a^2}{\max(m_a^2, m_{u_k}^2)}$$
$$+ \sum_{d_i=\{d,s,b\}} \frac{m_{d_k} (m_a^2 + \hat{m}_{d_k}^2)}{16\pi^2 f_a^2 m_{d_i}} \text{Im} \left(C_Q^{ik} C_{d_R}^{*ik} \right) \log \frac{f_a^2}{\max(m_a^2, m_{d_k}^2)}$$

Neglecting threshold corrections

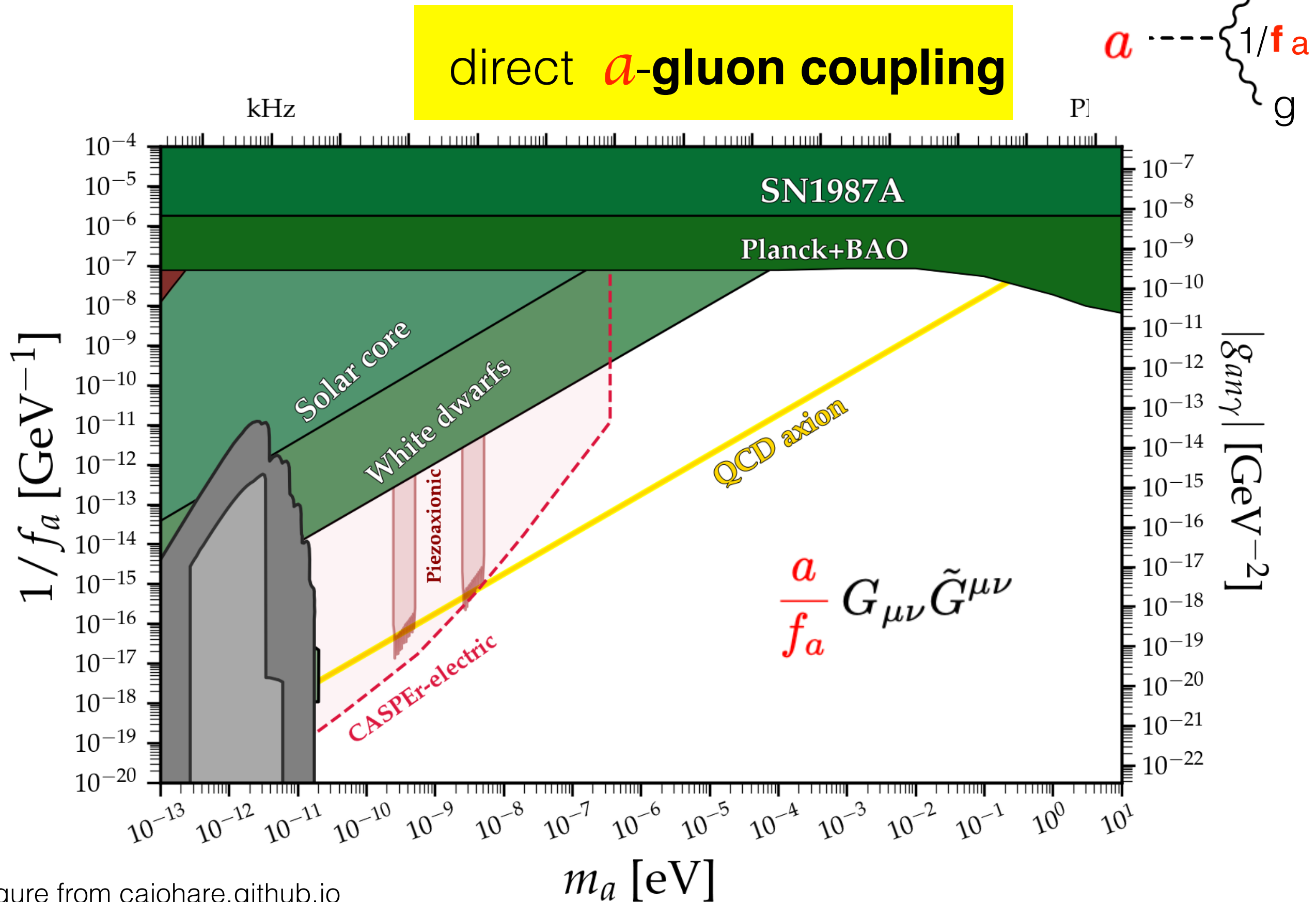
For a generic scalar:

$$\bar{\theta}(\mu_{IR}) \simeq \bar{\theta}_0 + \frac{v^2}{16\pi^2\Lambda^2} \times \left(\sum_{i,k} \left[\frac{m_{u_k} \text{Im}(K_u^{ik} K_u^{ki})}{m_{u_i}} - \frac{m_\phi^2 \text{Im}(F_u^{ik})}{m_{u_i}} \right] \log \frac{\Lambda^2}{\max(m_\phi^2, m_{u_k}^2)} \right. \\ \left. + \sum_{i,k} \left[\frac{m_{d_k} \text{Im}(K_d^{ik} K_d^{ki})}{m_{d_i}} - \frac{m_\phi^2 \text{Im}(F_d^{ik})}{m_{d_i}} \right] \log \frac{\Lambda^2}{\max(m_\phi^2, m_{d_k}^2)} \right)$$

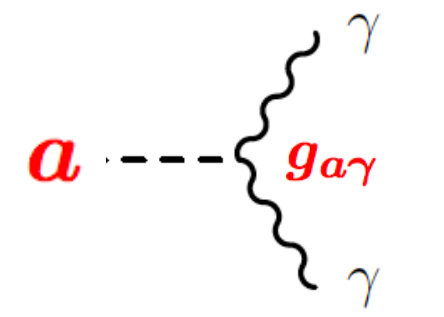
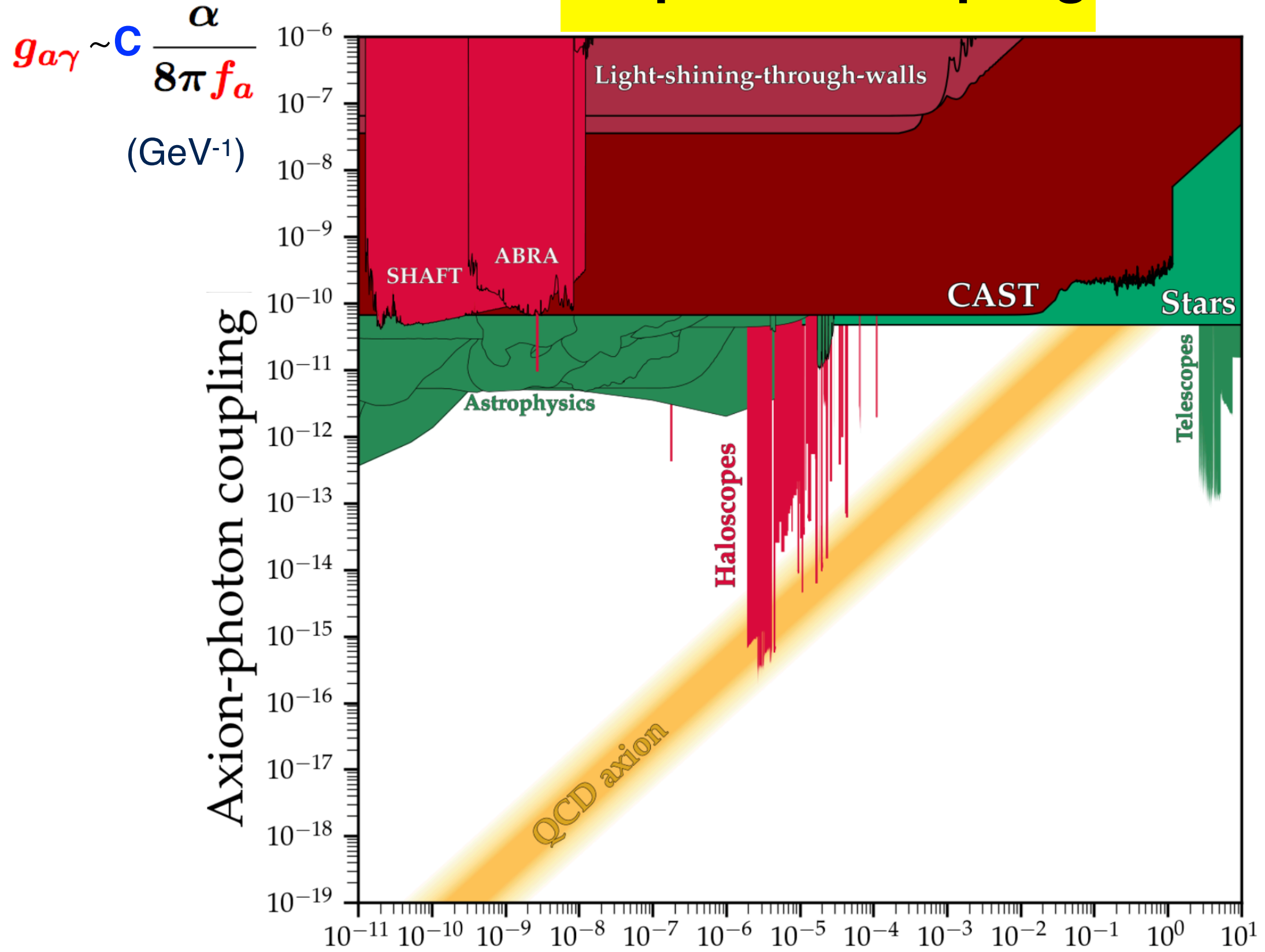




Intensely looked for experimentally...

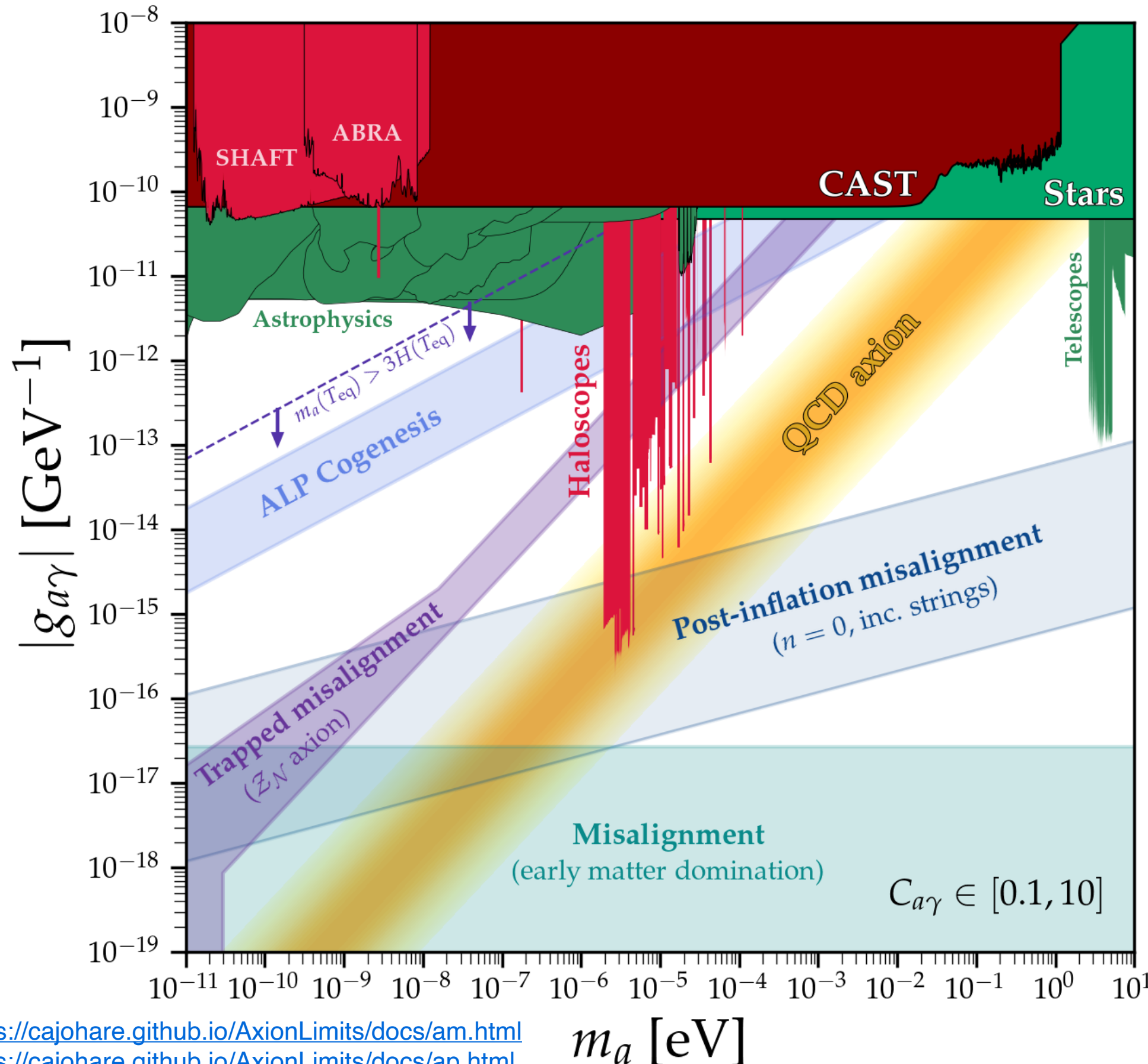


a -photon coupling



$$\frac{a}{f_a} F_{\mu\nu} \tilde{F}^{\mu\nu}$$

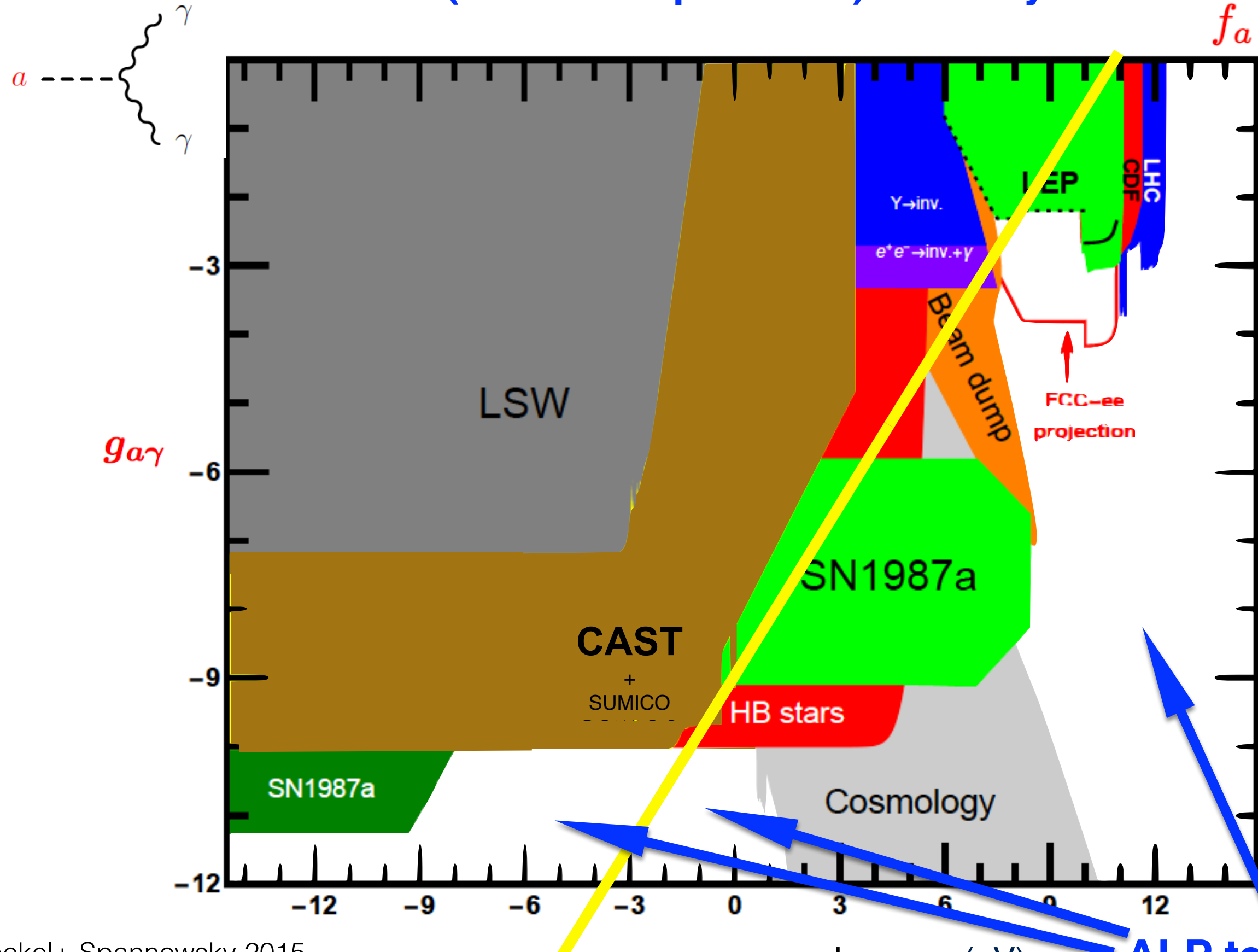
Axions and ALPs can explain Dark Matter



within the blueish bands
axions/ALPs would account for all the DM

ALPs (axion-like particles) territory

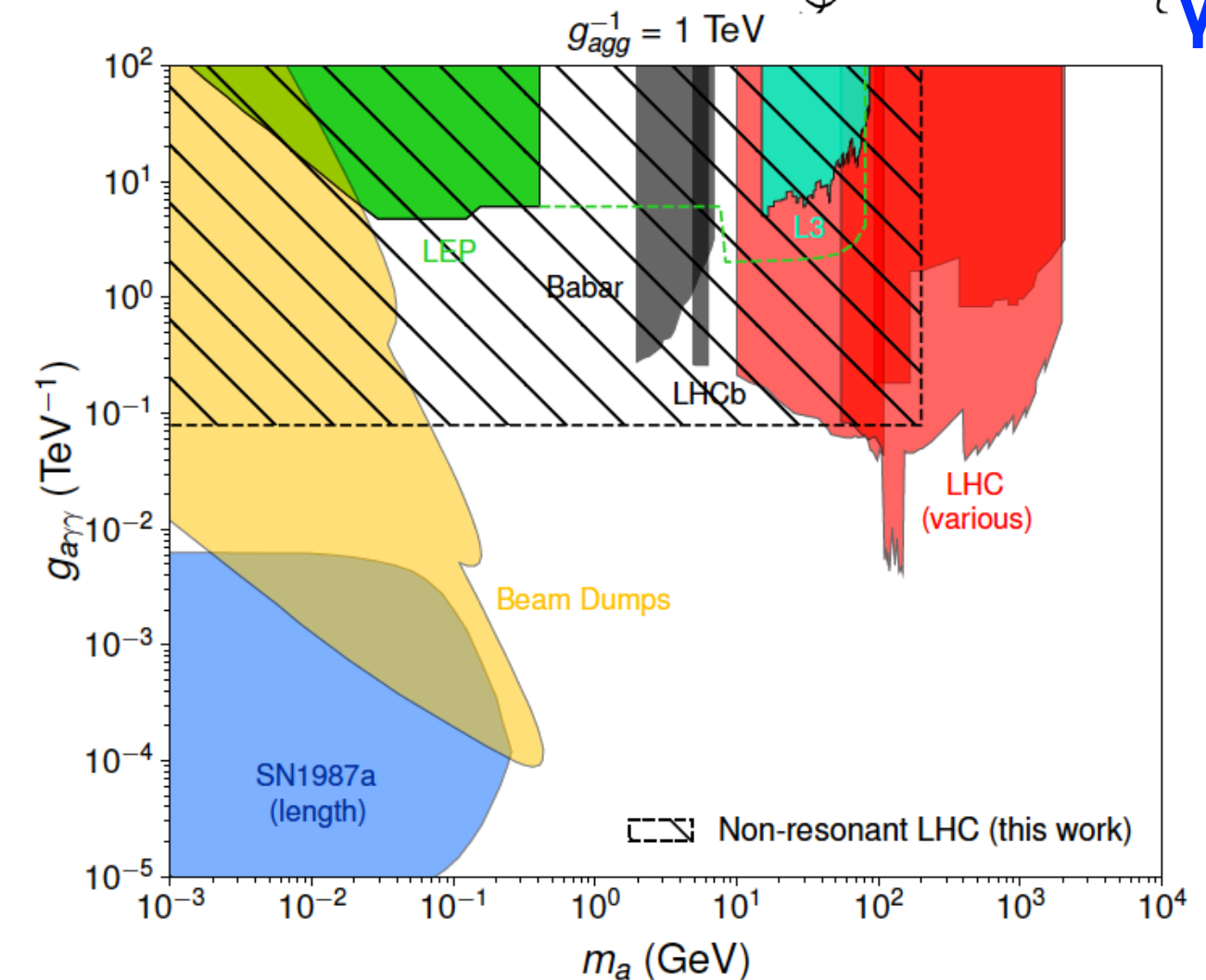
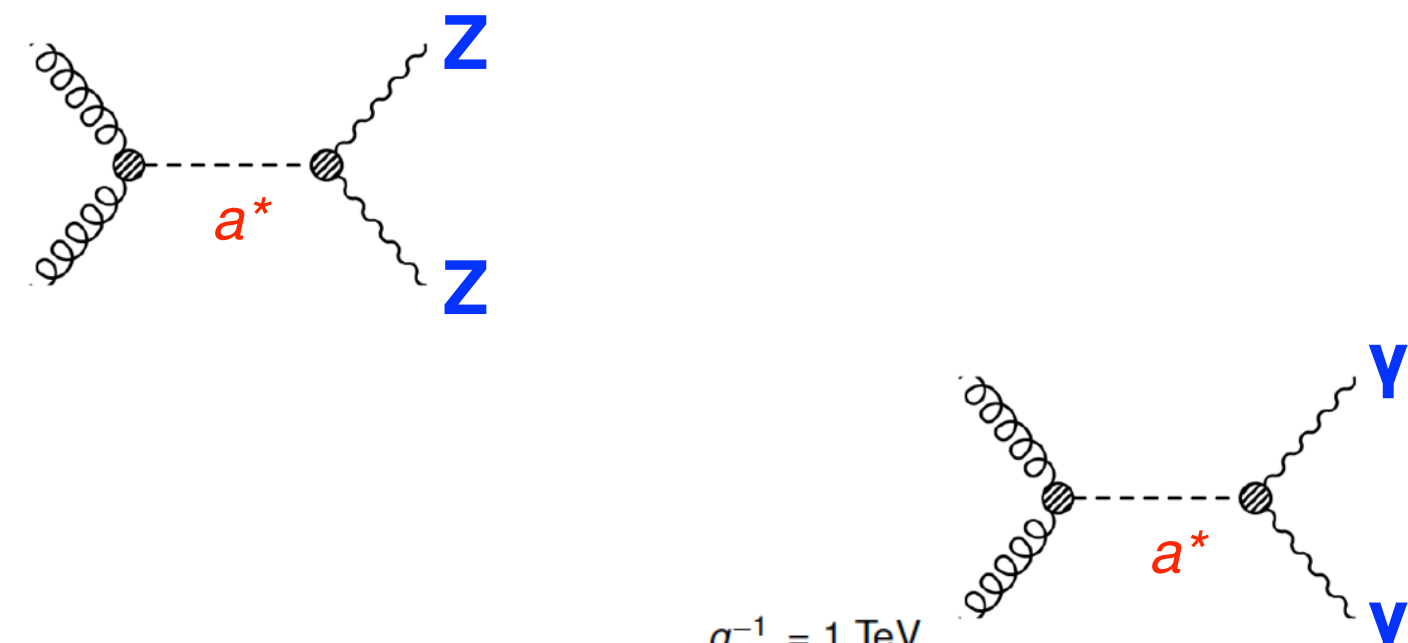
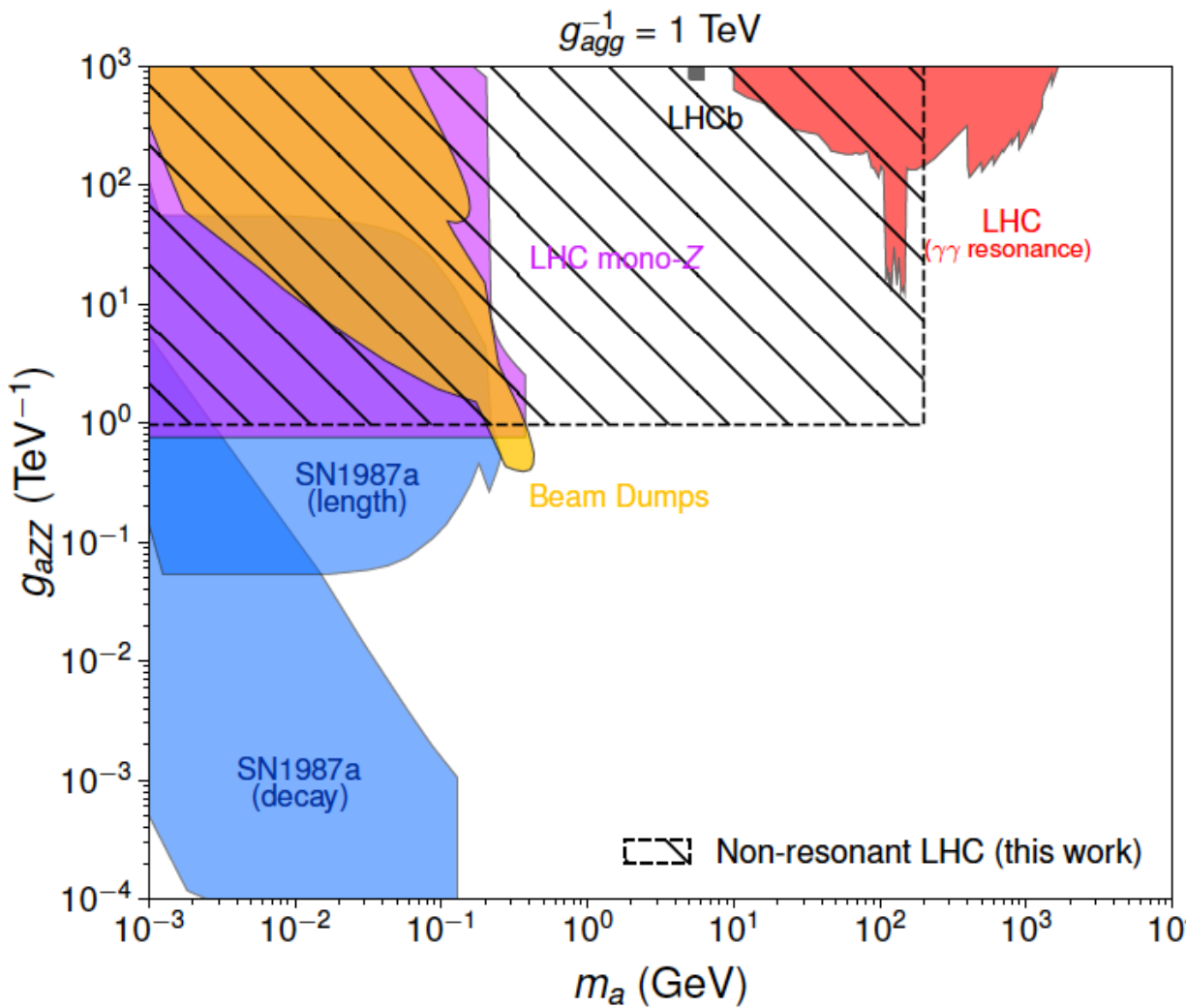
$$\frac{a}{f_a} F_{\mu\nu} \tilde{F}^{\mu\nu}$$



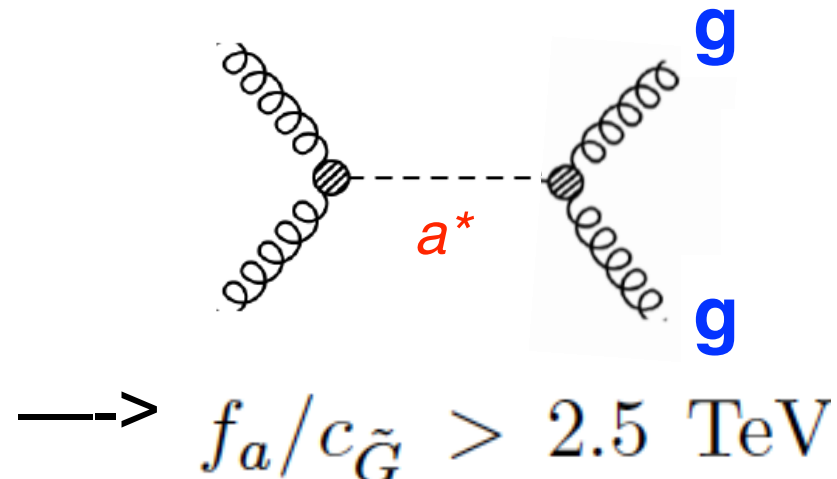
Other new ways to probe ALPs at LHC

(Fdez. de Troconiz, Gavela,
No, Sanz, 2019)

Non - resonant diboson searches

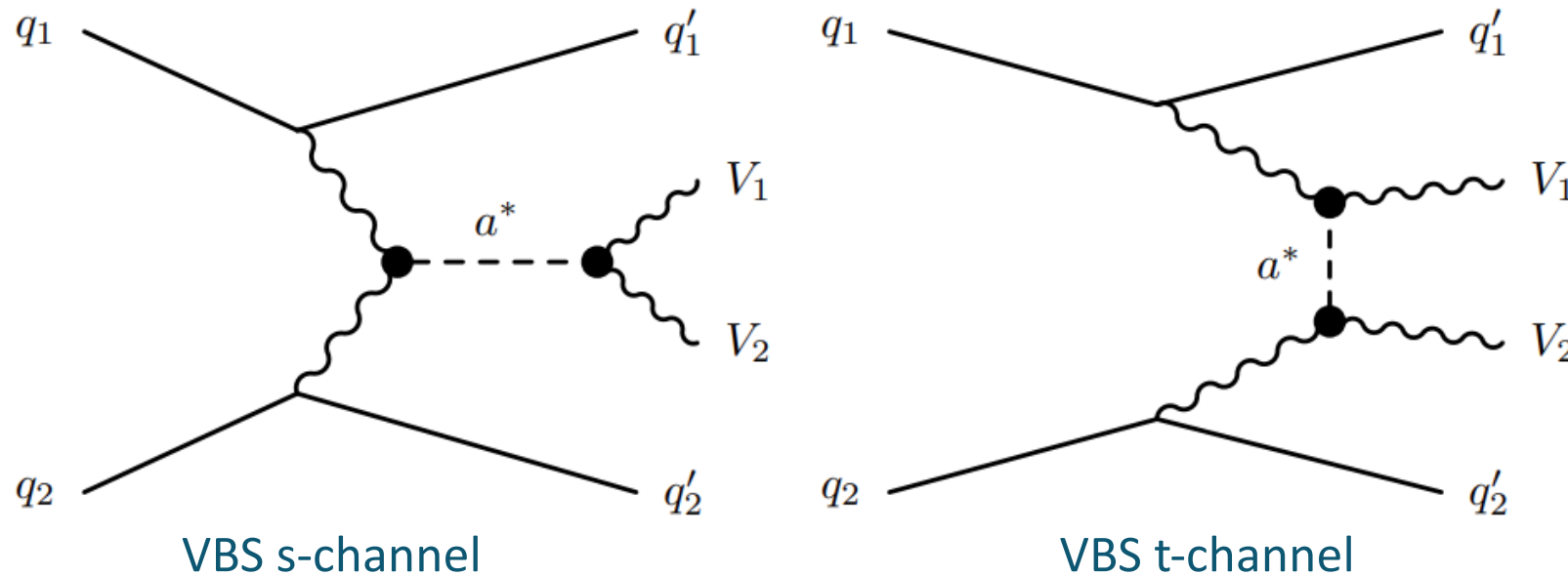


We also looked at two jets:



2022: ALP-mediated EW VBS (vector-boson fusion)

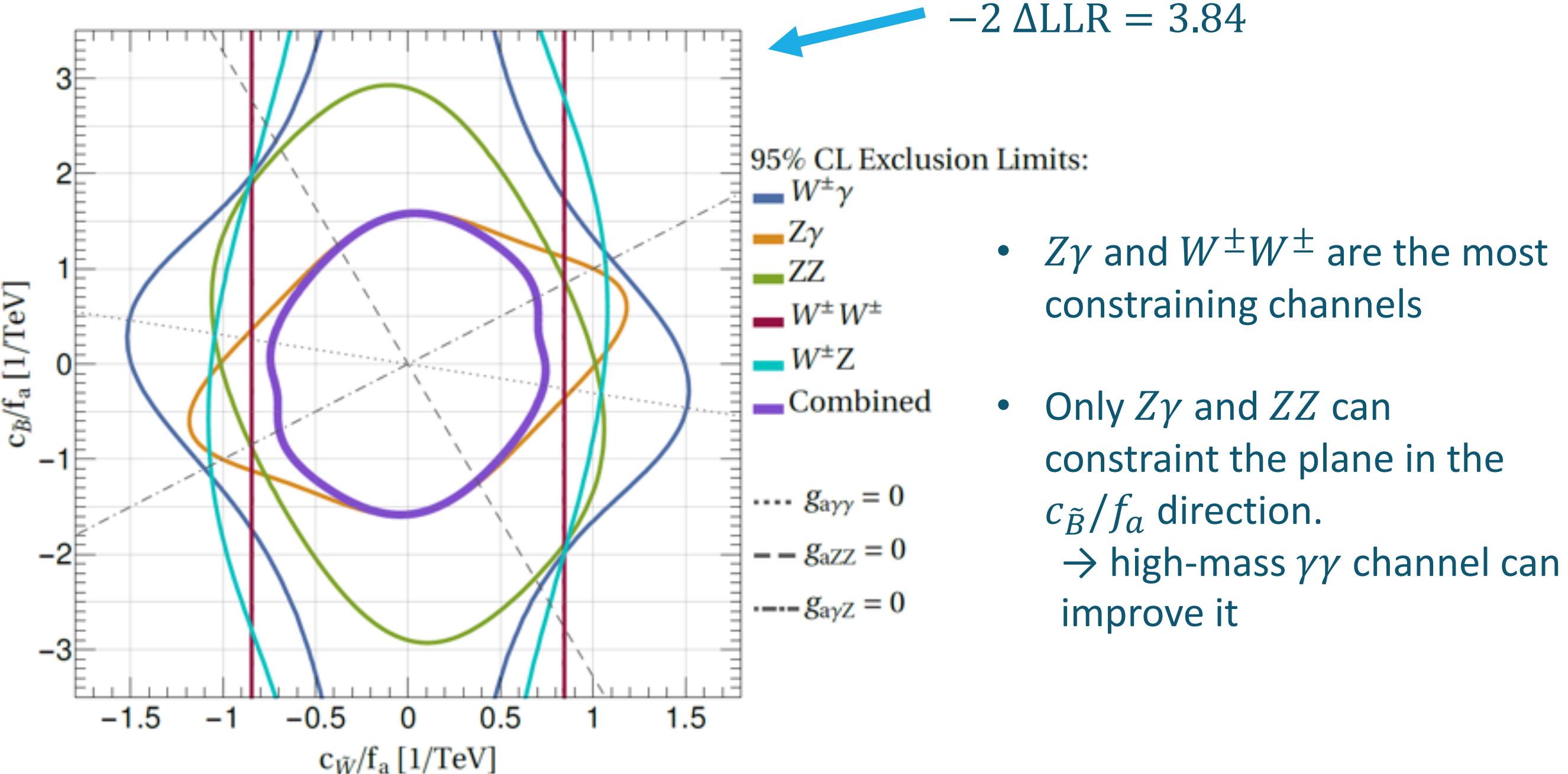
- **Vector Boson Scattering**
 - production of a diboson pair + 2 face-to-face jets with high invariant mass
 - explore **ALP EW couplings** with reduced dependence on the gluon coupling
- EW ALP-mediated processes $q_1 q_2 \rightarrow q'_1 q'_2 V_1 V_2$



Reinterpretation of Run 2 CMS analysis:
 $V_1 V_2 = ZZ, Z\gamma, W^\pm\gamma, W^\pm Z, W^\pm W^\pm$

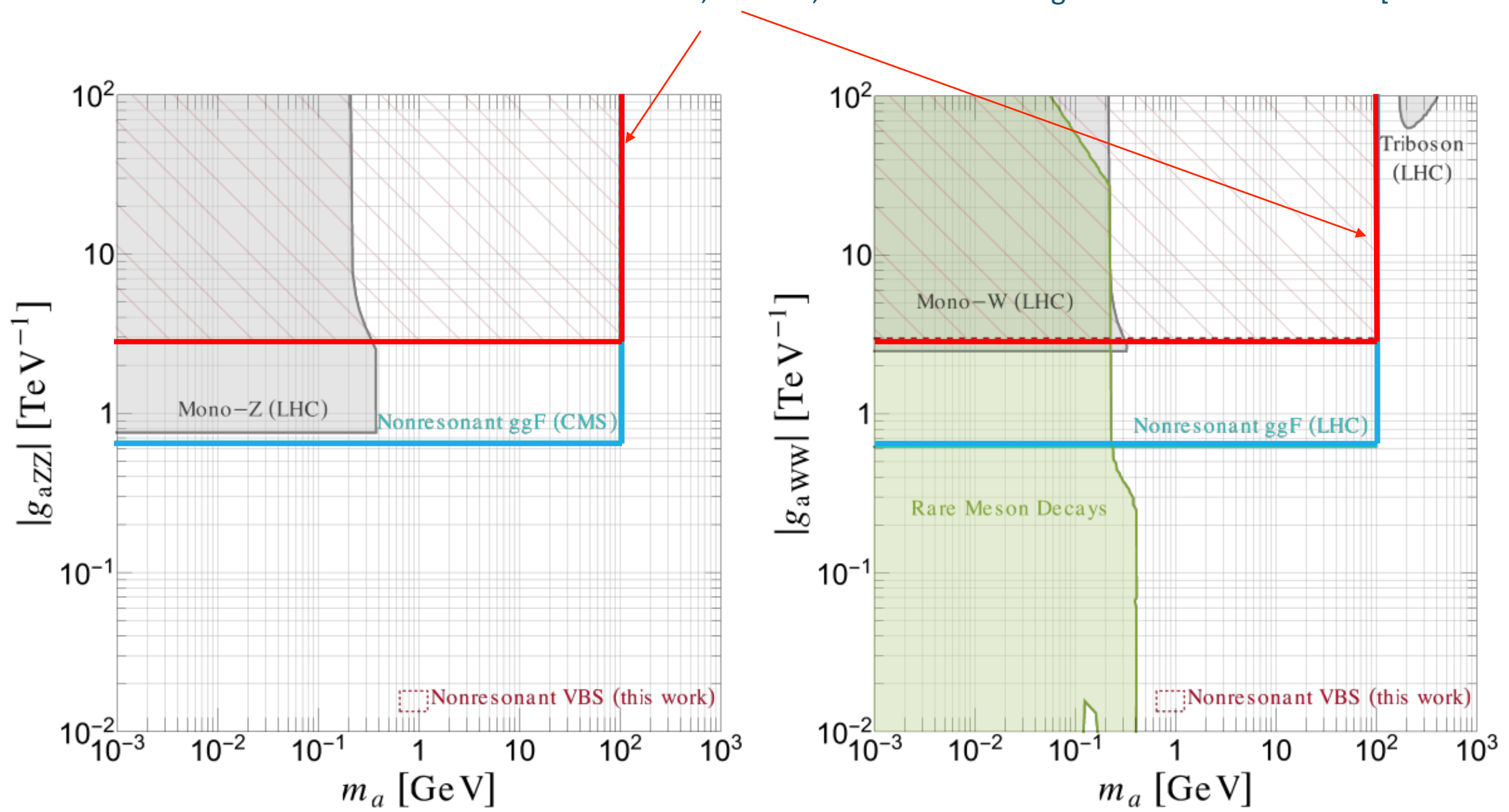
CMS-SMP-20-001, CMS-SMP-20-016,
CMS-SMP-19-008, CMS-SMP-19-012

RESULTS

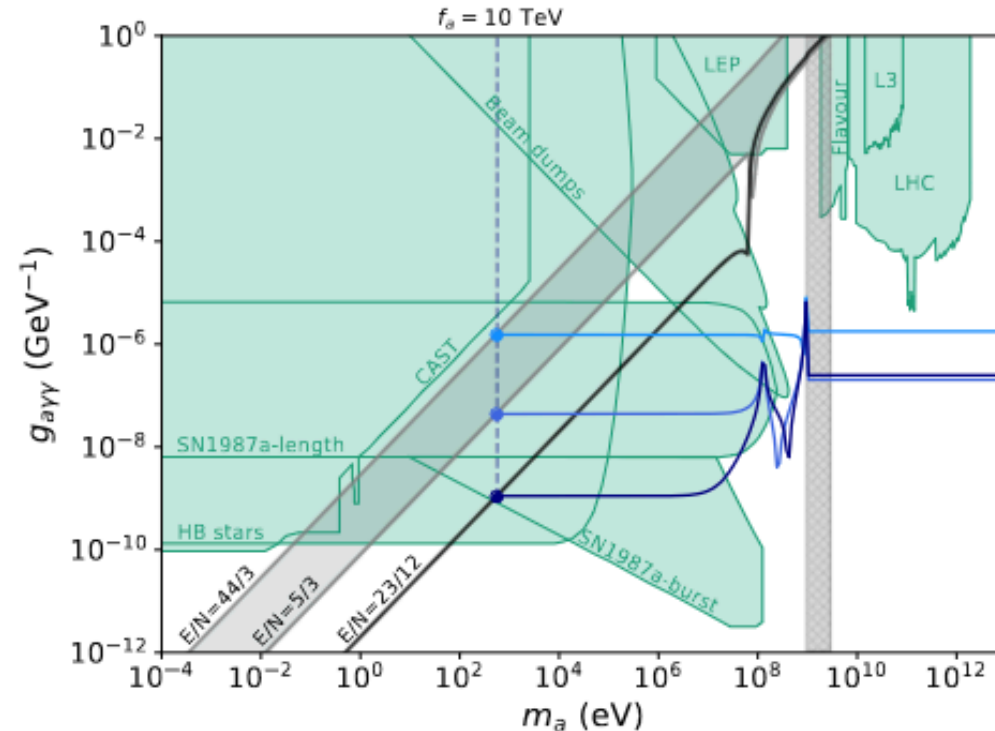


Comparison with existing bounds

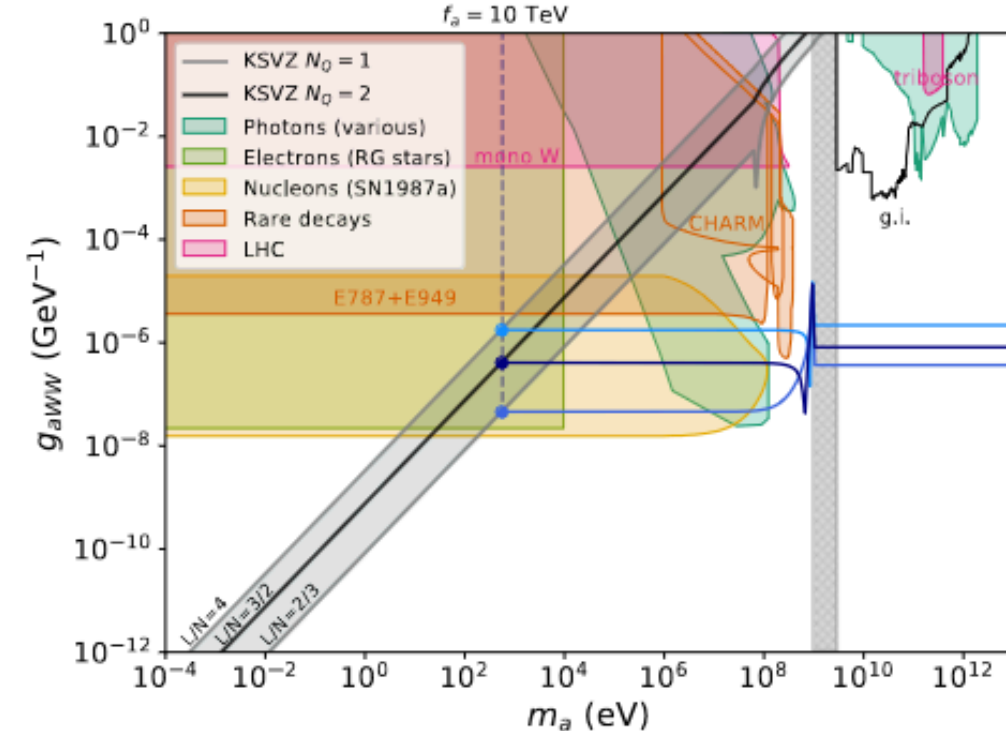
J. Bonilla, I. Brivio, J. Machado-Rodríguez and J. F. de Trocóniz [2202.0345]



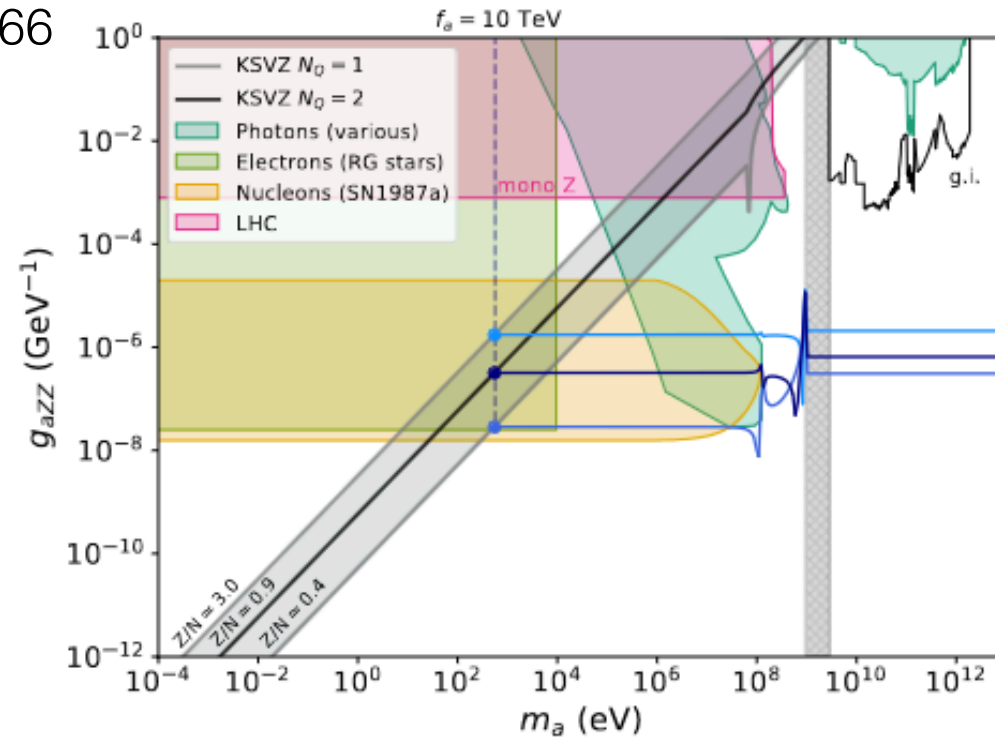
Alonso-Alvarez,
Gavela, Quilez,
arXiv:1811.05466



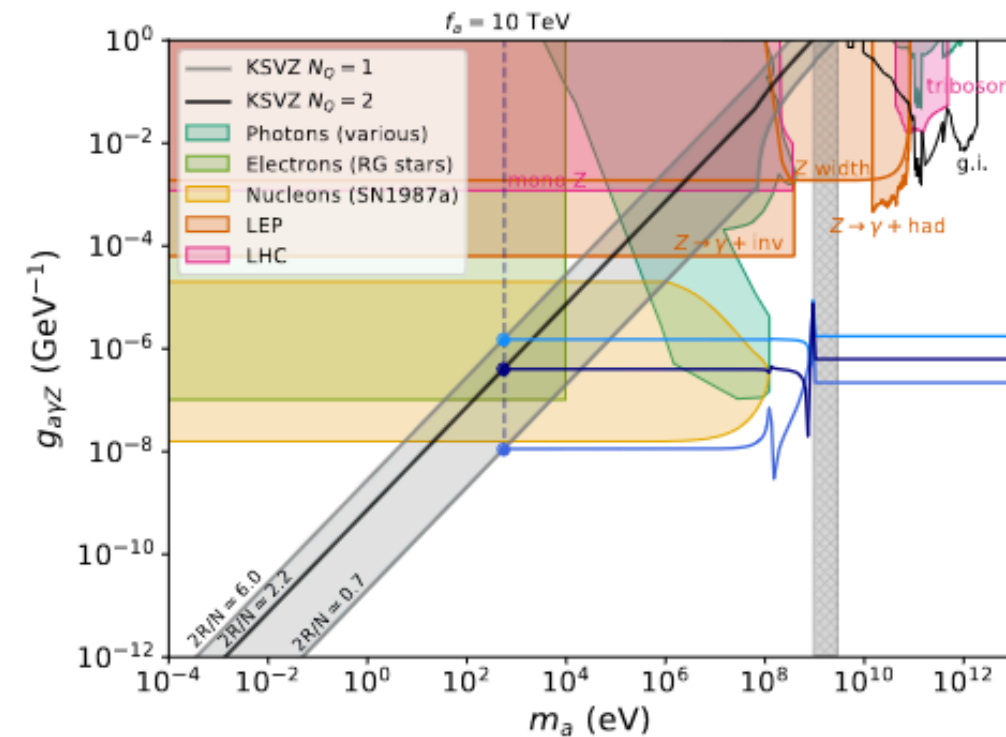
(a) Coupling to photons.



(b) Coupling to W bosons.



(c) Coupling to Z bosons.



(d) Coupling to a photon and a Z boson.

Figure 4: Coupling to EW gauge bosons. A two-operator framework is used: each panel assumes the existence of the corresponding electroweak coupling plus the axion-gluon coupling. The

e.g. Casper electric

$\{m_a, 1/f_a\}$: direct **a - gluon coupling**

$$\mathcal{L} \supset \frac{a}{f_a} \frac{\alpha_s}{8\pi} G \tilde{G}$$

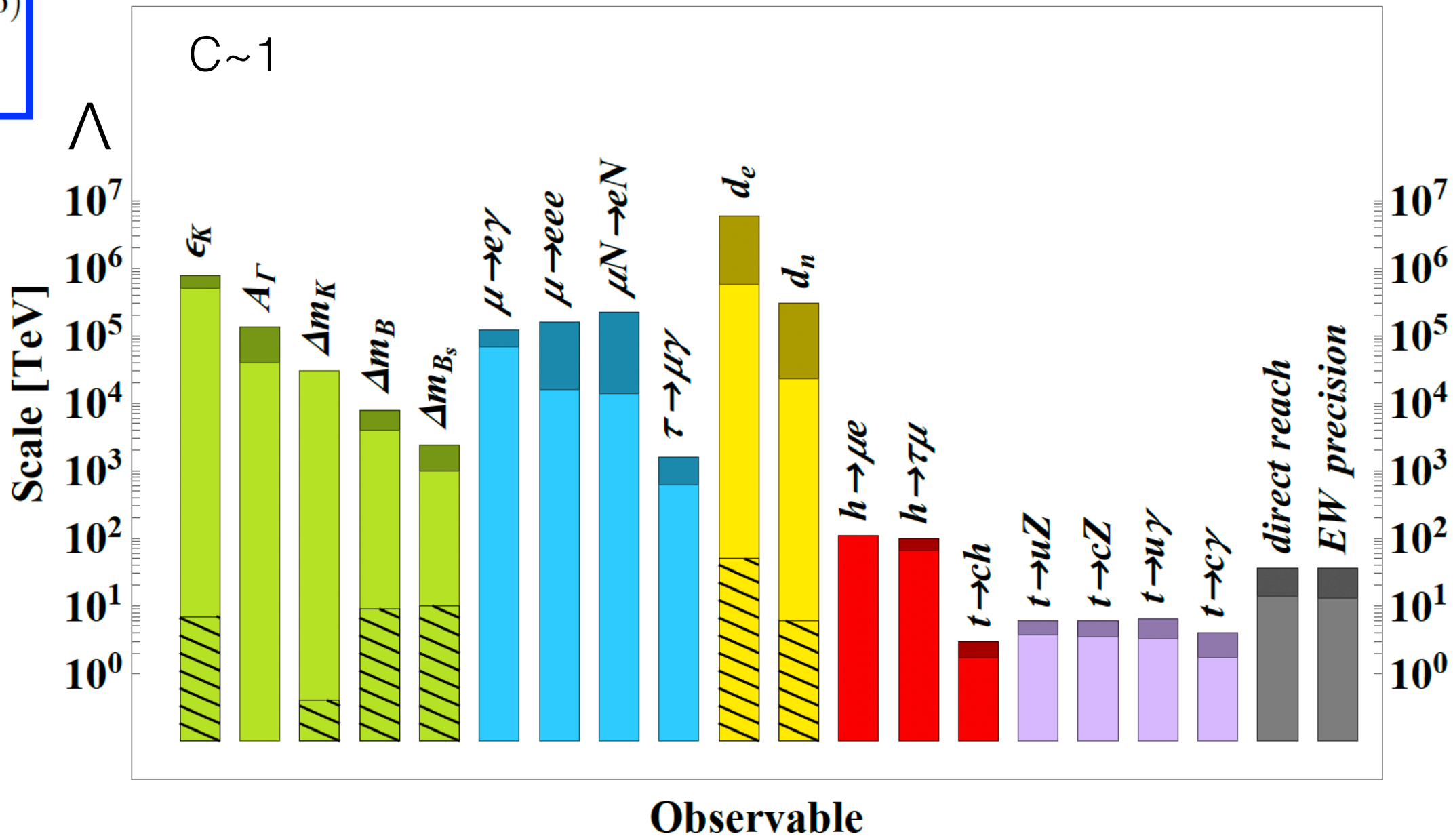
$$\delta \mathcal{L} \equiv -\frac{i}{2} \frac{0.011 e}{m_n} \frac{a}{f_a} \bar{n} \sigma_{\mu\nu} \gamma_5 n F^{\mu\nu}$$
$$\equiv g_{a\gamma n}$$

$$m_a^2 f_a^2 \simeq m_\pi^2 f_\pi^2 \frac{m_u m_d}{(m_u + m_d)^2}$$

Coupling to the
nEDM

Axion mass

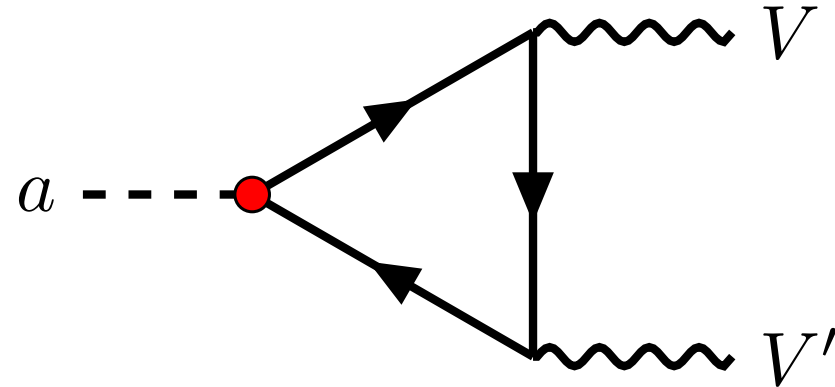
$$\frac{C_6^a}{\Lambda^2} \mathcal{O}_a^{(6)}$$



D. Aloni, A. Dery, M.B. Gavela, Y. Nir

Fig. 5.1: Reach in new physics scale of present and future facilities, from generic dimension six operators. Colour coding of observables is: green for mesons, blue for leptons, yellow for EDMs, red for Higgs flavoured couplings and purple for the top quark. The grey columns illustrate the reach of direct flavour-blind searches and EW precision measurements. The operator coefficients are taken to be either ~ 1 (plain coloured columns) or suppressed by MFV factors (hatch filled surfaces). Light (dark) colours correspond to present data (mid-term prospects, including HL-LHC, Belle II, MEG II, Mu3e, Mu2e, COMET, ACME, PIK and SNS).

One-loop induced couplings



$$g_{a\gamma\gamma}^{\text{loop}} = - \frac{\alpha_{\text{em}}}{\pi f_a} \left[\underbrace{\text{Tr}\{(\mathbf{c}_{ee})\}}_{\text{ANOMALOUS}} + 2 \sum_{\ell} (\mathbf{c}_{ee})_{\ell\ell} m_{\ell}^2 \mathcal{C}_0(0, 0, m_a^2, m_{\ell}, m_{\ell}, m_{\ell}) \underbrace{}_{\text{MASS-DEPENDENT}} \right]$$

$$g_{aZZ}^{\text{loop}} = - \frac{\alpha_{\text{em}}}{2 c_w^2 s_w^2 \pi f_a} \left[(1 - 2 s_w^2) \text{Tr}(\mathbf{c}_{\nu\nu}) + 2 s_w^4 \text{Tr}(\mathbf{c}_{ee}) + \mathcal{O}\left(\frac{m_{\ell}^2}{M_Z^2}\right) \right]$$

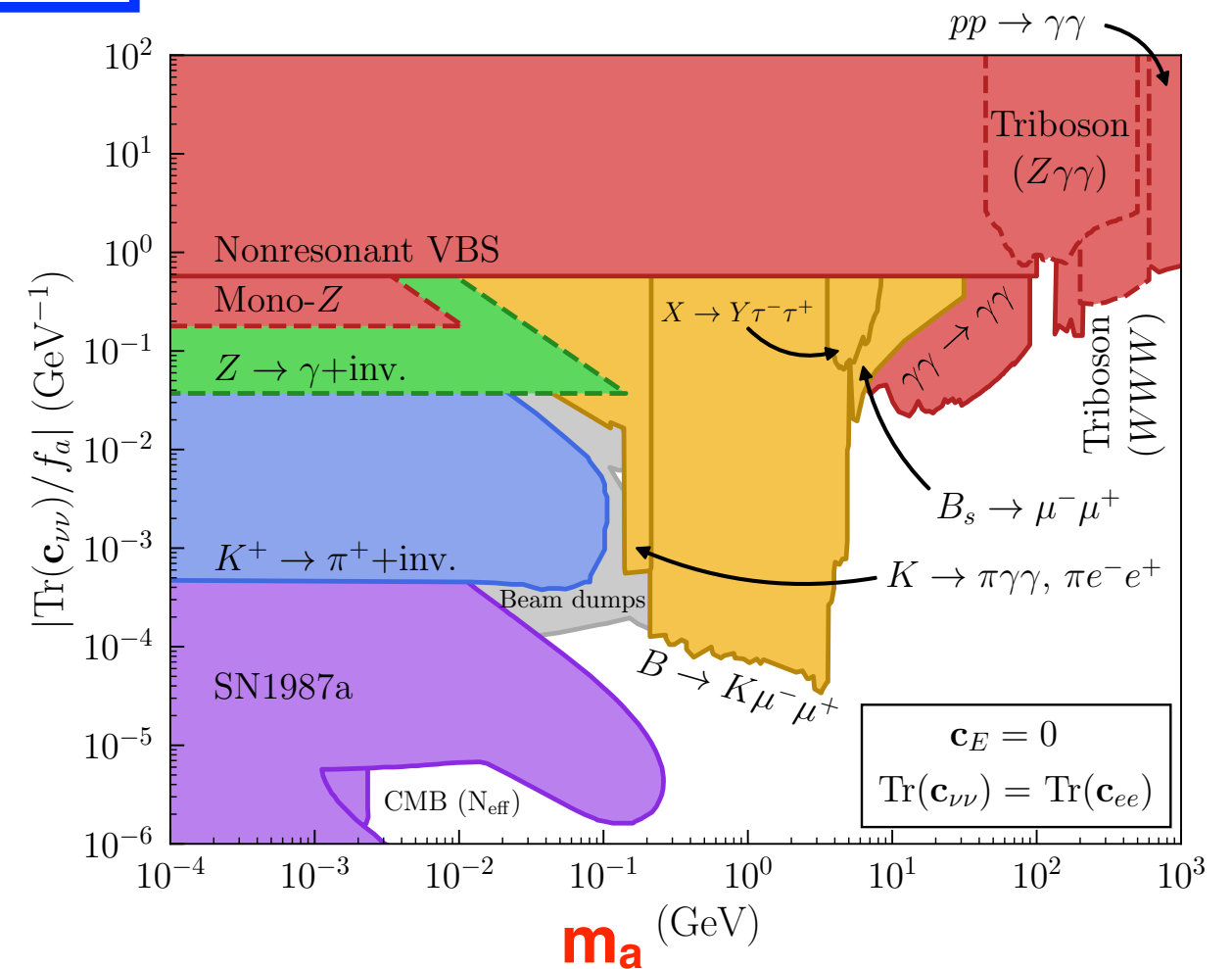
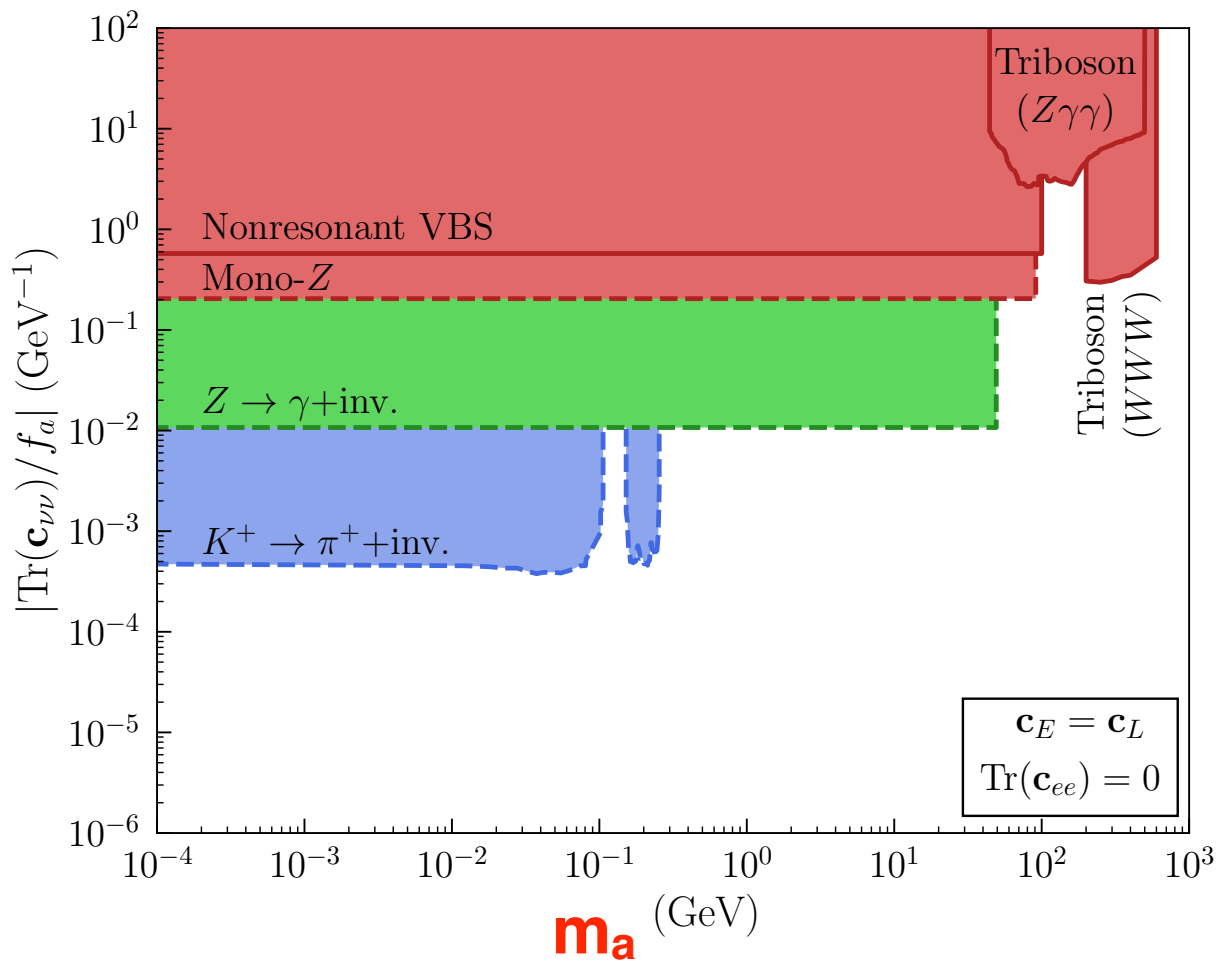
$$g_{a\gamma Z}^{\text{loop}} = \frac{\alpha_{\text{em}}}{c_w s_w \pi f_a} \left[\text{Tr}\{(\mathbf{c}_{\nu\nu})\} - 2 s_w^2 \text{Tr}\{(\mathbf{c}_{ee})\} + \mathcal{O}\left(\frac{m_{\ell}^2}{M_Z^2}\right) \right]$$

$$g_{aWW}^{\text{loop}} = - \frac{\alpha_{\text{em}}}{2 s_w^2 \pi f_a} \left[\text{Tr}(\mathbf{c}_{\nu\nu}) + \mathcal{O}\left(\frac{m_{\ell}^2}{M_W^2}\right) \right]$$

Package X, arXiv:1612.00009
FeynCalc, arXiv:2001.04407

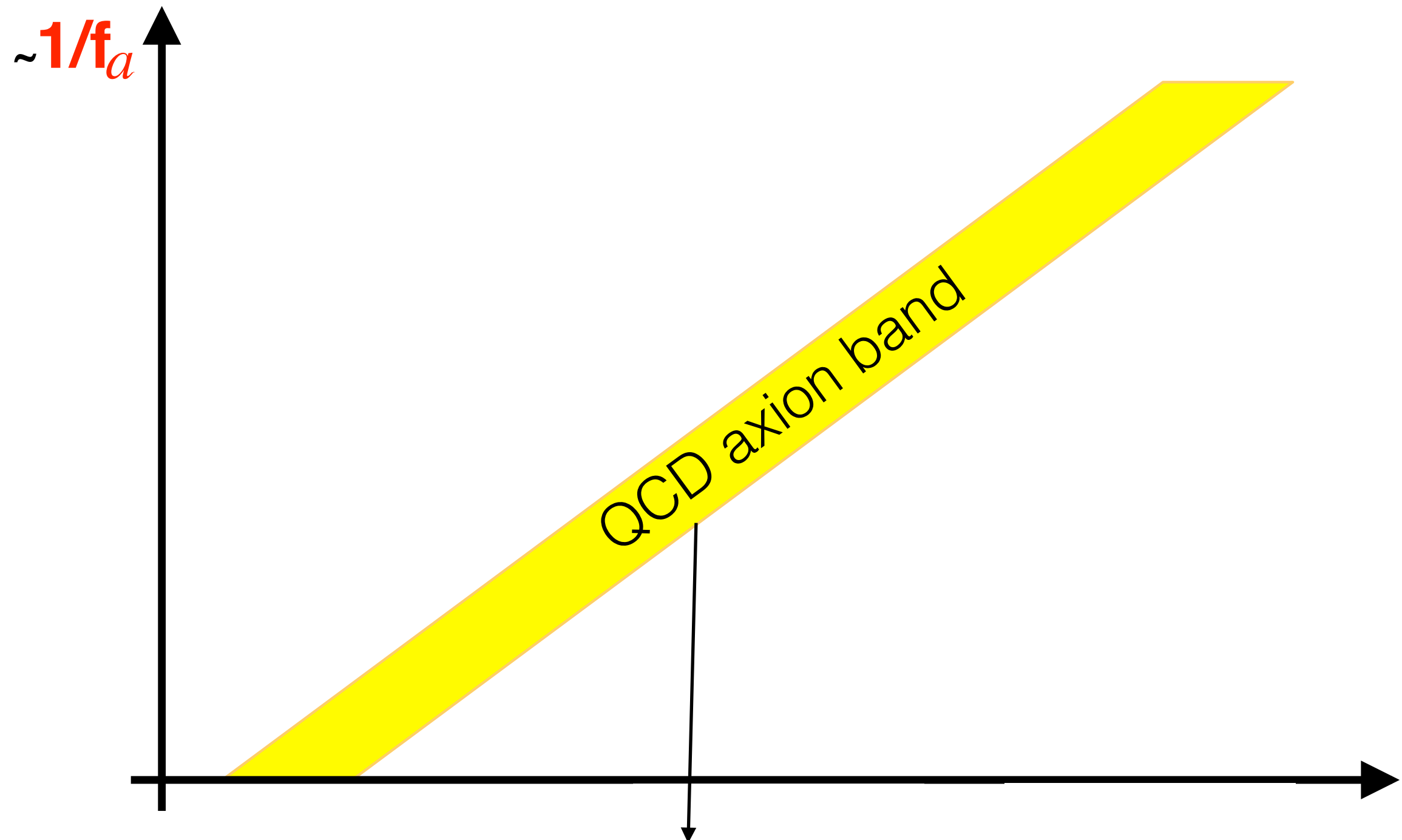
Bounds on ALP-neutrino coupling

$$\text{Tr}(\mathbf{c}_{\nu\nu}/f_a)$$

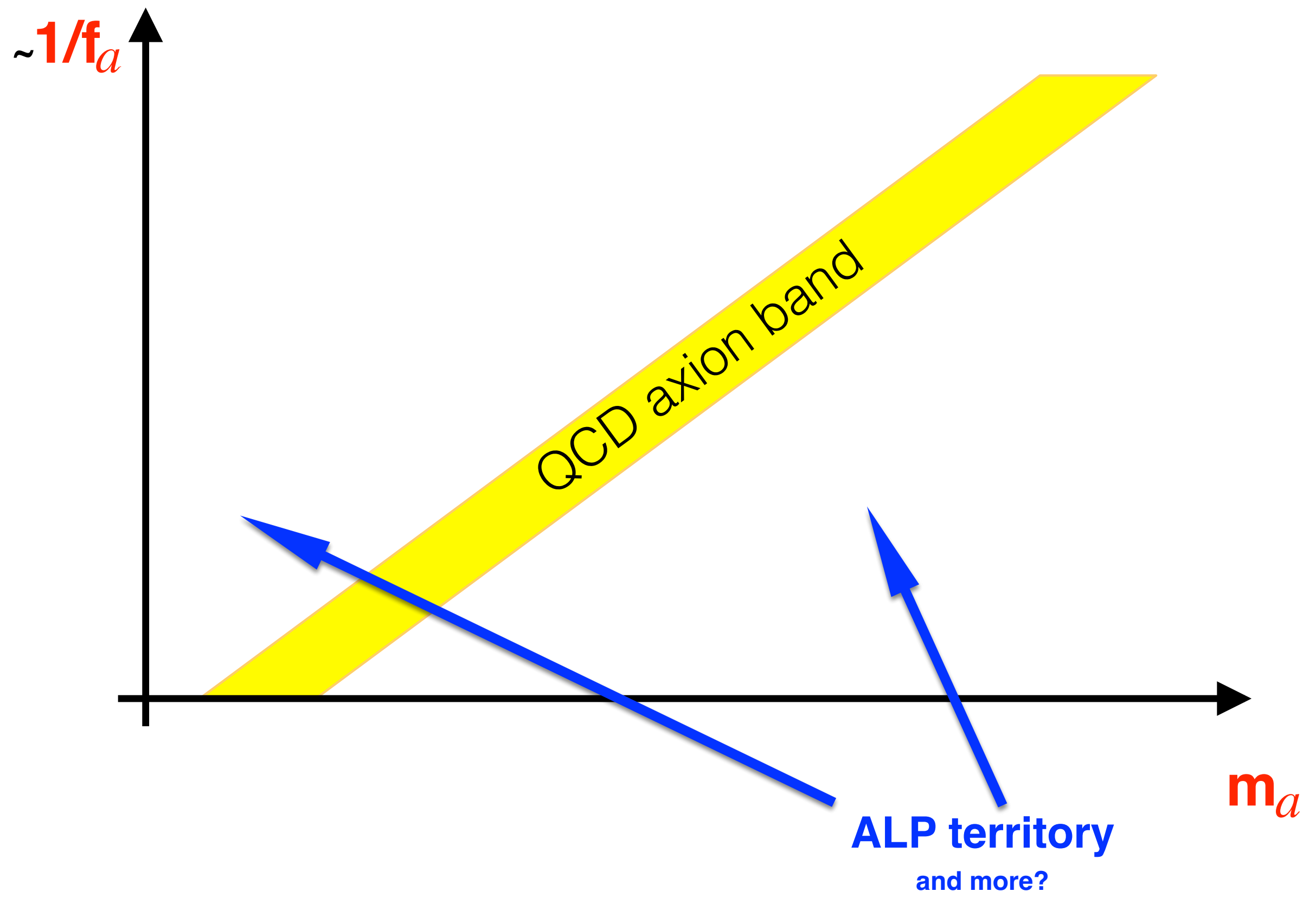


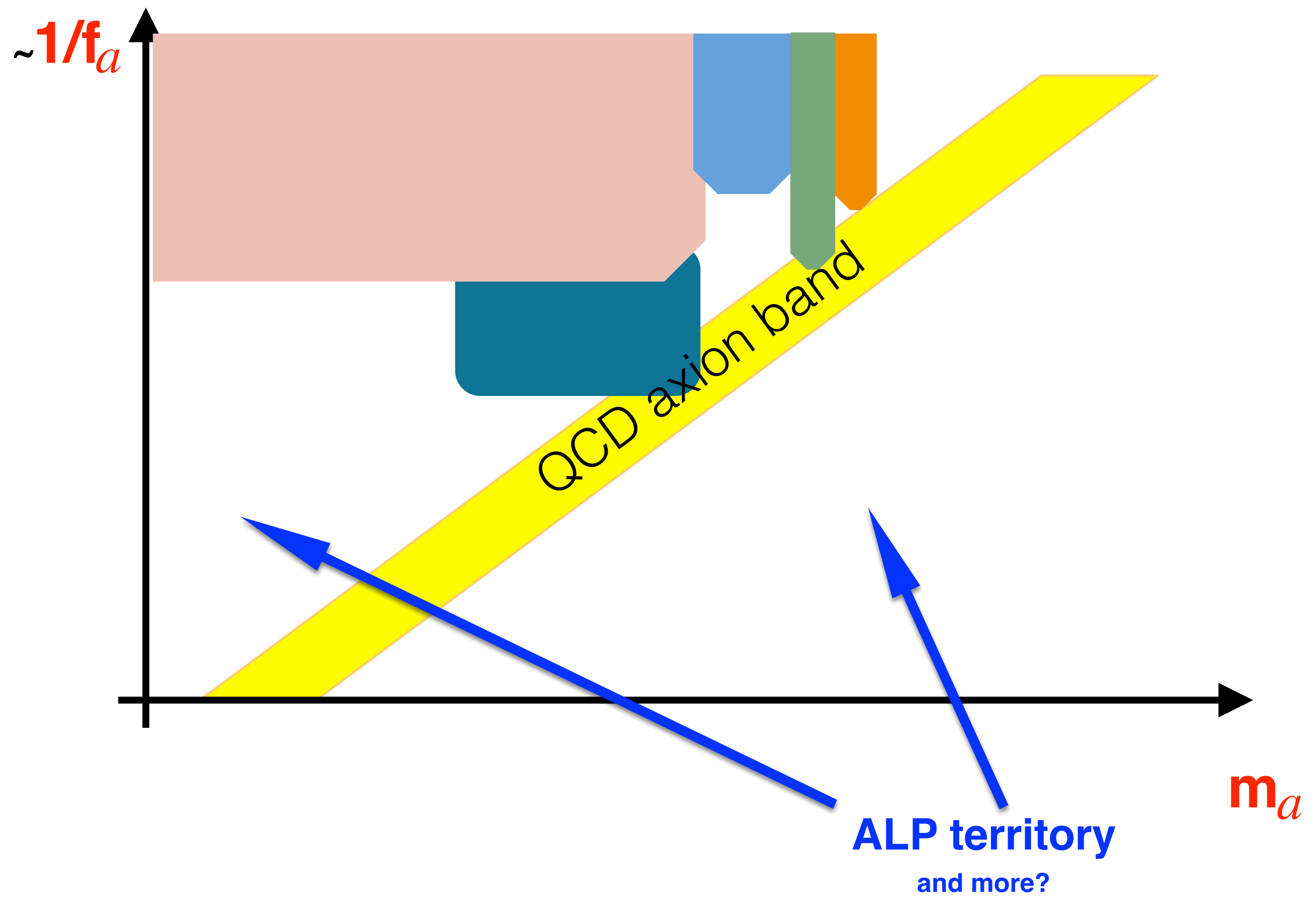
In “true axion” models (= which solve the strong CP problem):

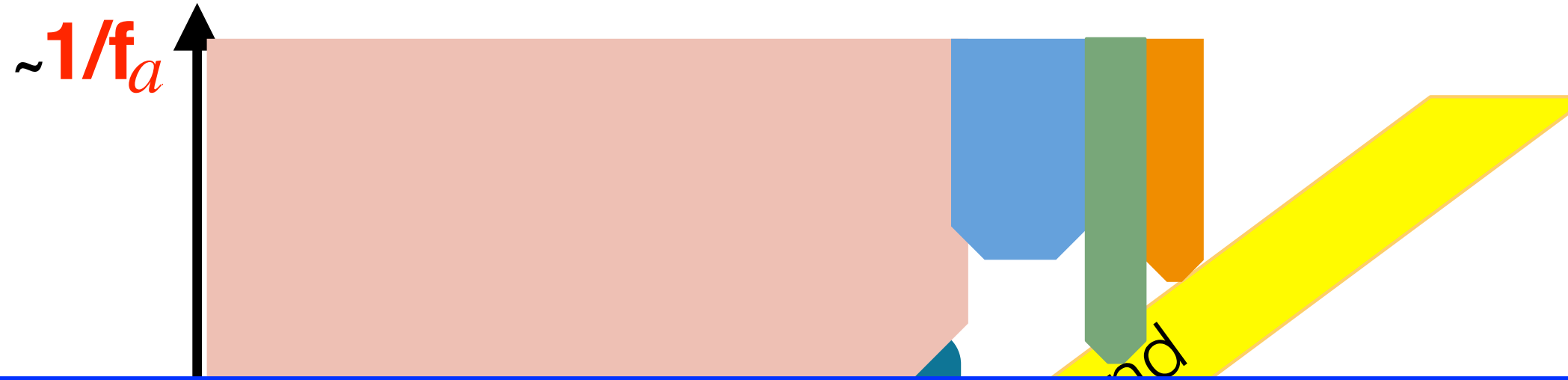
$$m_a f_a = \text{cte.}$$



$$m_a^2 f_a^2 = m_\pi^2 f_\pi^2 \frac{m_u m_d}{(m_u + m_d)^2}$$



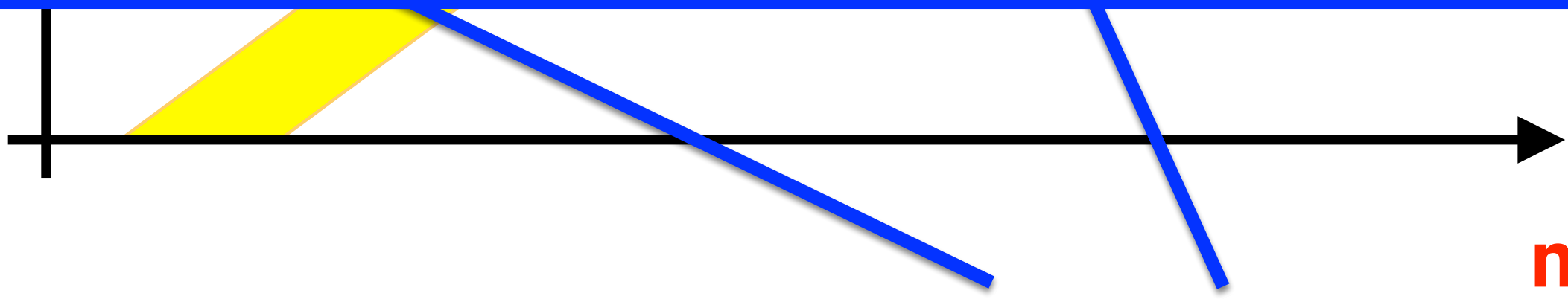




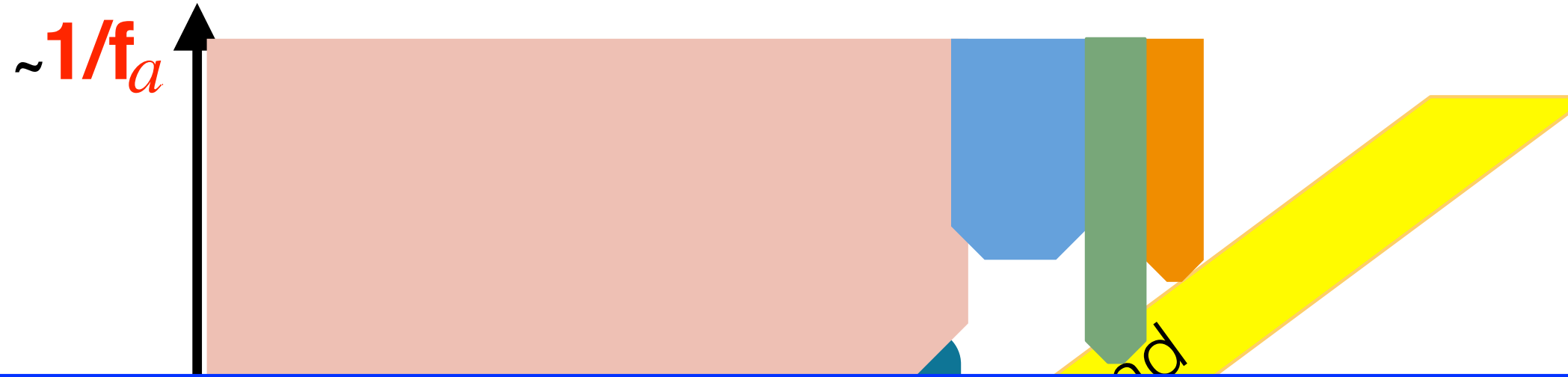
Difference between and ALP and a true axion:

an ALP does not intend to solve the strong CP problem

otherwise, the phenomenology is alike



**ALP territory
and more?**



Difference between the ALP and a true axion:

$$\{ m_a, f_a \}$$

are independent parameters for ALPs



m_a
ALP territory
and more?

a -neutron coupling

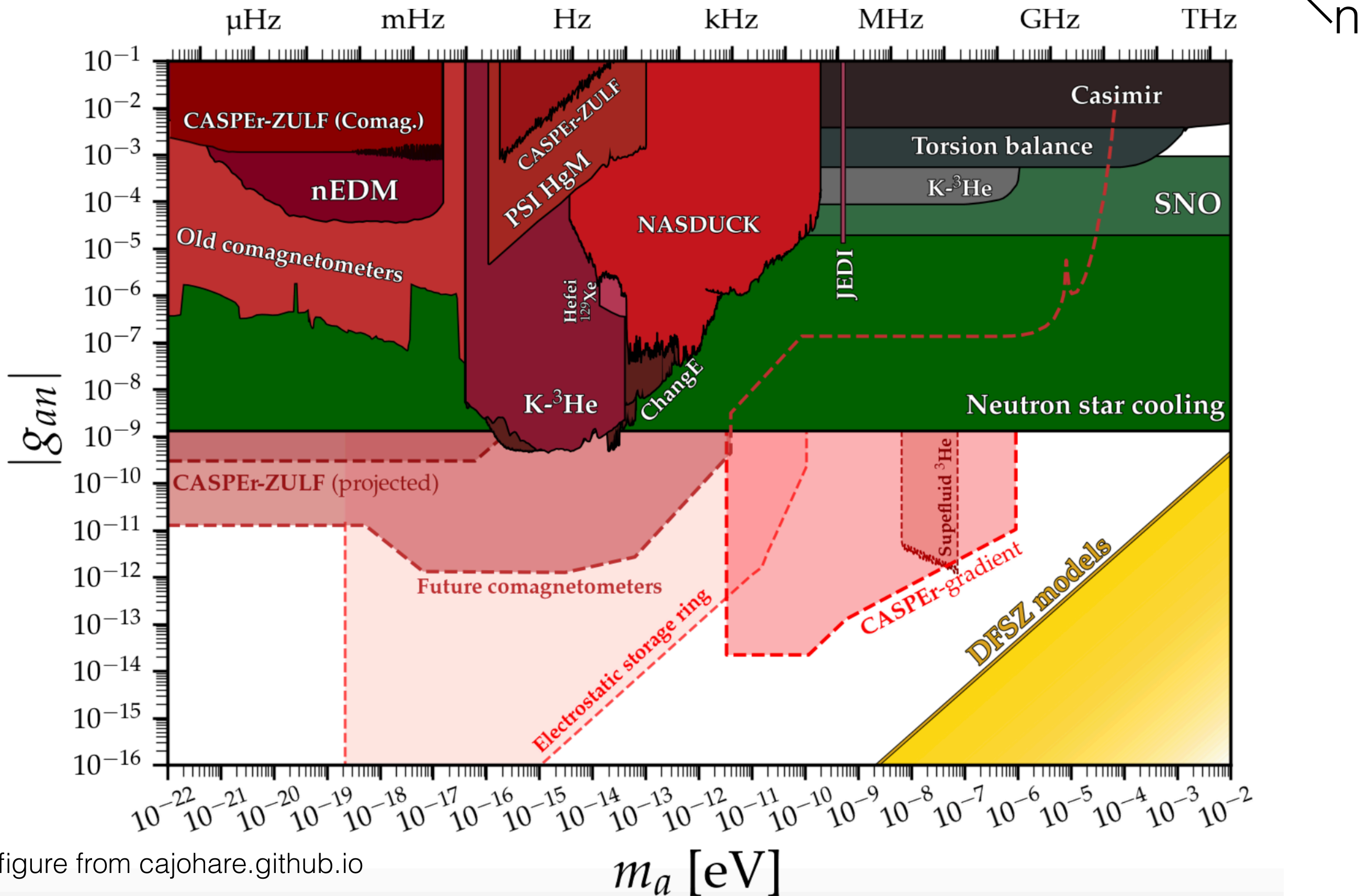
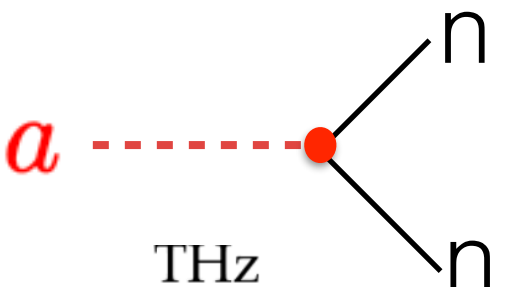
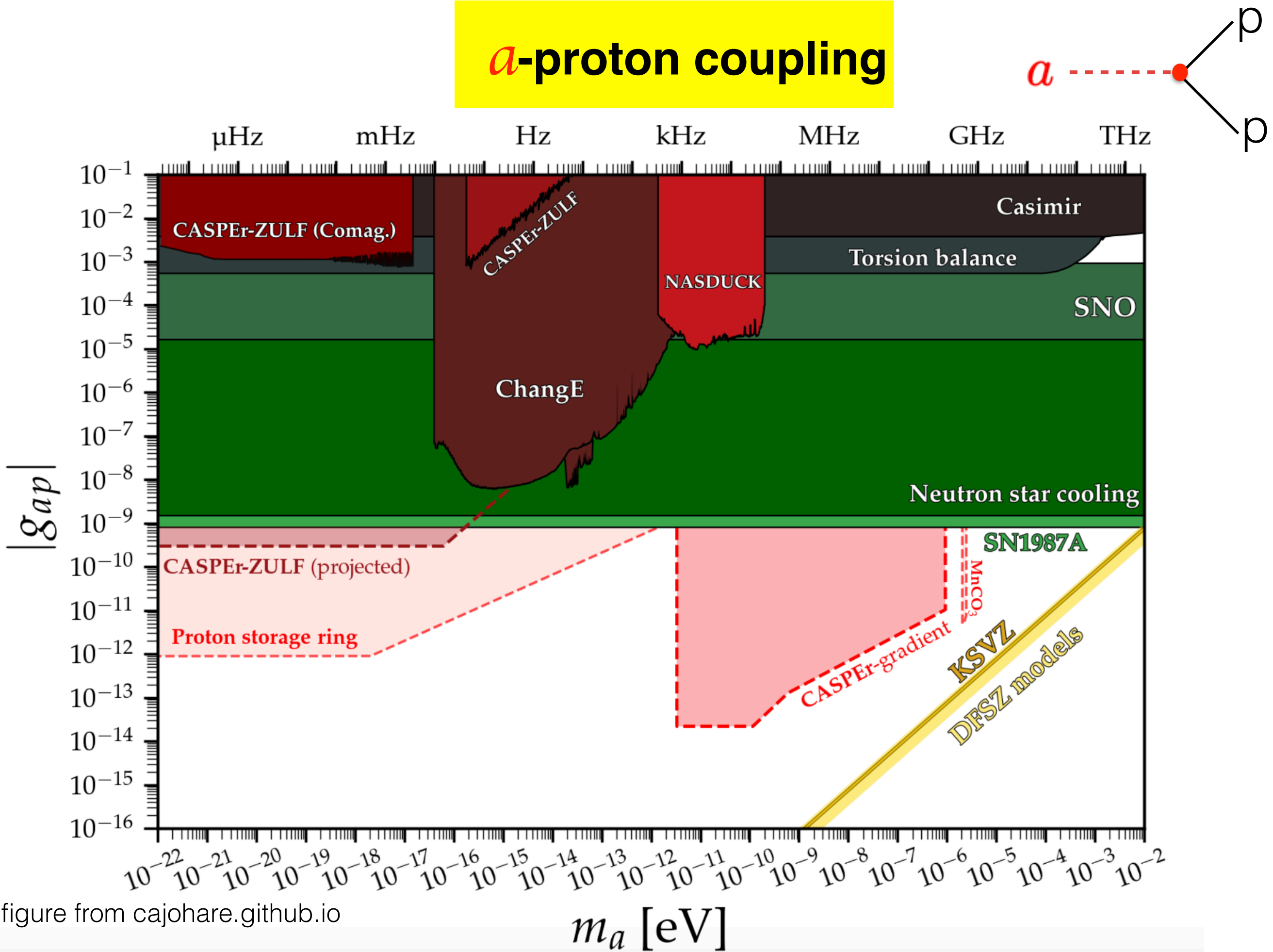


figure from cajohare.github.io

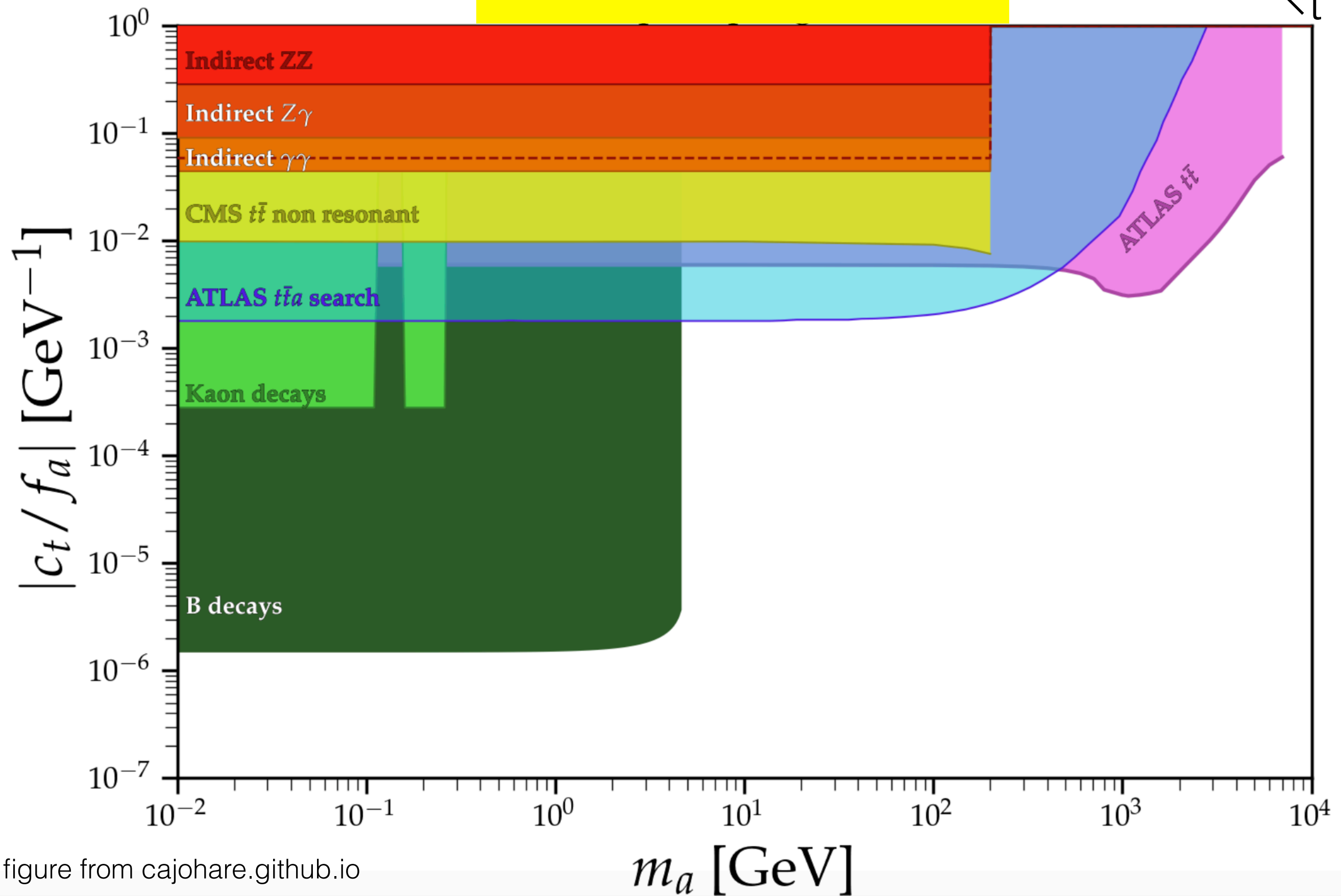
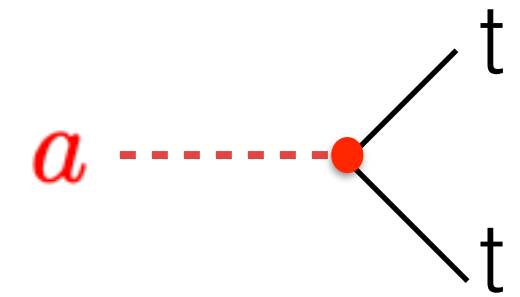
m_a [eV]



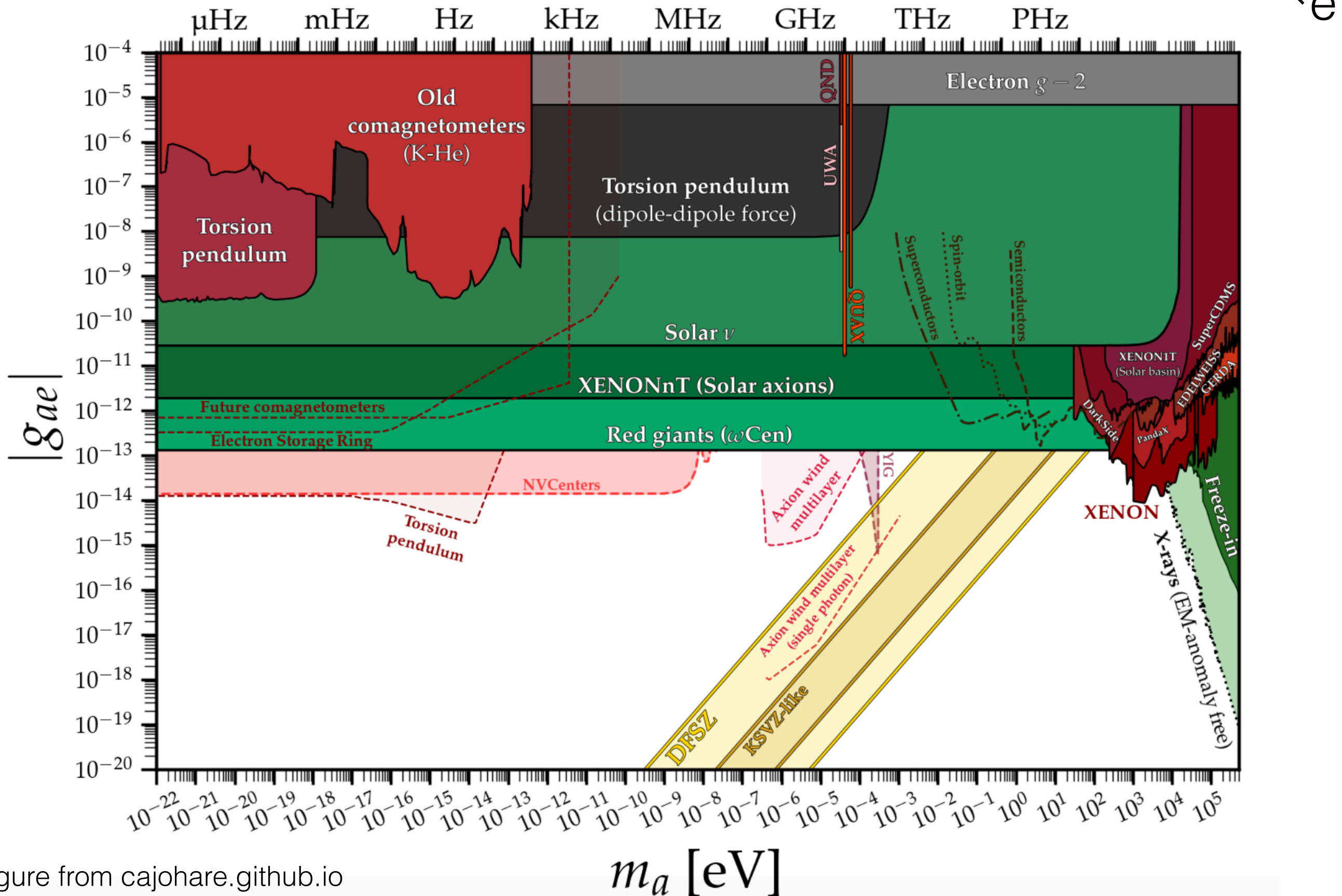
α -proton coupling



a -top coupling



a -electron coupling



a-neutrino couplings

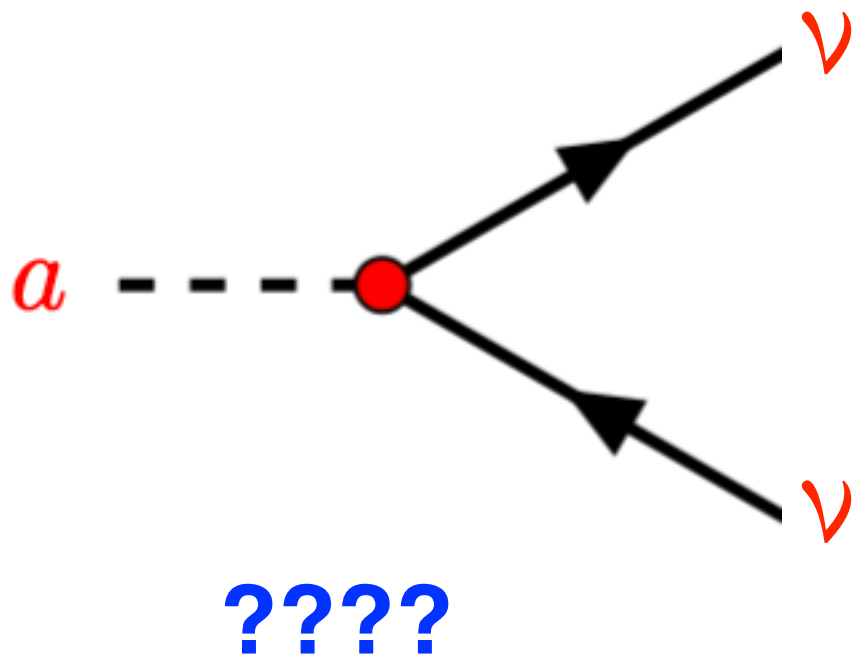
**Neutrinos are excellent messengers onto the dark sectors
of the universe**

What about *a*-neutrino couplings ?

Bonilla, Gavela, Machado [arXiv:2309.15910] Phys.Rev.D 109 (2024)

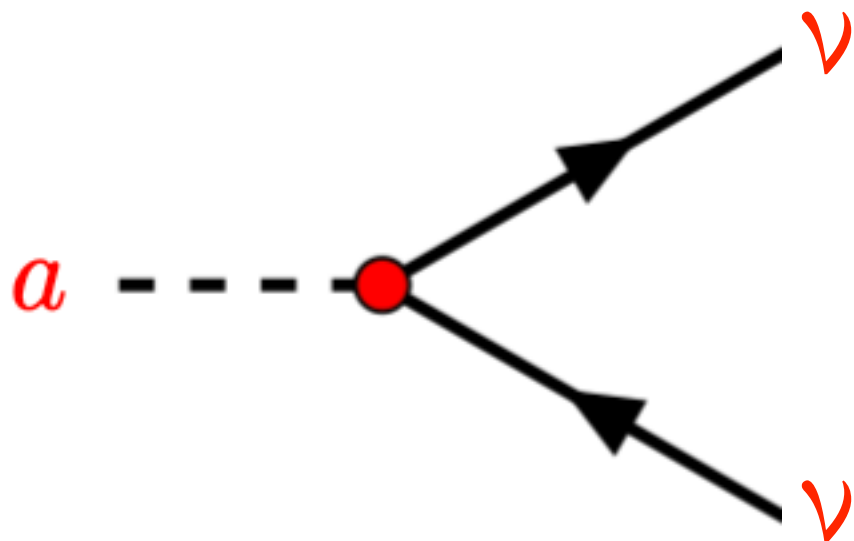
NEW

Bounds on ALP-neutrino couplings



$$\mathcal{L}_{\partial a}^{\nu} = \frac{\partial_{\mu} \textcolor{red}{a}}{f_a} \bar{\nu}_L \gamma^{\mu} \mathbf{c}_L \nu_L$$

Bounds on ALP-neutrino couplings

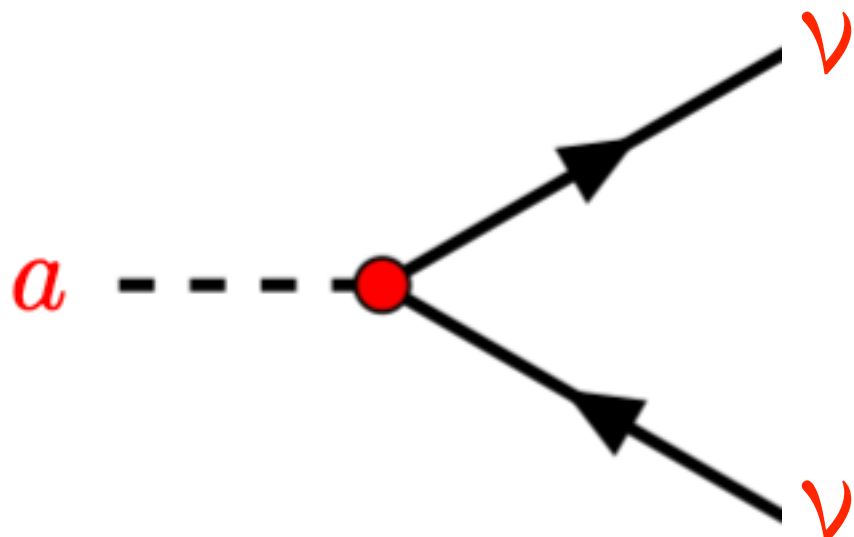


????

EOM

$$\mathcal{L}_{\partial a}^{\nu} = \frac{\partial_{\mu} a}{f_a} \bar{\nu}_L \gamma^{\mu} \mathbf{c}_L \nu_L = \left(i \frac{a}{f_a} \bar{\nu}_L \mathbf{M}_{\nu} \mathbf{c}_L \nu_R + \text{h.c.} \right)$$

Bounds on ALP-neutrino couplings



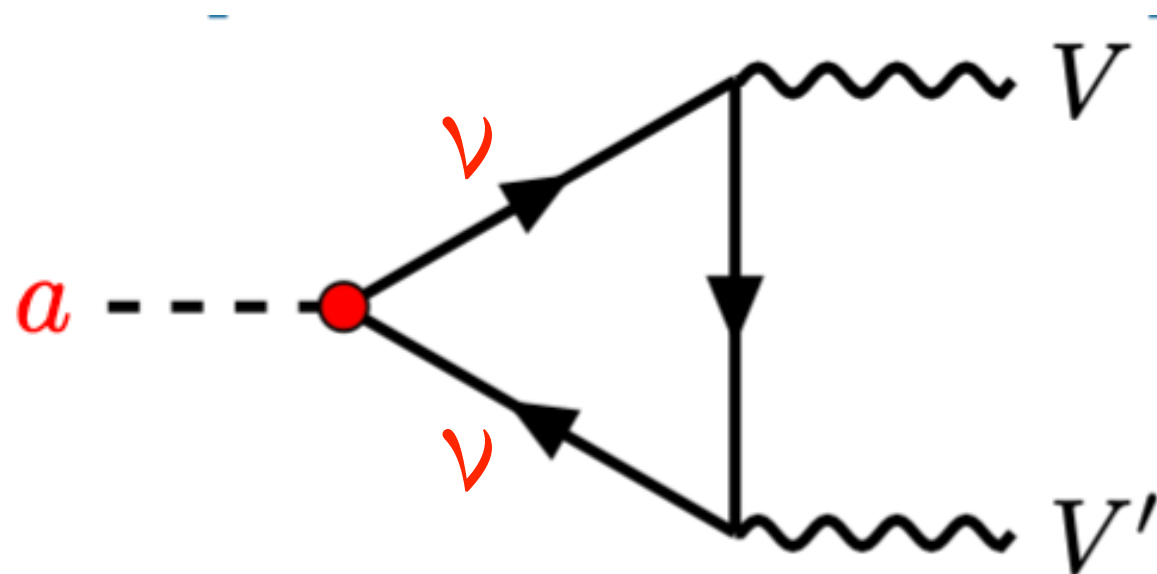
????

EOM

$$\mathcal{L}_{\partial a}^{\nu} = \frac{\partial_{\mu} a}{f_a} \bar{\nu}_L \gamma^{\mu} \mathbf{c}_L \nu_L = \left(i \frac{a}{f_a} \bar{\nu}_L \mathbf{M}_{\nu} \mathbf{c}_L \nu_R + \text{h.c.} \right)$$

$$- \text{Tr} [\mathbf{c}_L] \frac{a}{f_a} \left[\frac{g'^2}{64\pi^2} B_{\mu\nu} \tilde{B}^{\mu\nu} + \frac{g^2}{64\pi^2} W_{\mu\nu} \tilde{W}^{\mu\nu} \right]$$

Bounds on ALP-neutrino couplings



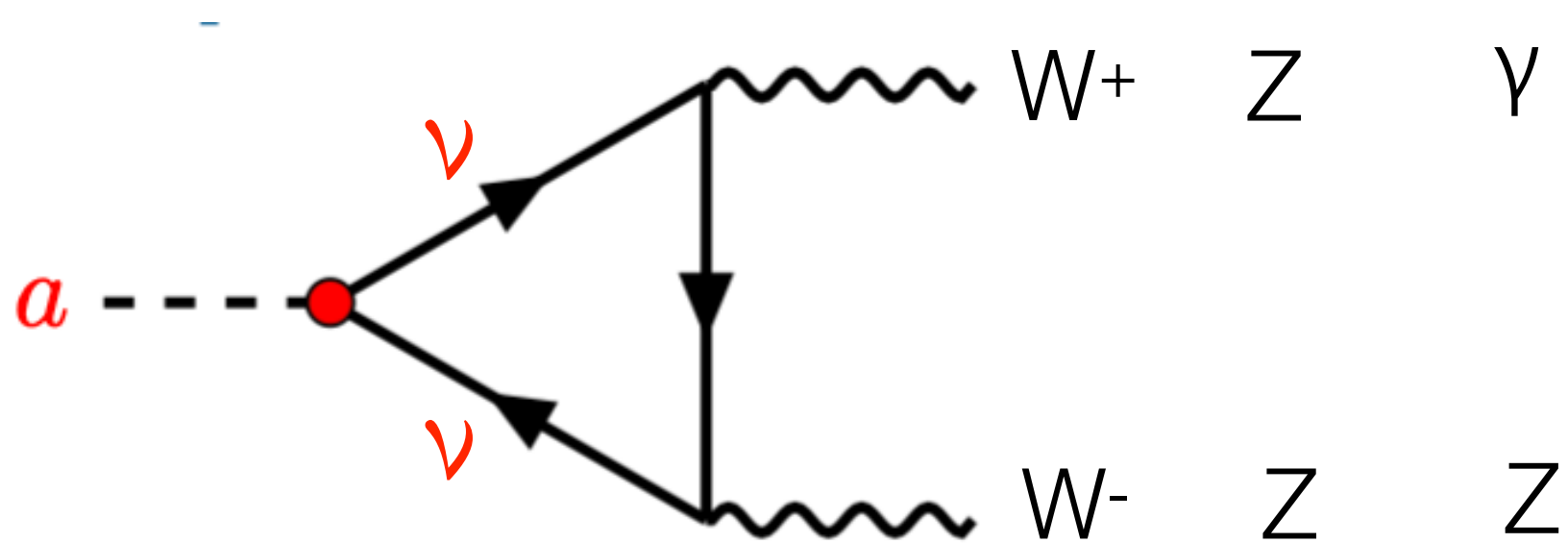
????

EOM

$$\mathcal{L}_{\partial a}^{\nu} = \frac{\partial_{\mu} a}{f_a} \bar{\nu}_L \gamma^{\mu} \mathbf{c}_L \nu_L = \left(i \frac{a}{f_a} \bar{\nu}_L \mathbf{M}_{\nu} \mathbf{c}_L \nu_R + \text{h.c.} \right)$$

$$- \text{Tr} [\mathbf{c}_L] \frac{a}{f_a} \left[\frac{g'^2}{64\pi^2} B_{\mu\nu} \tilde{B}^{\mu\nu} + \frac{g^2}{64\pi^2} W_{\mu\nu} \tilde{W}^{\mu\nu} \right]$$

Bounds on ALP-neutrino couplings



????

EOM

$$\mathcal{L}_{\partial a}^\nu = \frac{\partial_\mu a}{f_a} \bar{\nu}_L \gamma^\mu \mathbf{c}_L \nu_L = \left(i \frac{a}{f_a} \bar{\nu}_L \mathbf{M}_\nu \mathbf{c}_L \nu_R + \text{h.c.} \right)$$

$$- \text{Tr} [\mathbf{c}_L] \frac{a}{f_a} \left[\frac{g'^2}{64\pi^2} B_{\mu\nu} \tilde{B}^{\mu\nu} + \frac{g^2}{64\pi^2} W_{\mu\nu} \tilde{W}^{\mu\nu} \right]$$

$$L_L \equiv \begin{pmatrix} e_L \\ \nu_L \end{pmatrix} \quad \text{connected by gauge invariance}$$

$$\mathcal{L}_{ALP} \supset \frac{\partial_\mu a}{f_a} \bar{L}_L \gamma^\mu c_L L_L + \frac{\partial_\mu a}{f_a} \bar{e}_R \gamma^\mu c_E e_R$$

CLASSICAL EOM

$$\frac{\partial_\mu a}{f_a} \bar{e}_R \gamma^\mu c_E e_R = - \left(i \frac{a}{f_a} \bar{e}_L \mathbf{M}_E c_E e_R + \text{h.c.} \right)$$

$$\frac{\partial_\mu a}{f_a} \bar{e}_L \gamma^\mu c_L e_L = \left(i \frac{a}{f_a} \bar{e}_L \mathbf{M}_E c_L e_R + \text{h.c.} \right)$$

$$\frac{\partial_\mu a}{f_a} \bar{\nu}_L \gamma^\mu c_L \nu_L = \left(i \frac{a}{f_a} \bar{\nu}_L \mathbf{M}_\nu c_L \nu_R + \text{h.c.} \right)$$

Mass-suppressed

M. Chala *et al*, Eur. Phys. J. C 81 (2021), no. 2 181
 M. Bauer *et al*, JHEP 04 (2021) 063
 J. Bonilla *et al*, JHEP 11 (2021) 168

$$L_L \equiv \begin{pmatrix} e_L \\ \nu_L \end{pmatrix} \quad \text{connected by gauge invariance}$$

$$\mathcal{L}_{ALP} \supset \frac{\partial_\mu a}{f_a} \bar{L}_L \gamma^\mu c_L L_L + \frac{\partial_\mu a}{f_a} \bar{e}_R \gamma^\mu c_E e_R$$

CLASSICAL EOM

$$\frac{\partial_\mu a}{f_a} \bar{e}_R \gamma^\mu c_E e_R = - \left(i \frac{a}{f_a} \bar{e}_L \mathbf{M}_E c_E e_R + \text{h.c.} \right) + \text{Tr} [c_E] \frac{a}{f_a} \frac{g'^2}{16\pi^2} B_{\mu\nu} \tilde{B}^{\mu\nu}$$

ONE-LOOP EFFECT

$$\frac{\partial_\mu a}{f_a} \bar{e}_L \gamma^\mu c_L e_L = \left(i \frac{a}{f_a} \bar{e}_L \mathbf{M}_E c_L e_R + \text{h.c.} \right) - \text{Tr} [c_L] \frac{a}{f_a} \left[\frac{g'^2}{64\pi^2} B_{\mu\nu} \tilde{B}^{\mu\nu} + \frac{g^2}{64\pi^2} W_{\mu\nu} \tilde{W}^{\mu\nu} \right]$$

$$\frac{\partial_\mu a}{f_a} \bar{\nu}_L \gamma^\mu c_L \nu_L = \left(i \frac{a}{f_a} \bar{\nu}_L \mathbf{M}_\nu c_L \nu_R + \text{h.c.} \right) - \text{Tr} [c_L] \frac{a}{f_a} \left[\frac{g'^2}{64\pi^2} B_{\mu\nu} \tilde{B}^{\mu\nu} + \frac{g^2}{64\pi^2} W_{\mu\nu} \tilde{W}^{\mu\nu} \right]$$

Mass-suppressed

Mass-independent

M. Chala et al, Eur. Phys. J. C 81 (2021), no. 2 181
 M. Bauer et al, JHEP 04 (2021) 063
 J. Bonilla et al, JHEP 11 (2021) 168

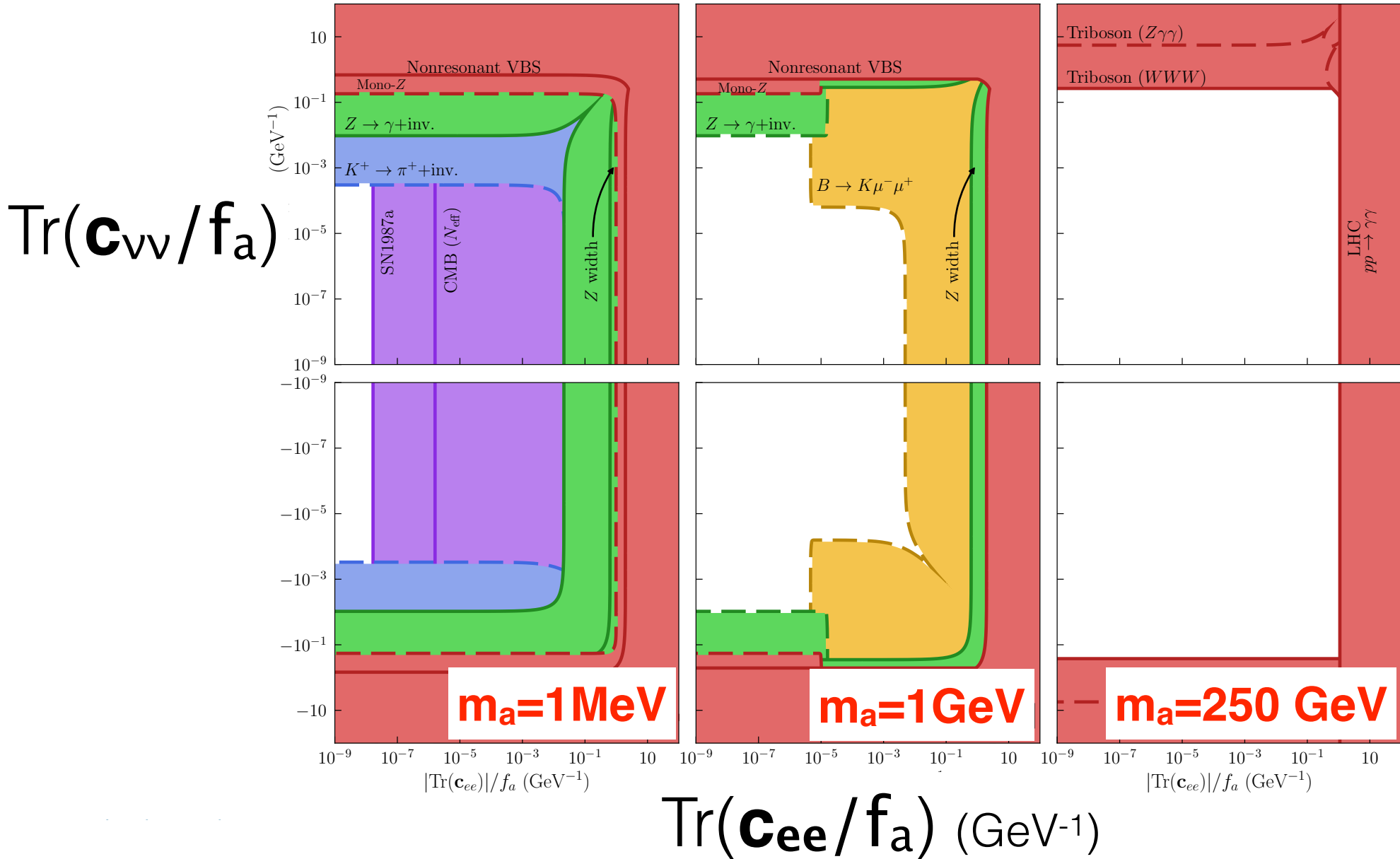
one-loop anomalous current

Bounds
**ALP-gauge
bosons**

Bounds
ALP-neutrino

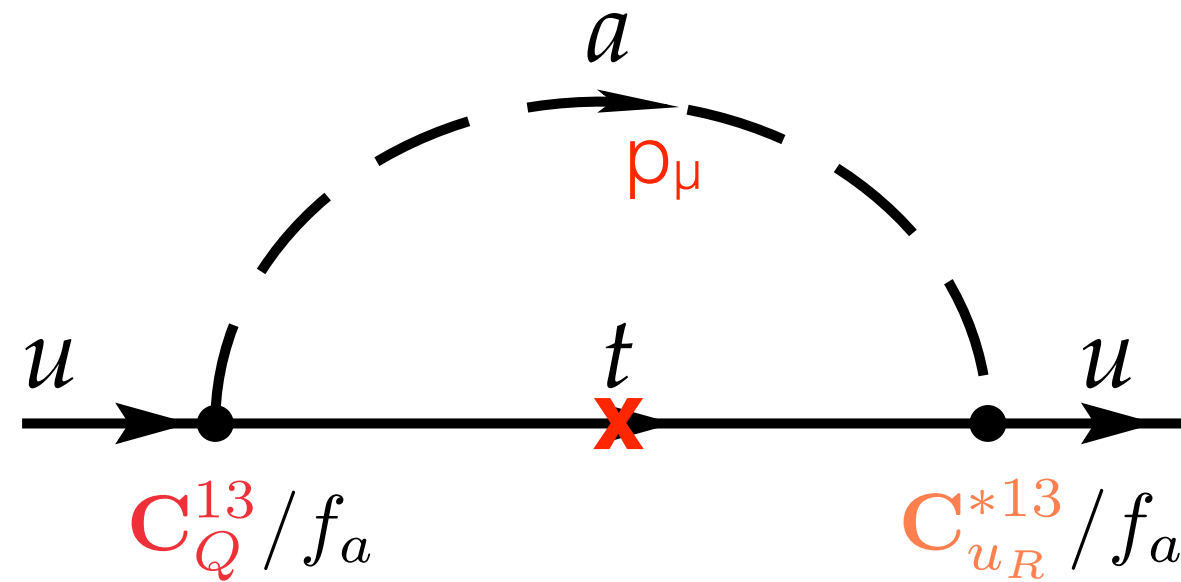
$$\text{Tr}(\mathbf{c}_{vv}/f_a) \text{ vs. } \text{Tr}(\mathbf{c}_{ee}/f_a)$$

Bounds on ALP-neutrino coupling



Lots of space to explore by LHC and future colliders

ALP contribution to $\bar{\theta}$



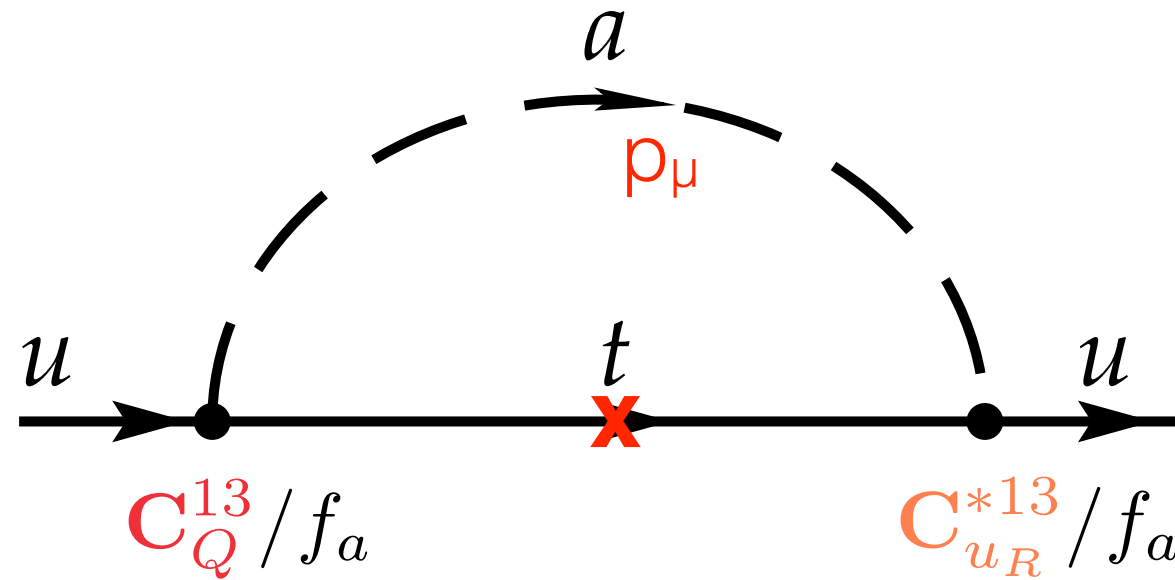
- * Factor m_t for chirality flip
- * Factor p_μ^2 from vertices

$$\begin{aligned} d_n &= 0.6(3) \times 10^{-16} \bar{\theta} [e \cdot \text{cm}] \\ &\quad - 0.204(11)d_u + 0.784(28)d_d - 0.0028(17)d_s \\ &\quad - 0.32(15) e \tilde{d}_u + 0.32(15) e \tilde{d}_d - 0.014(7)e\tilde{d}_s. \end{aligned}$$

M. Pospelov, A. Ritz,
hep-ph/0504321,
073015

J. Hisano et al.,
arXiv:1205.2212

ALP contribution to $\bar{\theta}$



- * Factor m_t for chirality flip
- * Factor p_μ^2 from vertices

$$d_n = 0.6(3) \times 10^{-16} \bar{\theta} [e \cdot \text{cm}]$$

$$- 0.204(11)d_u + 0.784(28)d_d - 0.0028(17)d_s$$

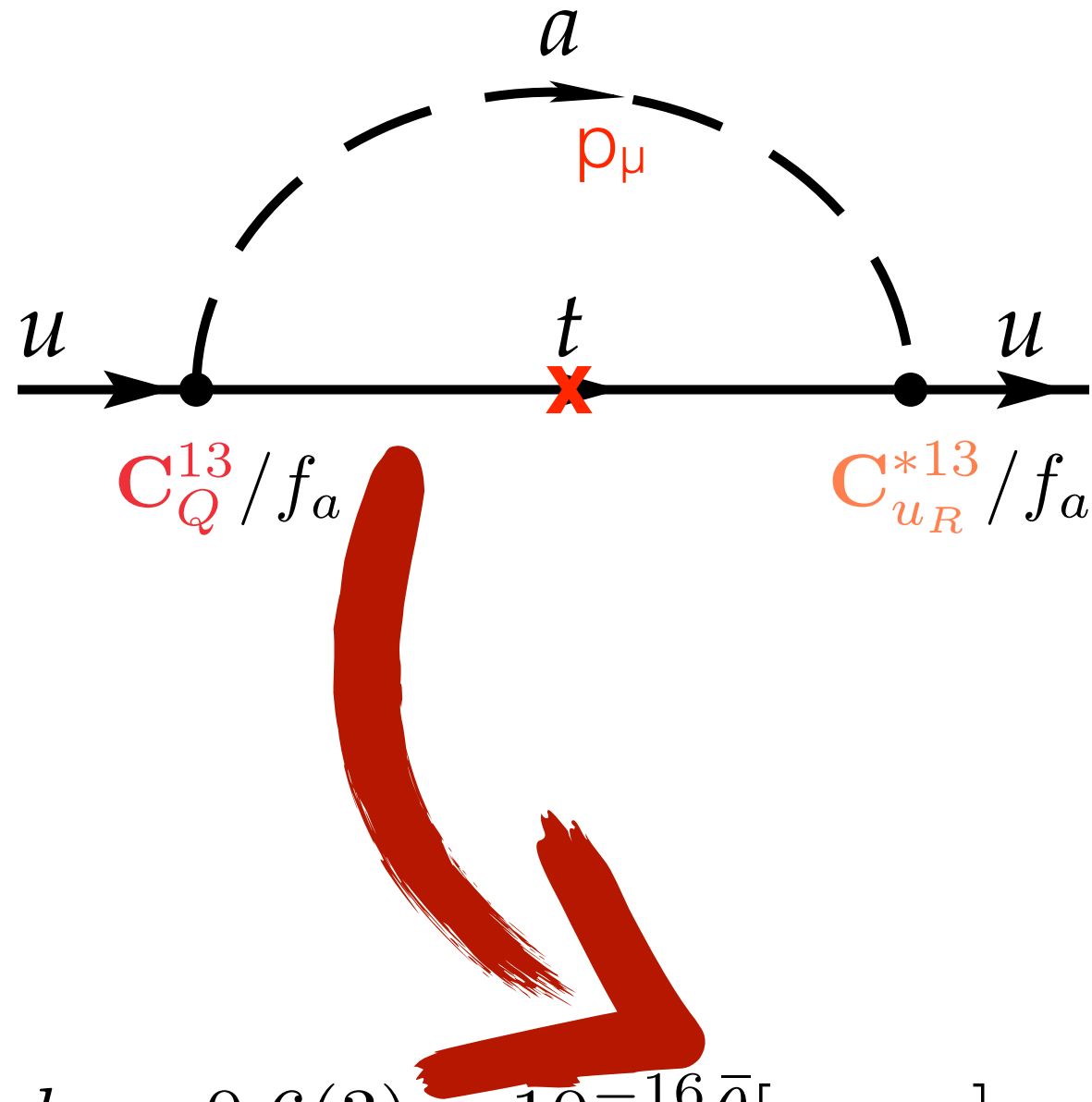
$$- 0.32(15) e \tilde{d}_u + 0.32(15) e \tilde{d}_d - 0.014(7)e\tilde{d}_s.$$

quark electric EDMs
quark chromo-electric EDMs

M. Pospelov, A. Ritz,
hep-ph/0504321,
073015

J. Hisano et al.,
arXiv:1205.2212

ALP contribution to $\bar{\theta}$



- * Factor m_t for chirality flip
- * Factor p_μ^2 from vertices

$$d_n = 0.6(3) \times 10^{-16} \bar{\theta} [e \cdot \text{cm}]$$
$$- 0.204(11)d_u + 0.784(28)d_d - 0.0028(17)d_s$$
$$- 0.32(15) e \tilde{d}_u + 0.32(15) e \tilde{d}_d - 0.014(7)e\tilde{d}_s.$$

M. Pospelov, A. Ritz,
hep-ph/0504321,
073015

J. Hisano et al.,
arXiv:1205.2212